Role of *lysX* gene from *Mycobacterium avium hominissuis* in metabolism and host-cell interaction

Inaugural-Dissertation

to obtain the academic degree

Doctor rerum naturalium (Dr. rer. nat)

Submitted to the Department of Biology, Chemistry and Pharmacy

of Freie Universität Berlin

by

GREANA KIRUBAKAR

from Chennai, India

Berlin, 2019

This work was accomplished between October 2015 and July 2019 at the Robert Koch Institute under the supervision of Dr. Astrid Lewin.

1st Reviewer: Dr. Astrid Lewin

2nd Reviewer: Prof. Dr. Rupert Mutzel

Date of Defense: 21.10.2019

Acknowledgement

I express my deepest gratitude to my doctoral guide, **Dr. Astrid Lewin** for giving me the opportunity to work in this prestigious Robert Koch Institute (RKI). Her constant guidance and encouragement has enabled me to successfully pursue this project. I appreciate all her contributions of time, ideas, and funding recommendations to make my PhD. experience productive and stimulating. I would also like to thank **Prof. Dr. Lothar Wieler**, the President of the Robert Koch-Institute, for providing me permission to carry out my PhD research work**.**

My sincere thanks to my second supervisor, **Prof. Dr. Rupert Mutzel,** for his insightful comments and valuable suggestions throughout the period of my thesis. I am also very thankful to Elisabeth Kamal, for her excellent technical assistance and taking care of both my experimental and personal issues. I also acknowledge Dr. Toni Aebischer for his valuable advice in my research project and his hard questions which incented me to widen my research from various perspectives.

In regards to the Proteomics experiments, I like to thank Dr. Jayaseelan Murugaiyan for collaborating with our institute. The research group of Dr. Uwe Roesler at the Institute for Animal Hygiene and Environmental Health and Dr. Murat Eravci, Dr. Christoph Weise from the Institute of Chemistry and Biochemistry, Free University Berlin have also contributed to the proteomics study.

The BIOLOG data analysis which is discussed in this dissertation would not have been possible without the contribution of Dr. Flavia Dematheis at the Institute of Microbiology and Epizootics, Free University Berlin. I appreciate this collaboration, as the metabolic analysis was conducted using the BIOLOG facility available the University lab.

For the microscopic examinations, Gudrun Holland and Dr. Christoph Schaudinn, from the ZBS4 division, Advanced Light and Electron microscopy, RKI, Berlin have made significant contributions and the inspirational discussions with Dr. Schaudinn regarding the experiments gave me newer perspectives in the research project.

I also appreciate the help of Dr. Hubert Schäfer and Barbara Kropp in the GPL experiments. I am also indebted for his motivational support, local expertise and sharing of knowledge during my research work.

I am also grateful to Dr. Volker Rickerts and the animal facility of RKI (MF3 division: Dr. Petra Kirsch, Annette Dietrich and Alice Stern) for enabling me to conduct in vivo experiment using the *Galleria mellonella* larval infection model.

I gratefully acknowledge the funding sources that made my PhD. work possible. I was funded by the Rosa Luxemburg fellowship for my first 3 years and was honored to receive the Georg & Agnes Blumenthal Stiftung and the Robert Winter Stiftung in my completion phase.

My time at RKI, Berlin, was made enjoyable in large part due to the many friends and groups that became a part of my life. I am thankful to the FG16 division group members at the RKI, who backed me up and were always ready to help. Especially, the lab members of our research group, Dr. Andrea Sanchini, Suriya Akter, Linus Fiedler, Anna Maria Oschmann and Alexander Lüders made my stay memorable by creating a friendly atmosphere. I truly appreciate the funtimes spent with them during the long working hours and some delightful trips together. My time in Germany was also enriched by the warm affections extended by the elders and fellow friends from the ODMC Church and the Berlin International Community church.

Lastly, I would like to thank my family for all their love, prayers and encouragement. For my parents, Kirubakar and Mercy Paulkani who raised me with a love to achieve greater heights in my education and supported me in all my pursuits. For the presence of my sister, Selina Kirubakar here in Berlin for the three of my years here. And most of all I would never forget the grace of God which enabled me to survive through every difficulty and obstacles that I needed to cross in this journey of my life.

GREANA KIRUBAKAR

Table of Contents

List of figures

List of Tables

List of Abbreviations

AIDS	Acquired immune deficiency syndrome
AMPs	Antimicrobial peptides
COG	Clusters of Orthologous Groups
DETA/NO	Diethylenetriamine/nitric oxide adduct
ELISA	Enzyme-linked immunosorbent assay
FAS	Fatty acid synthesis
FI%	Fusion index
GPL	Glycopeptidolipid
HBDM	Human blood derived macrophages
LAM	Lipoarabinomannan
L-PG	Lysinylated-phosphatidylglycerol
MAA	*Mycobacterium avium* subsp. *avium*
MAC	*Mycobacterium avium* complex
MAH	*Mycobacterium avium* subsp. *hominissuis*
MAP	*Mycobacterium avium* subsp. *paratuberculosis*
MGCs	Multinucleated giant cells
MTB	*Mycobacterium tuberculosis*
NTM	Non tuberculous mycobacteria
PBMC	Peripheral blood mononuclear cells
PG	Phosphatidylglycerol
ssGPL	species specific Glycopeptidolipid
TAG	Triacylglycerol
TB	Tuberculosis
TEM	Transmission electron microscopy
TLC	Thin-layer chromatography
WHO	World Health Organization

1 Introduction

Mycobacterial diseases still remain to be a potent problem to mankind and a far-reaching challenge for health systems [1]. Their complexity begins even at the level of species and subspecies classification as they differ widely in several traits, as of their pathogenic capacity in humans and animals, and growth dynamics in culture [2]. Tuberculosis, an infection caused by *Mycobacterium tuberculosis* (MTB) complex has been reported as one of the top ten reasons of death worldwide by the World Health Organization (WHO, 2018). Globally, it was estimated that around 10 million people developed TB disease in the year of 2017 and 1.6 million died from the disease (including 0.3 million among people with HIV) [3]. Drug resistance is a major obstacle in the treatment and control of tuberculosis [4].

Leprosy is another mycobacterial chronic infectious disease caused by *Mycobacterium leprae*, affecting the skin and peripheral nerves with lesions [5]. Its prevalence rate was estimated to be 0.3/10 000 population at the end of 2017, based on the occurrence of 193 118 cases(WHO, 2019).Though the number of cases are getting reduced, new cases are being re-emerged due to the active transmission capability of *M. leprae* which summons more effective interventions to prevent further infections [6]. The main drawback is that this bacterium is non-cultivable under axenic conditions, thus posing a big challenge to basic research and clinical management [7].

Apart from these pathogenic species, the nontuberculous mycobacteria (NTM) are a heterogeneous group consisting of more than 180 species of environmental mycobacteria with distinct human pathogenesis and varied geographic distribution [8]. They have been frequently isolated from water sources (household taps and natural water reservoirs), soil (potting soil and garden soil), dust and plants [9]. These NTM can cause opportunistic infections especially in immunosuppressed individuals (eg. AIDS, cystic fibrosis patients) and their clinical presentations include lymphadenitis, skin and soft tissue infections and disseminated infections. Immunocompetent patients are typically manifested with isolated pulmonary infections and this happens often to patients with a past history of lung disease [10]. Since the clinical symptoms of pulmonary infections caused by NTM are similar to tuberculosis and other pulmonary diseases, their diagnosis becomes very challenging and they are mostly underreported in developing countries [11]. Hence, the information on the

prevalence and the epidemiology of NTM cases are still incomplete. Further, as the NTMs are typically resistant to antituberculosis drugs [12], they are most often misinterpreted as multidrug-resistant (MDR) tuberculosis especially in countries where TB and AIDS are the major focal point of the healthcare system. A recent survey also reported that around 12-30% of the patients diagnosed with chronic and MDR TB were found to suffer from NTM infection in reality [13]. Nevertheless, the incidence of lung disease caused by NTM is increasing worldwide, posing it to be an emerging global health threat [14]. From the side of developed countries with the specialized healthcare facilities, it was also reported that the NTM diseases have risen to be greater disease burden than TB in countries such as US, Canada, Japan, Korea, Australia, and United Kingdom [15-19]. For example the annual incidence rates were elevated from 5.6/100,000 in England and Ireland during the year of 2007 to 7.6/100,000 in 2012 [19]. Likewise, the U.S. National Institutes of Health reported an increase in the pulmonary NTM diseases from 20 to 47 cases/100,000 persons (or 8.2% per year) among adults aged 65 years or older throughout the United States, with 181,037 national annual cases estimated in 2014 [2] .

Thus the lack of knowledge on NTM is a burning issue, wherein the imprecise diagnosis and ineffective treatment dosages contribute to disease progression and worsening of patient's health [8]. The NTM possess intrinsic bacterial resistance and also has a persistent nature making them more invincible [20]. Hence, the need to discover and develop new and more effective strategies to NTM treatment is indispensable. In order to attain the above goal, an understanding of the host-pathogen interactions and survivability of NTM by manipulating the host defense mechanisms is essential. "Todays' state of NTM drug discovery is reminiscent of the TB situation 20 years ago" [20] . In this project we have attempted to approach explanations to questions concerning resistance, persistence and pathogenicity of NTM which still remain unanswered. These questions without being unveiled have resulted in knowledge gaps and scientific obstacles in NTM drug discovery.

1.1 Genus *Mycobacterium*

Mycobacteria belong to the non-sporulating members of the actinomycete family and thrive in aerobic-to-microaerophilic environment [21]. They are gram-positive, non-motile and strongly differ from other bacteria in their cell wall architecture comprising of components with strikingly immuno-stimulatory properties [22]. Their lipid rich cell

envelope is the most prominent feature of mycobacteria that is uniformly present and distinctive to the genus [23]. This peculiar cell wall lipid composition makes them several-fold less permeable to chemotherapeutic agents and thus rendering the mycobacteria less susceptible to various antibiotic classes [24] .

Another distinguishing feature of the pathogenic mycobacterial species is attributed to their shifting metabolism in the intracellular environment. Initially, the bacilli access glucose and triacylglyerides as primary carbon sources during early replication under aerobic condition. As the infection progresses, they shift to more ultilization of lipids as they are exposed glucose-deficient macrophage environment [25]. Metabolic reprogramming is a vital virulence determinant during the course of acute and chronic mycobacterial infections [26, 27]. Several experimental studies have also identified the central carbon metabolism to be instrumental in pathogenic strategy [26, 28, 29].

Intracellular mycobacterial species possess the unique ability to organize their residence inside of the host organism and to proliferate within the host macrophages by overcoming the antimicrobial defense mechanisms. The tendency to establish chronic infections that produce similar pathologies in different hosts is one of the hallmarks of these pathogenic species. In particular, *M. tuberculosis*, *M. leprae*, *M. marinum*, and *M. avium*, are all capable of establishing these long-term infections [30]. Hence, it is necessary to understand the factors that contribute to the complex relationship between host and pathogen in order to modulate the clinical outcomes of mycobacteriosis [30].

In comparison to most other bacteria, they are slow growers requiring at least three days of incubation to produce visible colonies, with many showing visible growth only after one or more weeks [31]. Thus the *Mycobacterium* (*M.*) genus comprises of species with multiple behavioural characteristics including strict pathogens, opportunistic pathogens, and the nonpathogenic, saprophytic species [32]. Traditionally, the pathogenic mycobacterial species are classified based on their growing ability with the slow-growers group consisting of the three major human pathogens (MTB, *M. leprae* and *M. ulcerans*), while the NTMs which are prevalent among the immune-compromised individuals include fast growers such as *M. abscessus* and also slow growers like *M. avium*, *M. marinum*, *M. xenopi*, *M. gordonae* and *M. kansasii* [33].

1.2 *Mycobacterium avium hominissuis* (MAH)

M. avium is the most clinically significant NTM species causing infection in humans and animals. The *M. avium* complex comprises of four subspecies that have distinct pathogenic and host range characteristics: *M. avium hominissuis* (MAH) infecting pigs and humans in majority, *M. avium paratuberculosis* (MAP) causing Johne's disease in ruminants and the avian pathogens such as *M. avium avium* (MAA) , *M. avium silvaticum* [34, 35].

In the recent years, the incidence of NTM infections has been significantly increased, in which MAH alone accounts up to 72 % out of the mycobacterial infections in total [36-38]. Research surveys also report that MAH infection has a high incidence of reoccurrence and frequently results in antibiotic resistance over time. These consequences may be supported by the capability of MAH to produce biofilms in the lungs, which aid in the establishment of infection in the host and are strongly resistant towards antimycobacterial therapies [39, 40].

The MAH encompasses the highest level of genomic heterogeneity among the *M. avium* subspecies[41, 42]. Further, this subspecies is also different at the phylo-geographical level, suggesting different infection sources in different regions [43]. In addition, MAH strains comprises of highly variable phenotypic traits and this is already evident from their different colony morphotype. MAH isolates with different morphotype belonging to same strain can even show deviating virulence potentials [44].

MAH also produces lipid components that have been associated with immunomodulatory properties, such as lipoarabimannan (LAM), glycopeptidolipid (GPL) and a few non-characterized 'glycolipids'. These lipids are located on the outermost layer of the cell wall [45]. Amongst these GPL's are a special class of glycolipids, produced only by NTM's but are absent in other mycobacterial species. GPL's are associated with a variety of biological functions. They are highly antigenic and can be classified as serovar specific GPLs (ssGPLs) [46]. It was also demonstrated that the MAH GPL content is correlated with strain-to-strain variation in biofilm formation [47]. Further, the biosynthesis of GPL plays a role in the colony morphology of *M. avium* [46]. In addition, the core GPL is a primary requisite for adherent accumulation of MAH on some, but by no means all, surfaces.

Therefore, the GPLs are essential to colonize new environments and also play a part in the ingestion of MAC by humans cells [48].

1.3 Pathogenesis of MAH

The intracellular opportunistic pathogen MAH infects many host-cell types but the mononuclear phagocyte is the primary target. The ability of the bacterium to cross the mucosal barrier and infect submucosal macrophages is an important key for establishing infection in the host organism [49]. Antimicrobial peptides (AMPs) such as β-defensins, cathelicidin and Reg IIIβ are secreted by the human intestinal mucosa and they serve as a host innate response against a number of bacteria [50]. Recently it was shown that MAP, a subspecies closely related to MAH resists the actions of AMPs [51].

MAH are also fairly resistant towards reactive oxygen species (ROS) and nitric oxide (NO). In contrast to MTB, the survival of MAH is unaffected by the inactivation of induced NO in a mouse model. Even though it is known that the macrophage activation by the cytokines tumor necrosis factor alpha (TNFα) and interferon gamma (IFN-γ) have important roles in *M. avium* killing [52], the defense mechanisms achieving killing of intracellular MAH have not been identified so far. However , *M. avium* infections were shown to mediate NF-κB activation and enhanced gene expression of TNF-α and IL-1β, these proinflammatory cytokines influence multiple signal transduction pathways and inhibit macrophage apoptosis [53].

The immune responses induced by MAH are likely due to the diverse lipids in the outer layer of the cell wall (eg. Glycolipids, GPL)[54, 55]. However, previous studies have also proved that the NTM species with rough colony morphotypes containing a different pattern or lack of GPLs induced more inflammatory response when compared to the smooth phenotypes [56-58].

Once taken up by the macrophages, the MAH resides in cytoplasmic vacuoles, which does not acidify [49]. Thus they also escape from the docking stage of the late phagosome to lysosome, interfering with the normal course of maturation during infection. Though the MAH are less virulent than MTB, they still manage to survive within host macrophages by subverting the function of phagocytic cells [59].

Multinucleated giant cells (MGC) are the histologic hallmark of granuloma in mycobacterial infections [60]. Research studies have found that *M. avium* on exposing to human monocyte-derived macrophages, was bound to the adherent macrophages, inducing gene expression of chemokines and cytokines like TNF-α and IL-1 and adhesion molecules. During the later phase of infection, these adhesion molecules facilitate migration through the endothelial barrier to the site of infection, promoting cell-cell interactions resulting in the formation of MGCs which appear quite consistent with in in vivo events. At the MGC differentiation state, the macrophages are insufficiently microbicidal and provide a nonhostile environment to the mycobacteria [53, 61, 62].

MAH must encompass an array of virulence factors which enable them to survive amidst the defense mechanisms mounted by the host [63, 64]. However, a majority of the virulence factors and genes implicated for virulent phenotypes are still unknown. Although several studies have determined the MAH gene expression in phagosomes both vitro [65, 66] and in vivo [64], very few attempts have been made to identify the virulence genes necessary for survival in the host [49].

1.4 Cell envelope of MAH

The virulence and intrinsic multidrug resistance of MAH are attributed mainly to its cell wall characteristics [67]. The unusual mycobacterial cell wall corresponds to a permeability barrier of which mycolic acids constitute up to 60% of the lipid content [68]. The outermost layers are composed of different classes of glycolipids, that are species-specific [69]. Many of these cell wall glycolipids are considered important in mycobacterial pathogenesis. For example, the GPLs play a role in host-pathogen interactions, as they affect the initial or long-term response of the host. Since, the MAC bacteria are subjected to receptor-mediated phagocytosis by infected macrophages and further survive in mycobacterial phagosome, it has been suggested that GPLs can interact with host membranes promoting bacterial survival. Additionally, GPLs can also accumulate on the surface of MAC during extracellular growth and inside infected cells [70] [71]. Thus, GPL plays a major role, as their absence or modification also corresponded to an attenuated phenotype [55, 71].

Interestingly, NTM and MTB strains contain different cell wall components and henceforth exibhit differential immune reactivity. For example, when compared to the lipoarabinomannan of NTM, the mannose-capped lipoarabinomannan of MTB displays distinctive structural features and thereby elicits a different host-pathogen interaction [72]. In comparison, the cell envelope of NTM is considerable more impermeable than MTB, which enables the bacterium to survive in multifarious environments; eg. soil, dust , natural and man-made water systems and biofilms that also differ greatly with extremes conditions in temperature, humidity and nutrient availability [73].

In addition, the genes involved in cell-wall synthesis are also upregulated upon uptake of *M. avium* by macrophages. Studies have demonstrated that the expression of polyketide synthase encoding genes was enhanced in-vivo and the polyketides are involved in cell wall synthesis and integrity [66]. The mmpL (Mycobacterial membrane protein large) gene family which participates in the transport mechanism of polyketides to the bacterial surface were also reported to be overexpressed during infection of macrophages [65, 74]. MmpLs are essential for maintaining the structure of the cell envelope and directly support mycobacteria during infection and persistence inside the host [75].

1.5 The *lysX* gene

Some of the mycobacterial lipids present on the plasma membrane have no structural roles but they play important functional roles. These lipids mostly occur in low quantities and often remain unnoticed [76]. Recently, a research study on MTB reported the identification of a minor species of positively charged, membrane phospholipid known as lysylphosphatidylglycerol (L-PG). The L-PG synthesis mainly contributes to the resistance towards cationic antimicrobial peptides (CAMPs), thus protecting MTB from host-induced frontline defense. However, it was also demonstrated that the *lysX* gene which is a lysyl t-RNA synthetase, mediates the synthesis of lysinylated PG and a *lysX* deletion mutant also resulted in an alteration in the phospholipid metabolism and cell membrane integrity [77, 78]. It was also shown that the *lysX* gene was necessary for acquiring full virulence potential of MTB and it was proven to be essential for the survivability of the pathogen upon infection [77]. Another study showed that the *lysX* gene expression differed from strain to strain in the MTB species and those with the higher *lysX* expression exhibited increased levels of intracellular survival in vivo *and* in vitro [79]. Since the lysX

expression was represented as an important variable for the modulation of MTB virulence, further studies were performed and that uncovered the use of mutations in lysX SNP (single-nucleated polymorphism) marker for screening of tuberculosis Beijing and modern Beijing strains [80].

2 Aim and justification of the study:

MAH is an opportunistic pathogen able to reside as saprophytic organism in the environment but also as a pathogen within human phagocytic cells. The disclosure of the mechanisms enabling MAH to switch between a saprophytic and a pathogenic life style will facilitate the design of countermeasures against infections by this and related opportunistic agents. We were therefore interested in identifying genes predisposing MAH to survive outside their environmental habitat and instead replicate inside phagocytes of the human immune system. To this aim random mutant of MAH strain 104 were previously generated and among these a LysX-deficient mutant was identified that was now further analyzed.

The main objective of this thesis is to characterize a mutant of MAH with a deletion in the *lysX* gene, which is annotated as lysyl-tRNA synthestase. The study was targeted towards analyzing the functional role of the *lysX* gene in the growth, host-cell interplay and eventually its contribution towards virulence. The impact of this gene on the different functional pathways of MAH was to be examined through proteomic analysis and BIOLOG phenotype microarray for investigating the role of the gene in metabolism. Transmission electron and fluorescence microscopy techniques were to be applied to identify the structural features between the wild type, mutant and complemented strains. The survivability of the lysX mutant from MAH was tested in human blood-derived monocytes. To further decipher the impact of *lysX* for host-pathogen interaction, the resistance to host-inductive stresses, the inflammatory cytokine response and the MGC formation by human monocytes were planned to be experimented. Finally the impact of *lysX* for virulence was planned to be tested in the *Galleria mellonella* in-vivo model infection model.

3 Materials and Methods

3.1 Bacterial strains and growth conditions

Strain	Origin/Description	Reference / Source
*M. avium*104	HIV Patient	NRCM*, Borstel, Germany
lysXmut	*M. avium*104 mutant deterring the function of the *lysX* gene (*MAV_3128*), Hyg^R (Hygromycin resistance marker integrated in *lysX* gene)	RKI^+, Berlin, Germany[81, 82]
lysXcomp	*M. avium*104 lysXmut strain containing plasmid pFKaMAV3128 (Vector pMV306 with wild-type gene *lysX* inserted in restriction sites XbaI and HpaI).	RKI^+, Berlin, Germany[81, 82]

* National Reference Center for Mycobacteria, Borstel, Germany

+ Robert Koch Institute, Berlin, Germany

The mycobacterial strains were grown in Middlebrook 7H9 broth along with 0.05% Tween 80 and supplemented either with 10% modified ADC (2% of glucose, 5% of BSA, 0·85% of NaCl) or OADC (oleic albumin-dextrose-catalase; BD Biosciences) and Middlebrook 7H11 media with 0.5% Glycerol was also used for plating purposes. The strains were cultured without shaking at 37°C. If required the lysX mutant was grown in media supplemented with 50 μg/ml hygromycin B and the lysX complemented strain with 50 μg/ml hygromycin B and 50 μg/ml kanamycin.

3.2 Mass spectrometry - proteomic analysis

A total of six independent cultures of each of the strains were grown up to an OD (600 nm) of 1.8 to 2.0 (log phase), in Middlebrook 7H9 broth with 0.05% Tween 80, supplemented with 10% modified ADC without any antibiotic. Protein extraction and label free quantitative proteomic analysis was conducted using LTQ Orbitrap Velos mass Spectrometer (Thermo Fischer Scientific) along with MaxQuant –Andromeda software as described elsewhere [83]. The raw MS files were processed using a freely available software suit, MaxQuant (version. 1.3.0.5 / Max-Planck-Institute of Biochemistry, Martinsried, Germany). The difference in the protein expression levels amongst the three strains were computed using the Perseus software. The entire mass spectrometry proteomic data can be retrieved from the ProteomeXchange Consortium through PRIDE [84] partner repository, using the data set identifier PXD006470. These experiments were performed in collaboration with the facility available at Free University Berlin, in the Institute of Animal Hygiene and Environmental Health.

3.2.1 Mapping of differentially expressed proteins onto metabolic pathways

The functional characteristics of differentially expressed proteins in MAH were examined by performing a homolog search on the COG database (Clusters of Orthologous Groups) (https://www.ncbi.nlm.nih.gov/COG/). The online tool DAVID (Database for Annotation Visualization and Integrated Discovery) (https://david.ncifcrf.gov/) was utilized to classify each of the genes into biological modules. The Functional Annotation Chart was created using a threshold p-value < 0.05 and gene count >4 were set as the cut-off point. The genes from *M. avium paratuberculosis* (MAP) were selected as a background for the analysis, as it was the most closest relative to MAH available in DAVID. The pathway enrichment was also analyzed using the DAVID database by integrating the pathway information obtained from the KEGG database (Kyoto Encyclopedia of Genes and Genomes) (*https://www.genome.jp/kegg/pathway.html*).

The STRING-10.5 database (https://stringdb.org/) is an online resource which is useful in identifying the protein-protein interactions and constructing functional protein association networks. An interactome network was built for the differentially expressed MAH proteins with a setting of interaction score >0.9 (highest confidence score) to be defined as

significant. From the above analysis, the pathways which were found to be affected by the *lysX* mutation were combined together to form a network of pathways.

3.3 BIOLOG metabolic phenotype microarray

The substrate utilization of the bacterial strains was analyzed using the BIOLOG Phenotype Microarray™ (BIOLOG, Hayward, CA, USA) as instructed in the manufacturer's recommendations [85-87]. This technology analyzes the metabolization of specific substrates by the measuring of bacterial respiration. When the bacteria uses the substrate in a particular PM plate well (96-wells plates with different substrates) it releases NADH which thereby reduces the tetrazolium dye generating a purple colour. The change of colours is recorded for a time interval of every 15 minutes by a reporter instrument OmniLog™ (BIOLOG, Hayward, CA, USA). Different PM plates comprising for carbon (PM1 and PM2), nitrogen (PM3), phosphorous (PM4) and sulfur (PM4) substrates were used for the study. The bacterial strains were processed for the study as described in [88]. Kinetic response curves are generated for reach well and the raw data are exported as csv files using Omnilog PM management/kinetic analysis mode. This experiment was performed with the BIOLOG instrument present at the Institute of Microbiology and Epizootics, Free University Berlin. The significant differences between the substrate usage of the bacterial strains were analyzed by the maximum height obtained in the bacterial respiratory curves (parameter A) using the R-package opm. The comparison was performed using the mean point estimates and their 95% confidence intervals for the parameter, by employing the functions extract and ci-plot as illustrated elsewhere [89]. The substrates which are differentially metabolized by the strains are visualized using the R-package heatmap. The substrates Pyruvic acid and Acetic acid which showed a significant difference in metabolization between the strains were further analyzed by linking them to their associated metabolic pathway using the KEGG pathway database [90].

3.4 Bacterial pyruvate quantification

Intracellular pyruvate concentrations were determined using the Pyruvate Assay Kit (Sigma-Aldrich). Aliquots of bacterial cultures grown upto an OD_{600} of 1.8 to 2.0 (10 ml) were harvested by centrifugation at 4°C for 10 min at 8,000 g. The bacterial pellets were

washed twice with 1 ml of PBS and then re-suspended in 0.35 ml of pyruvate assay buffer, incubated for 20 min at 80°C, and lysed using lysing matrix B tubes in a FastPrep instrument (Precellys24, Peqlab). The lysates were centrifuged at 4°C for 5 min at 13,000 g Pyruvate concentrations were determined according to the manufacturer's protocol and normalized to the corresponding viable-cell counts at the time of harvest [91].

3.5 Electron microscopy

The wild type, mutant and the complemented strains were cultured in Middlebrook 7H9 media supplemented with 10% OADC at 37°C up to an optical density (600 nm) of 2. The bacteria were processed for Tokuyasu cryo-sectioning as per the protocol from [92]. Bacteria were fixed by adding an equal volume of a concentrated fixative (8% glutaraldehyde in 4 ×fold PHEM (Pipes, Hepes, EGTA and $MgCl_2$) pH 6.9 (containing 240 mM Pipes, 100 mM HEPES, 40 mM EGTA (Ethylene glycol-bis (2-aminoethylether)-N,N,N,N-tetraacetic acid, 8 mM $MgCl_2$) to the bacterial culture medium. The bacteria after incubation of 5 minutes were pelleted and the pellet was resuspended in 2 % glutaraldehyde in PHEM, pH 6.9 and incubated for 120 min at room temperature. These fixated bacteria were then processed for examination at the transmission electron microscope (Tecnail12; FEI). as described in our previous report [82]. For each of the strains comprising about 450 fully captured bacteria were examined and the total number of intracellular lipid inclusions in the different strains was determined.

3.6 Fluorescence microscopy

The log phase bacteria (OD600nm 1.8 to 2) were pelleted by centrifugation (6000 x g for 10 min) and then washed using 1 ml phosphate-buffered saline (PBS pH 7.4, 6000 g, 10 min).The fixation was done by adding 1ml of 4% paraformaldehyde and incubating overnight. The fixed bacteria were then washed twice with PBS (pH 7.4) and were adhered on a slide using cytospin (Beckman coulter). The bacteria were stained with Nile red (25 mg in 2.5ml DMSO) (incubation at dark for 20 minutes), to visualize the lipids. Additionally Ziehl-Neelson staining (TB-color staining kit; Merck) was performed in order to visualize the whole mycobacteria. The stained slides were further examined by using confocal laser scanning microscopy (LSM 780; Carl Zeiss). As the spectra of the

Nile red and Ziehl Neelson dyes were found to overlap with each other, the spectra of the individual stains were first recorded separately and then the bacteria stained with both the dyes were imaged. Later, the ZEN2011 software (Zeiss) was employed for unmixing the overlapping spectra of both the stains.

3.7 Antibiotic susceptibility test

The densely grown bacterial cultures from Middlebrook 7H11 agar plates were sweep transferred to a centrifuge tube containing 3-4ml of sterile water,by using a cotton swab. The bacteria were resuspended well by vortexing. Then the optical density was adjusted for the resuspended culture to OD 600 nm of 0.10-0.11. After which 50 µl of the bacterial dilution suspension were added to a tube of cation adjusted Muller-Hinton broth (ThermoFisher Scientific /Oxoid/Remel) .After thorough mixing, 100 µl of the suspension were transferred to each well of the sensititre plate (Sensititre TM SLOMYCOI, plate (Thermo Scientific/Oxoid/TREK Diagnostic) comprising of different antibitiotics at different concentrations. The plates were incubated at 35°C without additional CO_2. The growth of the *M. avium* was evaluated after 7, 10 and 14 days, respectively. The growth was read both visually using a mirror as well as by using the Sensititre Vizion System (Thermo scientific, TREK Diagnostic,UK) and thus the minimal inhibitory concentration (MIC) defined as the lowest concentration showing no growth was computed for each of the strains**.**

3.8 Intracellular growth measurement

For the infection studies, buffy coats from anonymous healthy donors were obtained from the German Red Cross. The human blood derived monoctyes were isolated by the gradient method using Ficoll–Paque and Percoll (GE Healthcare) as per the manufacturer's recommendations and described elsewhere [93]. The isolated monocytes were resuspended in IMDM (Iscove's Modified Dulbecco's Media) cell culture medium supplemented with 10% human serum and distributed in 24 wells cell culture plates (TPP) with one million cellsper well and incubated overnight for adherence at 37°C with 5% CO_2. .Then the cells were activated with IFNγ (100/ml) overnight.After that the cells were infected at an MOI of 10 with the MAH strains wild type MAH 104, lysX mutant and lysX complemented

strain. Then the cells were washed with fresh media after 4 hours of infection. Following that the cells were treated for 2 hours with high concentration of amikacin (200µg/ml) in order to terminate the extracellular bacteria. The cells were washed everyday with fresh media for the removal of extracellular bacteria. The infection samples were harvested after specific time points post infection (4 hours, then every 24 hours during 7 days). The cells were lysed in 1 ml of sterile water at 37°C for 20 minutes and the lysates were collected. The intracellular bacterial numbers were quantified by diluting the sample lysates and plating in triplicates for the CFU counting.

3.9 Stress resistance tests

The resistance of the mycobacterial strains against stress by H_2O_2 (reactive oxygen species), NO stress and the effect of Human beta defensin-1 (HBD-1) was determined by 96-well microplate (nunclon) assays. Log phase bacterial cultures (OD of 1.8) grown in Middlebrook 7H9 broth were added to the wells of the microplate. The bacterial suspensions were then exposed to different concentrations (20 mM and 100 mM) of H_2O_2 and were incubated at 37°C. To measure the sensitivity towards H_2O_2, the ATP content was quantified after 4 hours and 7 hours post exposure to H_2O_2 stress. A luminescence based kit was employed for this purpose (BacTiter-Glo Microbial Cell Viability Assay, Promega) according to the manufacturer's protocol. The plates were read using a luminometer (Tristar LB 941 Multimode microplate reader, Berthold technologies) and the luminescence were recorded as relative light units (RLU). The bacterial viability was determined with stress treatment as well as without stress treatment so as to measure the percentage survival for each strain.

The bacterial strains were also exposed to a NO donor, DETA/NO (diethylenetriamine/nitric oxide adduct), of 25 mM concentration for 4 hours incubation. As in the case of H_2O_2 susceptibility test which is described above, the difference in survival percent between the MAH strains was determined in the same manner.

The phenotypic susceptibility of the MAH strains towards host inductive defensins was tested by exposing the bacterial cultures to 0.5 µg/ml and 1µg/ml of HBD-1 . Since the defensin was soluble only in 0.01% acetic acid, the acetic acid was also added to the

controls. The growth inhibitory activity of the defensin was also evaluated using ATP measurement as explained in the above stress resistance tests.

3.10 Cytokine measurement in infected human PBMC

Peripheral blood monocytes (PBMCs) were isolated from human buffy coats from healthy donors using Ficoll-Paque (GE Healthcare) differential gradient centrifugation method, according the protocol recommended by the manufacturer and described previously in [93]. 24-well cell culture plates (TTP) were used for the infection experiment, where one million cells were seeded in each well. The cells were maintained at 37°C with 5% CO_2 for 24 hours before infection. The PBMCs were stimulated with the MAH strains (wild type, lysX mutant and lysX complemented) at a MOI of 10. Negative controls (uninfected cells) were also included in the study. The infection experiment was monitored for a course of seven days post infection and culture supernatants were harvested after particular time points (24 hours and 120 hours post infection). The cytokine released in response to the infection was measured by conducting ELISA assay with the infection supernatants (in appropriate dilutions, eg. 1:10 for TNFα) , as per the instructions of the manufacturer (Human IL-1β, IL-10, TNFα and IL-12 (P40) ELISA Ready – SET-Go! Kit, Thermo Fischer Scientific).

3.11 Evaluation of macrophage fusion during MAH infection

The fusion rate of macrophages upon infection was determined by employing human blood derived monocytes extracted from human buffy coats (from healthy individuals) as described previously in [94]. The isolated monocytes were pre-activated with IFNγ (100 units/ml)overnight and then were infected with the MAH strains at a MOI of 10. Special microscopic ibidi cell culture dishes (ibidi GmbH) were used for these infection experiments. These dishes were embedded with labelled grids and this was helpful for an accurate quantification of the multinucleated giant cells (MGCs). Additionally the cell culture dishes also facilitated an improvised optical quality for a high resolution microscopy.

The infection course was investigated for 7 days to spot the fusion events and the infection samples were fixed with 4% paraformaldehyde at the 5^{th} day post infection (desirable

timepoint). Uninfected cells were used as negative control. The samples were double stained with the lipophilic stain Nile red (25 mg/ml) and the nucleic acid specific DAPI stain (5 mg/ml (stock), 1:100 diluted in dimethyl sulfoxide). After staining for 20 minutes in the dark, the samples were washed with sterile water and then were examined using a confocal laser scanning microscope (LSM 780; Carl Zeiss). Specific grids were selected at different areas of the cell culture dish and the total number nuclei as well as the nuclei in the MGCs were counted for each sample. At least 500 nuclei were counted for every preparation and the fusion index (FI) was computed with the formula mentioned below: (ref:[94])

$$FI\% = \frac{\text{Number of nuclei in multinucleated cells}}{\text{Total number of nuclei}} \times 100$$

3.12 In vivo study using *Galleria mellonella*

An invertebrate infection model, *Galleria mellonella* (Greater wax moth) was used for survival experiments to check the virulence of the MAH strains. The larvae were received in boxes (140-200 numbers from the in-house animal breeding facility (MF3 division) at the Robert Koch Institute. Only the healthy looking larvae with a pale colour without any dark shade and those which weighed around 250 mg were selected for the experimental purpose. The larvae chosen for the study were placed overnight in a 37°C incubator before infection The bacterial inoculum was prepared by washing and diluting in sterile PBS supplemented with Tween 80 to give the appropriate infection dosage of 10^6 bacteria per larvae. The larvae were injected into one of the last set of prolegs with 20 µl of the prepared inoculum (n= 30 larvae per group) using a 30G insulin syringe needle (Omnican, Braun). Safe handling of the syringe was accomplished by handling the worms using forceps. The infected worms were placed individually in 12-well cell culture plates (TPP) in an alternative manner to prevent any transfer of material between the neighboring infected larvae. Woodchips were also added to the wells. The plates were tightly taped and then placed in a sealed plastic box for incubation at 37°C. Throughout the course of

infection (about 20 days), the wax worms were inspected daily for phenotypic changes. The events of death and pupation were recorded accordingly. Graph pad prism was used to perform the survival analysis.

To measure the growth of the bacteria in vivo, the infected larvae (3-5 per strain), which were still alive, were freeze-killed by incubating at -20°C overnight. A set of larvae were sacrificed immediately after infection, in order to check for contamination if any and to confirm equal infection doses. Then an equal number of larvae were sacrificed at different infection time points (5^{th} and 10^{th} day post infection). The surfaces of freeze-killed larvae were disinfected with 70% ethanol and then the larvae were homogenized with glass beads (0.11 mm diameter, Sartorius) in PBS-Tween 80, using the Precelly-24 tissue homogenizer (Peqlab). The survival of the MAH strains was determined by plating the serially diluted homogenized larvae material on to Middlebrook 7H11 agar plates supplemented with cycloheximide (25 µg/ml) and vancomycin (2 µg/ml) (Sigma). These antibiotics were added to the agar plates in order to inhibit the growth of the intrinsic bacterial and fungal flora found in *G. melonella*. Finally, the mean CFU for each of the strain was calculated for the enumeration of intracellular bacteria.

3.13 Extraction of glycopeptidolipids (GPL)

The MAH strains were grown to log phase (OD_{600} of 1.8-2-0) in Middlebrook 7H9 broth (Becton Dickinson) with 0.05% of Tween 80 and supplemented with modified ADC at 37°C. The harvested bacteria were washed three times, heat killed and frozen at -80°C until use. The extraction of total lipids and GPL purification were performed as previously explained in [95, 96]. For total lipids, the dried bacterial pellets (from 50 ml culture) were treated with 10 ml of choloroform-methanol mixture (2:1; vol/vol) and were ultra-sonicated (Branson sonifier-450 D, G. Heinemann) with 100% power for a minute. After centrifugation (8000 g for 10 minutes), the liquid phase obtained was transferred to a separate tube and then was hydrolyzed by adding 0.2 N NaOH in methanol (3 ml each). To remove the alkali–labile lipids, the reaction mixture was incubated at 40° C in a water bath for 2 hours with vortexing from time to time. Then the GPL was purified by neutralizing the lipid extract to pH 7 with 6 N HCl and 1 M NaOH. Then chloroform (6 ml) and water (5 ml) were added one after the other with intensive shaking. The phase-separation was achieved by centrifugation (8000 g for 10 minutes) and the bottom phase containing the

GPL was collected and evaporated. The GPL extracted was dissolved in 1ml of chloroform–methanol mixture (2:1 ; vol/vol) and then the GPL preparations were loaded on to silica coated TLC plates (Analtech). The GPL expression pattern was scrutinized by performing thin layer chromatography (TLC) in a chloroform-methanol (90:10; vol/vol) solvent system. The plates were sprayed with 10% H_2S0_4 in ethanol and then exposed to hot-air to visualize the GPL bands.

3.14 Measurement of GPL-Antigenic reactivity using ELISA assay

The MAH GPL extracts diluted in PBS (1:1000) were deposited (100 µl/well) in a polystyrene microplate well (Nunc-Maxisorp, Thermo fischer scientific). Then the plates were sealed and incubated overnight at 4°C. For the ELISA, blocking was done by adding 3% BSA in PBS (200 µl/well) and incubating overnight at 4° C. After that the wells were flipped and washed twice using PBS followed by the addition of serum from MAH infected patients as well as healthy individuals (approval from the ethics committee of the Charite – Universitätsmedizin Berlin (EA2/093/12). The sera were diluted (1:1000) in 1% BSA (dissolved in PBS) and were added (100 µl/well) to the appropriate wells. GPLs in the absence of serum were employed as negative controls. After an hour of incubation at room temperature, PBS-Tween 20 was used to wash the plate (five times) and then the secondary antibody, Horseradish peroxidase (HRP)-goat anti-human IgG (Jackson Antibodies)(diluted (1:5000) in 1%BSA dissolved in PBS) was added to each of the wells (100 µl/well). Post incubation (1 hour at room temperature), the plates were washed again for five times with PBS-Tween 20 and then with PBS twice. Finally, the TMB ELISA substrate (Sera care) was added (90 µl/well) to the wells and after ten minutes, the reaction was stopped using 0.16 M H_2SO_4 (90 µl/well). The absorbance value was measured in a microplate reader (Infinite M200 PRO, Tecan) at a wavelength of 450nm.

4 Results

The target gene *lysX* was phenotypically characterized under extracellular conditions in the first part of the study. Initially, we analyzed the influence of the gene with respect to the protein expression, metabolism, antibiotic resistance and its impact on the capacity to multiply in human monocyte-derived macrophages [82].

The second part of the study was focused on the role of the *lysX* gene in MAH pathogenesis. Here, we examined the effect of the mutation during MAH infection of the host by measuring the reactivity against host defense mechanisms (ROS, RNI, defensins), inflammatory responses and survival in vivo.

4.1 Proteomic analysis of the MAH strains

In order to analyze the impact of the gene *lysX* on the protein expression pattern, we applied a proteomic approach and quantified the protein expression changes between the wild type, the mutant lysXmut and the complemented strain lysXcomp containing an intact copy of *lysX* [81]. Orbitrap analysis was performed on six biological replicates (independent broth cultures) of each of the three strains. Label-free proteomic analyses involved trypsin digestion and the separation of peptides was done by liquid chromatography (LC) coupled to electrospray ionization. Peptide analysis applying mass spectrometry unfolded certain interesting expression patterns showing proteome level differences between the three strains of MAH (Supplementary Table S1).

In total, 1347 mycobacterial proteins were identified out of which 282 proteins were differentially expressed in the lysX mutant when compared to the wild type strain. Of these 282 proteins, 169 were upregulated in the mutant and 113 were downregulated. The results of the statistical analysis for all identified proteins are listed in Table S1 in the supplementary material. The differentially expressed proteins in the lysX mutant were analyzed and segregated based on their functional categories using a database of Clusters of Orthologous Groups of proteins (COGs). This database helps in phylogenetic classification of the proteins from completely sequenced genomes on the basis of the orthology concept [97]. The proteins were distributed in 15 different COG categories but nevertheless there were still many which were poorly characterized or uncharacterized

(Fig. 1). Amongst the groups, a majority of the genes (57%) were found to be involved in metabolism, in particular in the lipid transport and metabolism. This already indicates the influence of the *lysX* gene on the metabolic activity of MAH.

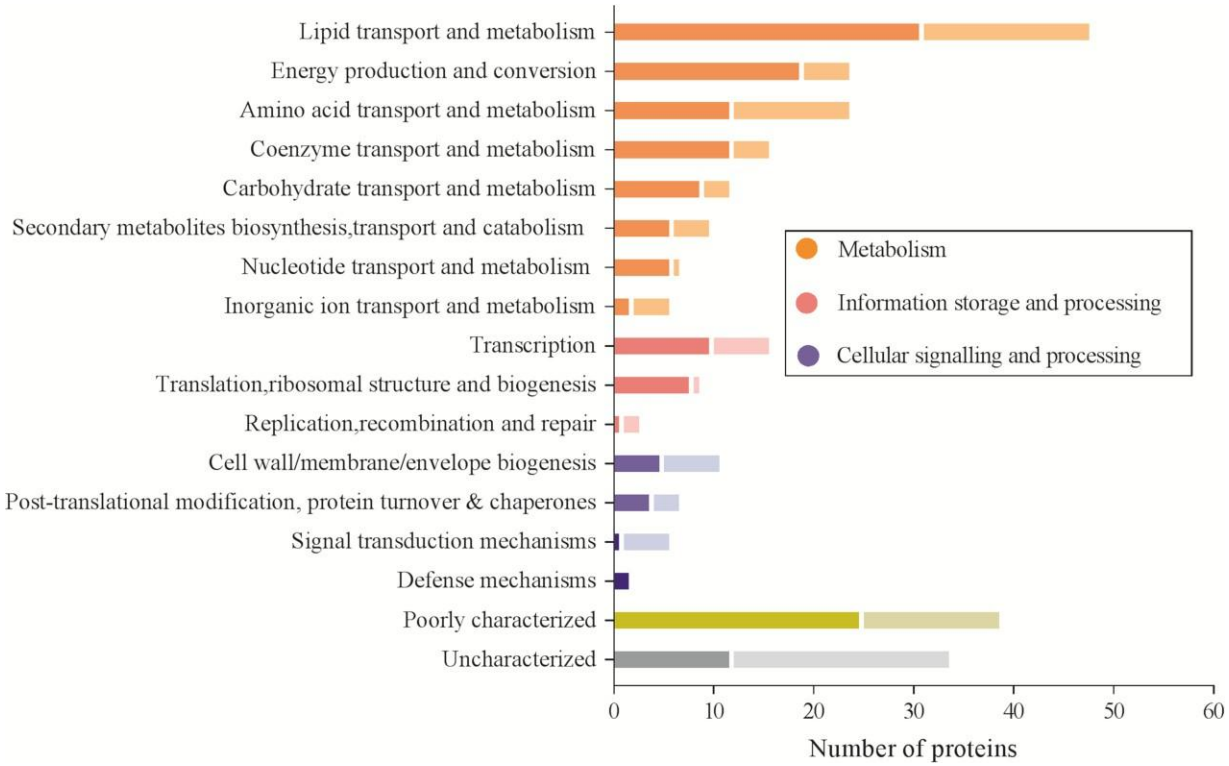

Figure 1: COG classification of differentially expressed proteins in lysX mutant compared to wild type (MAH 104). *The proteins identified from the proteomic analysis were classified based on their functional orthologues and the COG categories are indicated in specific colors. The darker shade of the bars indicates upregulated proteins and the lighter shade indicate downregulated proteins.*

DAVID enrichment analysis [98] was performed with the set of genes upregulated in the mutant and with the set of genes downregulated in the mutant to classify the pathways affected by the mutation. DAVID offers an individual gene pathway analysis and our data resulted in seven pathways from the list of upregulated proteins and three pathways were related to downregulated proteins. Tricarboxylic acid cycle, Biosynthesis of secondary metabolites, Fatty acid metabolism, Proponoate metabolism and Butanoate metabolism were the ones which contained the highest percentage of genes involved, having the highest enrichment scores (Supplementary Table S2a). Particularly, three of these pathways (Fatty acid metabolism, Proponoate metabolism and Butanoate metabolism) were accounted to be related with 60% of the differentially regulated genes in the mutant

strain. In order to generate energy and for the sake of lipid synthesis, the mycobacteria degrade the fatty acid and cholesterol into short chain fatty acids (eg. Acetate and propionate)[99]. The assimilation of short chain fatty acids involving the proponoate metabolism is considered to be crucial for the survival and virulence of MTB[100] . A recent study on the metabolic phenotyping of MAH isolates from different sources also revealed the butyric acid and propionic acid to be the most preferred carbon source[88].

The STRING database was also used for analysis of the same data sets as used for DAVID to have an overview of the proteome-scale interaction network .The STRING analysis provided us an interactome network which predicted the protein-protein interactions and their functional associations [101]. We found that the proteins upregulated in the lysXmut were involved in 18 pathways and the downregulated proteins were linked to three pathways. The output from STRING analysis was coincidental with that of the results from DAVID .Totally, seven pathways from the upregulated genes and two pathways from the downregulated genes were identical for both DAVID and STRING analysis while the rest of the pathways were also found in both of the analysis but the level of significance was varied (Supplementary Table S2b).The differentially expressed proteins were mapped using KEGG pathway database, specifically in functional pathways of *M. avium* . On pooling all the affected pathways we identified many enzymes being involved in the central metabolism, also in the adaptive pathways which are essential for the growth and survival of MAH during infection of the host (for eg. β-oxidation of fatty acids and glyoxylate cycle) (Fig. 2).

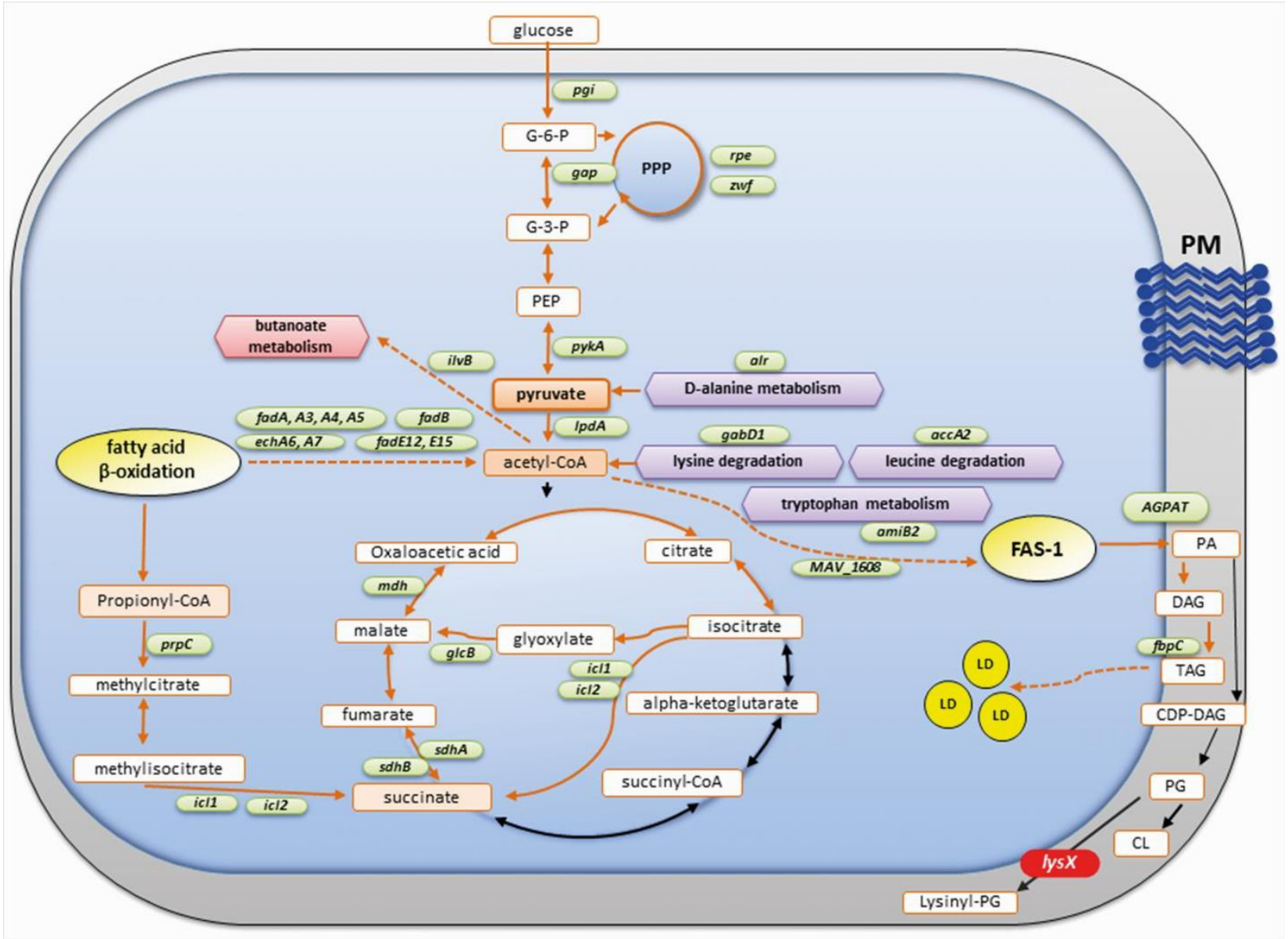
glucose
pgi
G-6-P
PPP
rpe
zwf
gap
G-3-P
PEP
pykA
butanoate metabolism
ilvB
alr
D-alanine metabolism
pyruvate
lpdA
fadA, A3, A4, A5
fadB
echA6, A7
fadE12, E15
fatty acid β-oxidation
gabD1
accA2
lysine degradation
leucine degradation
acetyl-CoA
tryptophan metabolism
amiB2
MAV_1608
Oxaloacetic acid
citrate
mdh
malate
glyoxylate
isocitrate
glcB
icl1
icl2
alpha-ketoglutarate
fumarate
sdhA
sdhB
succinyl-CoA
succinate
Propionyl-CoA
prpC
methylcitrate
methylisocitrate
icl1
icl2
PM
AGPAT
FAS-1
PA
DAG
fbpC
TAG
LD
LD
LD
CDP-DAG
PG
CL
lysX
Lysinyl-PG

Figure 2: Pathway network of the central metabolism of MAH with differentially regulated genes. *Proteomic analysis was conducted for MAH 104, lysX mutant and lysX complemented strains. This figure is a schematic diagram showing changes in the expression of enzymes in the biosynthetic pathways that are affected by the lysX mutation. The enriched pathways in the lysX mutant are marked with brown arrows (according to DAVID and STRING analysis). The metabolites which are predicted to be overproduced (eg. Pyruvate) are shown by filled-in brown boxes. The mutated lysX gene is indicated in red. The intracellular lipid droplets (LD) are marked in yellow. The bacterial plasma membrane (PM) is represented as the surrounding gray area. G-6-P, glyceraldehyde 6-phosphate; PPP, pentose phosphate pathway; PEP, phosphenolpyruvate; FAS-1, fatty acid synthase-1; TAG, triacylglycerol; AGPAT, 1-acylglycerol-3-phosphate O-acytransferase; CDP-DAG, cytidine diphosphate diacylglycerol; PA, phosphatidic acid; PG, phosphatidylglycerol; CL, cardiolipin.*

We also compared the differentially regulated genes in the lysX mutant with a list of mycobacterial genes which are differentially expressed during infection of human macrophages from other research studies [65, 102-104]. This analysis revealed that out of the 282 differentially regulated proteins, 65 proteins were identified to be related with the intracellular survival in the host (Supplementary Table 3). Among those listed, some of the virulence factors of MTB were also identified: isocitrate lyase icl (glyoxylate cycle) [105], choD and fadE29 (cholesterol catabolism), lpqH and pstS1(lipoproteins), rmlB2 and murC (cell wall modifier), ahpC, katG and ndk (resistance towards reactive oxygen and reactive nitrogen species), nuoG and pknD (inhibition of apoptosis), sigA (sigma factor) and phoP (2-component system) [106].

4.2 Metabolic phenotype characterization

Since the *lysX* mutation was found to have an effect on the bacterial metabolism, we analyzed the capacity of metabolizing different substrates in the wild-type and lysX mutant. A high throughput phenotypic microarray analysis (BIOLOG) was applied for this purpose. The BIOLOG sytem measures the respiration of bacteria in the presence of different substrates. The usage of 379 substrates was tested, which contained 190 carbon, 95 nitrogen, 59 phosphorus and 35 sulphur substrates. In total 335 out of these 379 substrates were not metabolized by both the strains and only 6 of them were utilized by

both the wild type and the mutant strains (Supplementary Table S4). In comparison, 15 substrates were differentially metabolized by the strains. The differential utilization of these substrates by the two strains is displayed in the heat map in Fig.3. Significant differences were observed between the strains lysXmut and the wild type for the usage of Acetic acid and Pyruvic acid. Analysis using the "Kegg pathway database" revealed that Acetic acid was involved in Glycolysis, Pyruvate metabolism, Proponoate metabolism and others, while the Pyruvic acid was involved in Tricarboxylic acid cycle, Glycolysis, Pentose phosphate pathway, Benzoate degradation, Pyruvate metabolism, D-alanine metabolism and others. The pathways identified by the Kegg pathway analysis correlated with the pathways enriched according to DAVID and STRING using the data from the proteomic data analysis (Supplementary Tables 5).

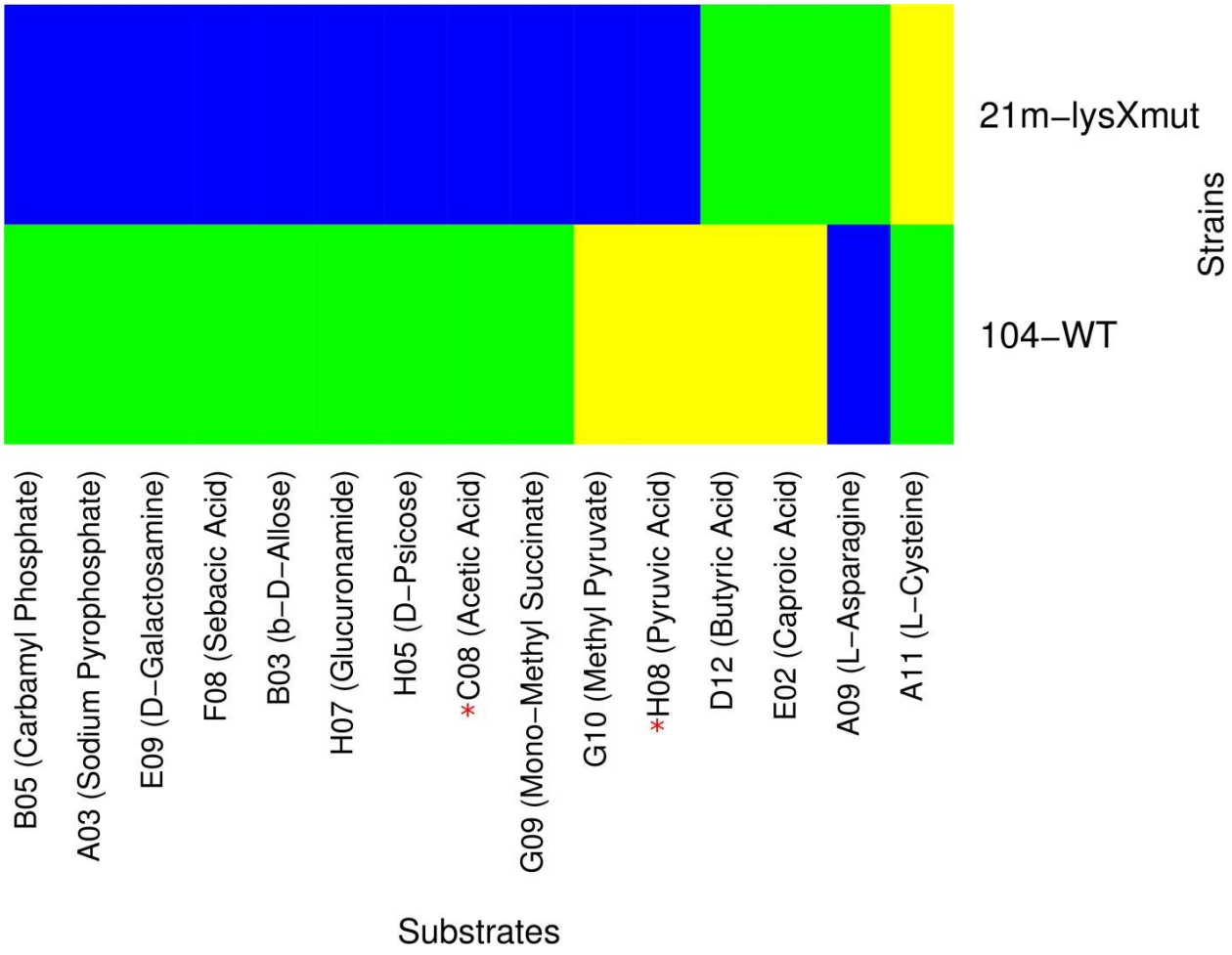

Figure 3: Heatmap showing the 15 substrates that were differently metabolized by the wild type (104-WT) and lysX mutant (21m-lysXmut) strain. *The color key scale for the substrate is based on the dye reduction quantified by Omnilog units. The yellow color denotes strongly positive substrate metabolization, green color denotes moderate*

metabolization and blue color refers to no substrate metabolization. Substrates which showed a statistically significant metabolization are marked with red stars.

Pyruvate is a key metabolite and plays a major role in carbon metabolism and since the BIOLOG assays had shown that the mutant cannot use Pyruvate, the intracellular pyruvate concentrations in the wild type, lysXmut and lysXcomp strains was measured using the Pyruvate Assay Kit (Sigma-Aldrich) (Fig.2b). As anticipated, the *lysX* mutation led to the accumulation of pyruvate in the mutant; and the mutant showed a double fold increase in pyruvate concentration when compared to the wild type and complemented strains.

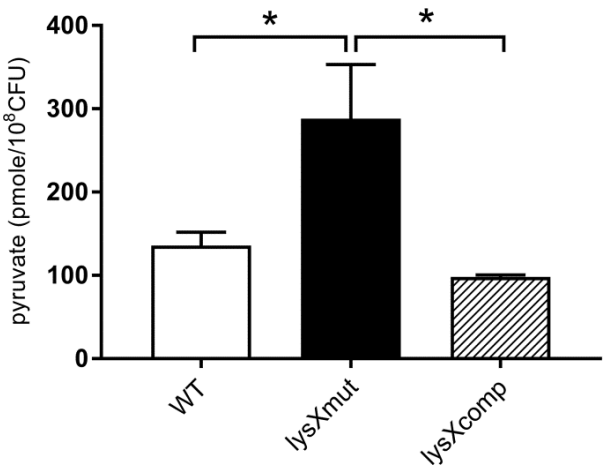

Figure 4: Intracellular pyruvate quantification. *Pyruvate assay kit (Sigma-Aldrich) was used to determine the concentration of pyruvate in the bacterial strains cultured in Middlebrook 7H9 broth with 0.05% Tween 80 and supplemented with 10% modified ADC. CFU,colony forming units. Data are means ± standard deviation of the results from three independent experiments.* $^{*}P < 0.05$*, by two-tailed, paired Student T-test.*

4.3 Structural examination of MAH strains

Our proteome analysis had shown an upregulation of metabolic steps required for TAG synthesis in the mutant. TAG is stored in lipid bodies of mycobacteria and we therefore intended to visualize lipid bodies in the analysed strains. We wanted to see if there were any consequences that would be visible as a result of this deviation in metabolism. Hence, the densely grown cultures were processed for transmission electron microscopy for studying the structural features of the strains. Interestingly, the lysXmut strain displayed a

higher number of lipid-like vacuoles in the cytoplasm in comparison to wild type and the complemented strains (Fig. 5a, 5b, 5c). The lipid inclusions were quantified by counting 450 bacteria per strain at the microscope. The quantification confirmed that the mutant strain with 31.7% comprised of the highest percentage of bacterial cells containing lipid inclusions, while in the case of wild type and the complemented strain only 15% and 24.3% of the cells contained lipid inclusion. (Fig. 5g)

In order to confirm whether these inclusions were truly lipids, fluorescence staining with a neutral lipid stain (Nile red) was performed. In the staining, the lysX mutant was found to show a more intensive staining pattern as when compared to the wild type and the lysX complemented strains (Fig. 5d, 5e, 5f).

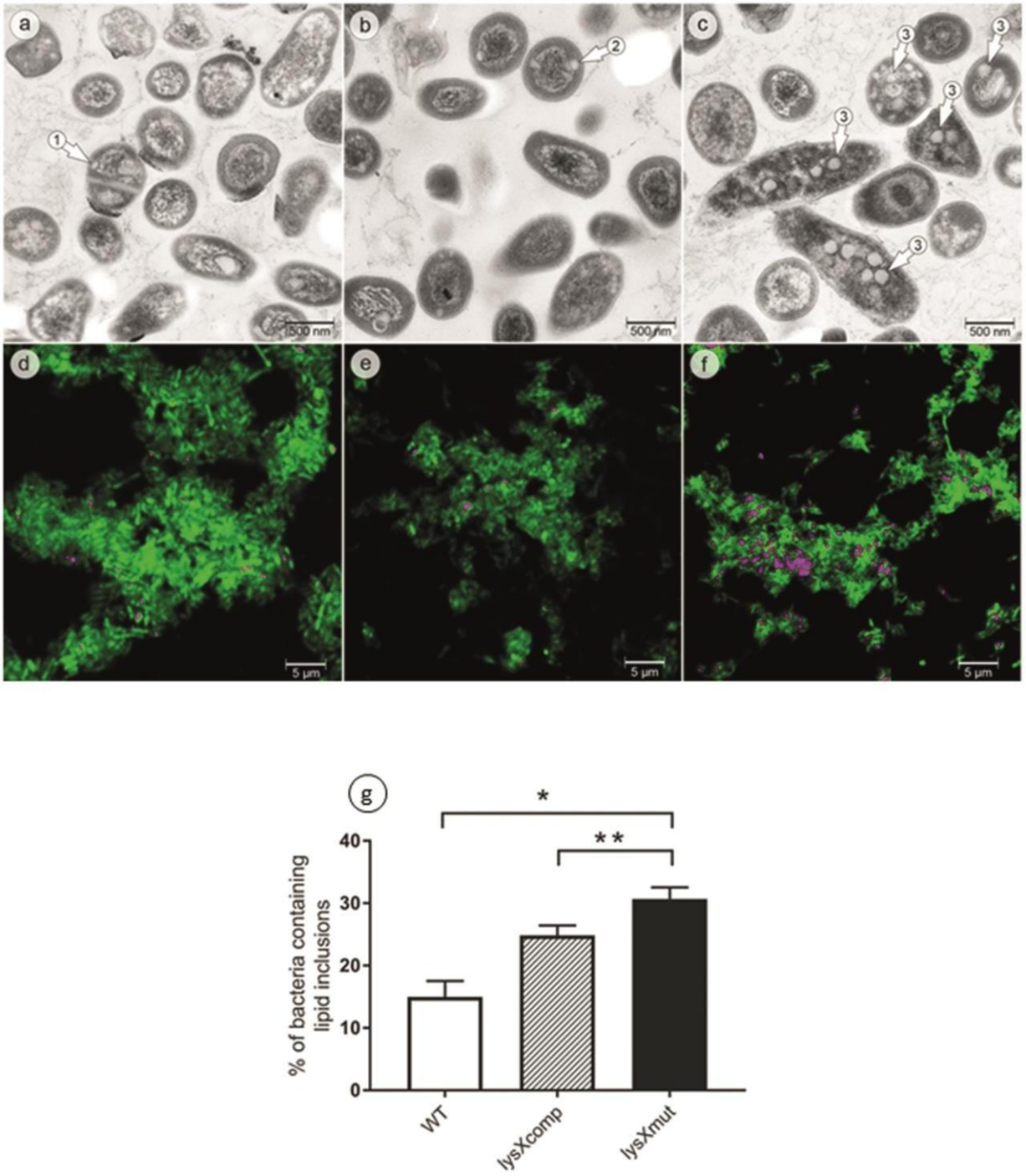

Figure 5: Representative images of the bacterial strains showing lipid accumulation. *Transmission electron microscopy (TEM) pictures of M.avium strains cultured at 37°C (wild type (a); lysX complement (b); lysX mutant (c)), The white arrowheads point towards the lipid bodies. lysX mutant (c) exhibited an accumulation of lipid inclusions; Fluorescence microscopic images of Nile red staining of the strains -wild type (d), lysX complement (e), and lysX mutant (f) for visualization of the lipid content. The violet fluorescence shows Nile red staining of intracellular bacterial lipids and the green*

*fluorescence indicate the stained mycobacteria. The lysX mutant (f) was found to be stained brighter than the wild type (d) and lysXcomp (e) strains. The images were taken with a confocal laser scanning microscope at 100× magnification with scale bars representing 5 μm. Fig.5g: The lipid inclusions were quantified by counting 450cells per strain at the microscope and the percentage of cells with lipid inclusions were determined. It was found that the mutant strain comprised of the highest percentage of lipid-like vacuoles (Fig.5g). Data are means ± standard deviation of the results from three independent experiments. *P<0.05 and **P<0.01 by two tailed Student T-test.*

4.4 Antibiotic susceptibility testing of the MAH strains:

The LysX is involved in the neutralization of the negative charge of the bacterial cell membrane, which decreases the membrane permeability and susceptibility towards cationic antimicrobial peptides and antibiotics. Hence, we tested the impact of LysX mutation on the antibiotic susceptibility of our strains by measuring the MIC values for 14 clinically relevant antibiotics. The lysX mutant displayed a significant difference in the susceptibility towards clarithromycin, ethambutol and streptomycin in comparison to the other strains. The mutant strain exhibited hypersensitivity to the above mentioned cationic antibiotics which is an evidence of the *lysX* mutation affecting the membrane properties (Table 1).

Table 1: Antibiotic susceptibility of the *M. avium* strains wild type104, lysX mutant (lysXmut) and lysX complement (lysXcomp)

Antimicrobial agents	MIC (µg/mL) WT	lysXmut	lysXComp
Aminoglyoside			
Amikacin	30	5.5	30
Streptomycin**	36	16	32
Tetracycline			
Doxycycline	>16	>16	>16
Macrolide			
Clarithromycin**	2.5	1.06	1
Oxazolidinone			
Linezolid	44	24	16
Quinolone			
Ciprofloxacin	9	4	7
Moxifloxacin	2.25	1	2
Sulfonamide			
Sulfamethoxazole/ Trimethoprim	90.25/4.75	90.25/4.75	52.25/2.75
Anti-mycobacterial			
Ethambutol*	9	1.37	5.5
Ethionamide	2.46	2.17	1.85
Isoniazid	5.5	5.5	2
Rifabutin	<=0.25	<=0.25	<=0.25

The values are the means of four independent experiments.

[a]MIC – Minimal Inhibitory Concentration

Statistical analysis was done by Student's t test. $P < 0.05$ was considered as significant (*) and $P<0.01$ was considered as very significant (**).

4.5 Intracellular survival of MAH strains in human blood monocytes

We examined whether our lysX mutant was also sensitive to the positively charged CAMPs such as polymyxinB (PMB) and to lysozyme. Similar to the results seen with the cationic antibiotics, PMB and lysozyme significantly reduced the viability of lysX mutant compared to the wild type and lysX complemented strain (data not shown).Since antimicrobial peptides synthesized by macrophages play an important role in fighting mycobacterial infections, we were interested in exploring the capacity of the lysX mutant to replicate within human monocyte-derived cells. IFN-γ activated human blood derived monocytes were infected with the wild type, lysX mutant and the lysX complemented strains. The growth of the intracellular mycobacteria were quantified by lysing the infected macrophages and by plating colonies at a particular time course of incubation post infection. The three strains initially showed a uniform decrease in numbers but later they continued to grow constantly. At 96 hours post infection, a sudden elevation of bacterial numbers was found in the lysX mutant (Fig. 4). These results suggest that the lysX mutant strain has a similar capacity to grow in culture (data not shown) as well as a similar rate of infectivity like the wild type strain, but that it has a greater capacity to proliferate within host cells.

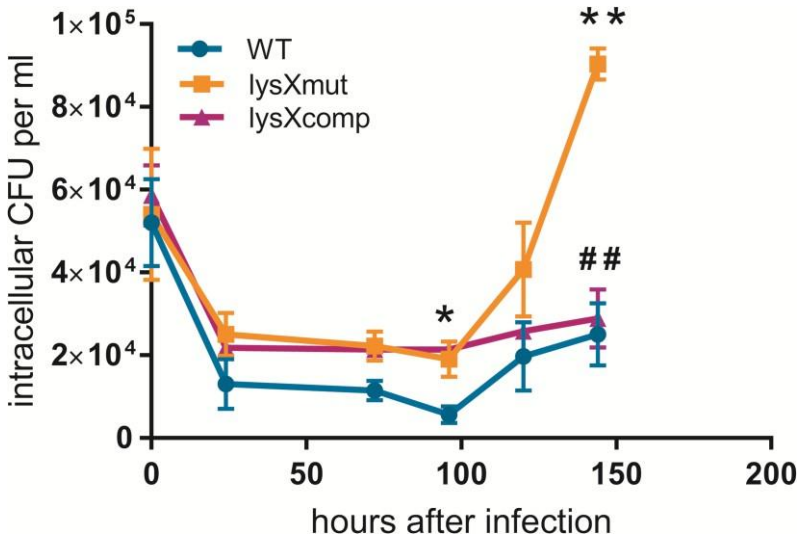

Figure 6: Growth of the *M. avium* strains in monocyte derived macrophages . *Human blood monocytes (1.0x10^6) from healthy volunteers were infected (MOI 10) with the wild-type, lysXmut and the lysXcomp strains. Intracellular bacteria were quantified at the indicated times following infection by lysis of the macrophages and the viability of the*

mycobacteria was determined by CFU counting. The mutant exhibited a significant growth after 96 hours from infection. Data are representative of three independent experiments (three buffy coats). **P<0.05, **P<0.01,* $^{\#\#}$*P<0.01 (* lysX mut vs wild type; # lysX mut vs lysX comp) by two tailed Student T-test.*

4.6 Effect of H_2O_2, NO and defensins on the growth and viability of MAH strains

As we had witnessed the enhanced intracellular growth of the lysX mutant, it was suggested to identify the underlying mechanisms which enabled the mutant bacteria to exhibit a virulent phenotype. The production of reactive oxygen and nitrogen intermediates by activated macrophages is a critical part of the human innate immune response during the infection process. Our MAH strains grown up to a mid-logarithmic phase were treated with hydrogen peroxide of 20 mM and 100 mM concentrations. After 4 hours and 7 hours of incubation, the ATP content was quantified using the BacTiter-Glo™ Microbial Cell Viability Assay with relative light units (RLU). Amongst the three strains, the lysX mutant was found to show a substantial decrease in cell viability (Fig 5a). Considering the untreated to have a 100% RLU, on the exposure to 20mM H_2O_2 the wild type reduced to 36% but the mutant reduced to 17% showing a significant difference in sensitivity. The sensitivity of the strains was also tested with a NO donor (25 mM DETA/NO) treatment. The ATP quantification only showed a minor difference between the strains, with the wild type exihibiting a decrease to 51% and 42% by the lysX mutant strain. However, the lysX mutant proved to be the most sensitive to NO exposure (Fig 5b).

Since the *lysX* gene is involved in the modification of cell surface charge, which in turn is associated with the CAMP resistance, we intended to investigate the effect of defensin, an antimicrobial peptide,a on the strains. The Human Beta Defensin–I (HBD-I) which belongs to the cationic antimicrobial peptide family was used for this purpose. When the bacterial strains were treated with HBD-1 with a concentration of 0.5 µg/ml, all the strains displayed a strong reduction in cell viability after 120 hours of post incubation. However by comparing the ATP content with the untreated (100% RLU) control, the wild type reduced to a value of 17%, lysX mutant to 10% and the lysX complemented strain to 21% (Fig 5c). Thus we could see an effect of the lysX mutation on resistance towards defensins in MAH.

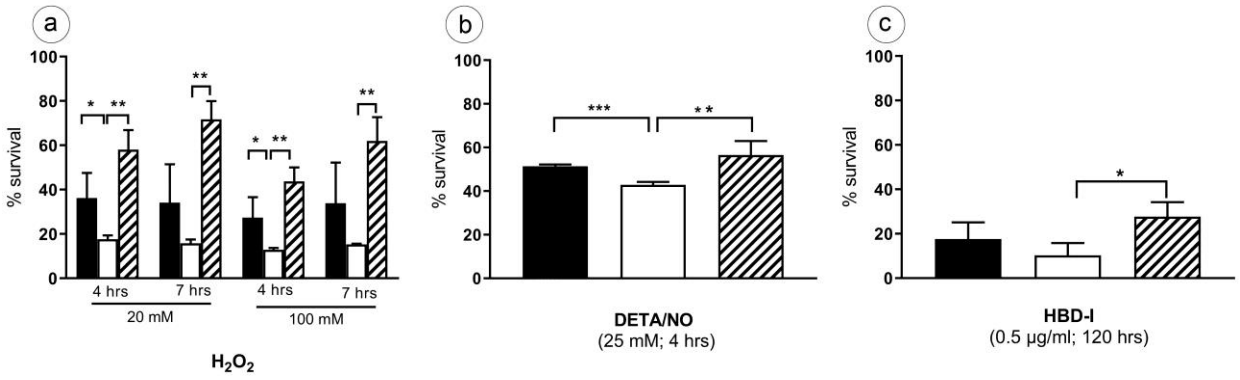

Figure 7: Effect of H_2O_2, NO and defensin (Human Beta Defensin-1) stress on survival of the MAH strains. *The three strains (wild type (MAH 104) (black bar), lysX mutant (open bar) and lysX complemented strain (striped bar)) were incubated with a) 20 mM and 100 mM H_2O_2 for 4 hours and 7 hours or (b) 25 mM DETA/NO for 4 hours or (c) 0.5 µg/ml Human Beta Defensin-1 for 5 days and the sensitivity towards the stresses was determined through survival percent calculation by measuring ATP production using luminescence assay kit (BacTiter-Glo Microbial Cell Viability Assay, Promega). Data are means ± standard deviation of the results from three independent experiments, (performed in triplicates with three individual cultures per strain). *P < 0.05; **P < 0.01; *** P < 0.0001; two-tailed, unpaired Student's t test.*

4.7 Cytokine responses of human PBMCs infected with *M. avium strains*

Mycobacterial infections induces the host immune cells to produce inflammatory cytokines such as tumor necrosis factor-alpha (TNF-α), IL-6 and IL-10. In view of the improved survival of the lysX mutant in human monocytes, we aimed to examine the inflammatory response produced during the infection of the host cells with our MAH strains. PBMCs were infected with the wild type, mutant and the complemented strains (MOI 10) and the secretion of selected cytokines was investigated in the course of infection for five days post infection. Culture supernatants were collected at particular time points (24 hours and 120 hours post infection (120 hrs was the time point wherein the lysX mutant showed a sudden elevation in the intracellular growth in monocytes [82]). The cytokines (pro-inflammatory: IL-1β, IL-12(p40) and TNF-α; anti-inflammatory: IL-10) released were quantified using ELISA assay. Overall, the lysX mutant showed the highest inflammatory cytokine secretion in every kind, when compared to the wild type and the lysX complemented

strains (Fig. 6a, 6b, 6c and 6d). Although the difference in the TNF-α secretion was not as significant as the others, still they were overproduced in the lysX mutant. The differences in the cytokine release were more evident after 24 hours compared to the 120 hours infection time point.

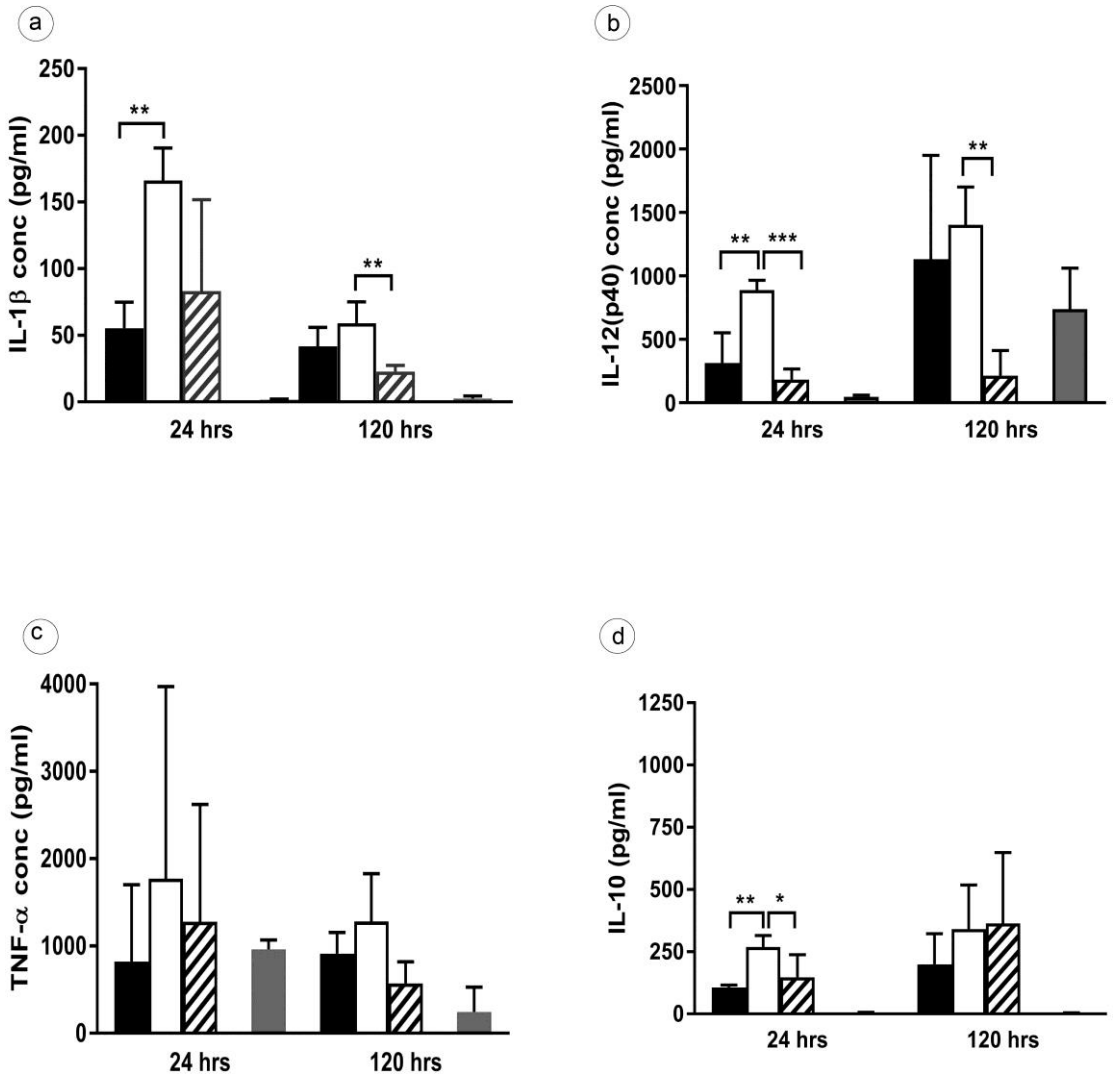

Figure 8: Induction of cytokine secretion by human blood derived PBMCs after infection with the MAH strains *Human PBMCs were infected (MOI 10) with wild type (Black bar), lysX mutant (Open bar), lysX complemented strain (striped bar). After 24 hours and 120 hours post infection, cytokines IL-1β (a), IL- 12 (b), TNF-α (c) and IL-10 (d) from supernatants were measured by ELISA using kits (ELISA Ready-SET-Go! Kit,*

*Thermo Fischer Scientific). Uninfected cells were used as controls (grey). Data are means ± standard deviation of the results from three independent experiments (using three buffy coats). *P < 0.05; **P < 0.01; *** P < 0.0001; two-tailed, unpaired Student's t test.*

4.8 Multinucleated giant cell formation on macrophage infection with MAH strains

During chronic mycobacterial infections, the infected macrophages fuse to form multi-nucleated giant cells which are stated as a hallmark granulomatous inflammatory structure. So, we were interested in analyzing the effect of the *lysX* mutation on the macrophage fusion process, as it was already revealed to induce severe inflammatory responses. The human blood derived monocytes were infected with the three bacterial strains (MOI 10) and the giant cell formation was examined for five days post infection. Infected cells were fixed at a particular time point (fifth day after infection), stained with Nile red and DAPI and were examined for macrophage fusion events by fluorescence microscopy (Fig. 9a, 9b and 9c). The fusion index (FI) was calculated for each of the strains by counting the nuclei in fused and not-fused cells (Fig 9d). The lysX mutant showed a higher amount of fusion events with an FI of 23%, while wild type and the lysX complemented strains caused an FI of 14% and 9%, respectively. The uninfected controls had a FI below 5%.

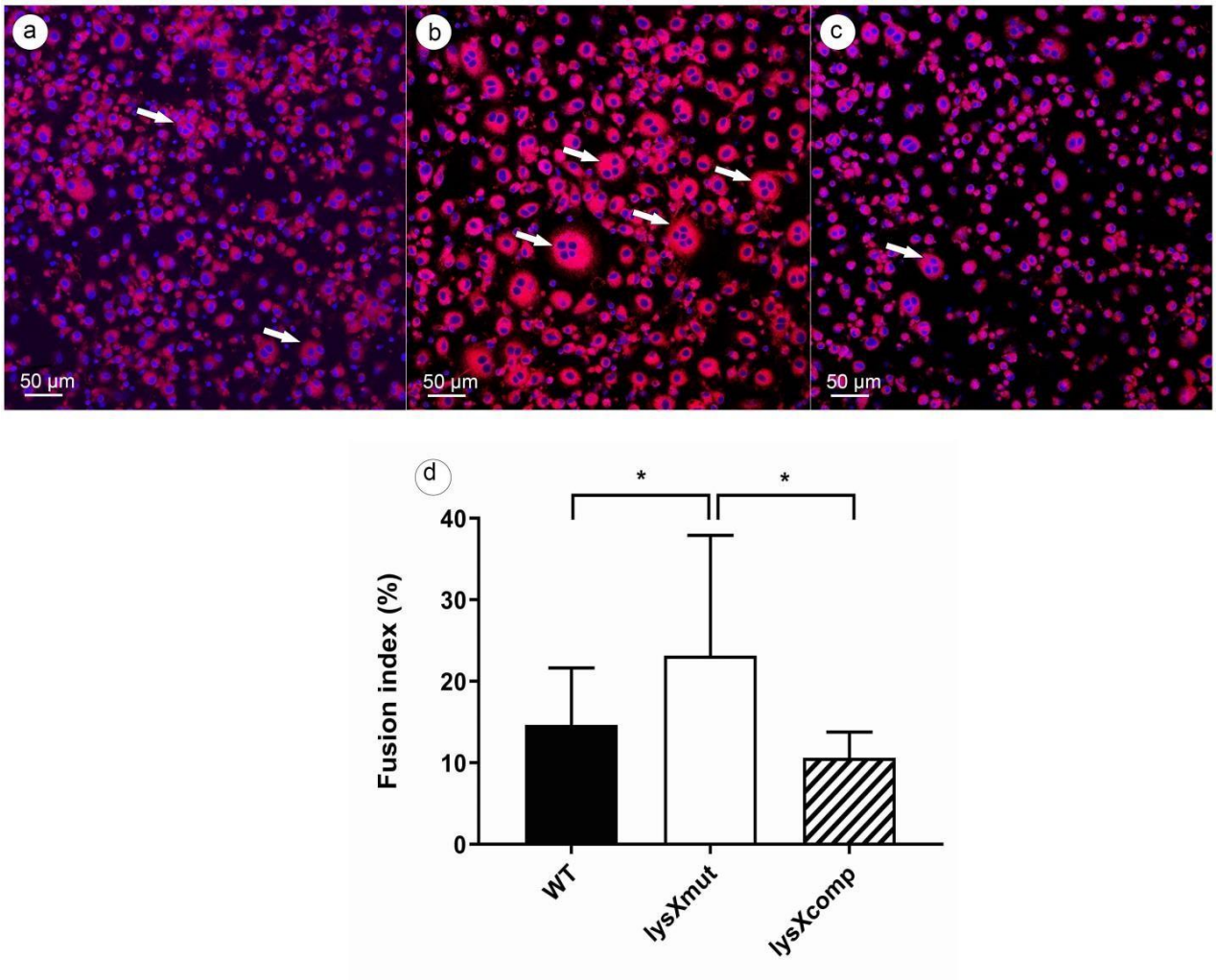

Figure 9: Microscopic examination and quantification of multinucleated giant cells formed by MAH infected macrophages. IFN-γ activated *human blood monocytes were infected with (a) wild type (WT), (b) lysX mutant (lysXmut) and (c) lysX complemented strain (lysXcomp) and the infection samples were fixed at 5th day post infection. The samples were stained with Nile red (red fluorescence) and DAPI (blue fluorescence). Examplary some MGCs are marked with white arrows.. Scale bars: 50 µM. The total number of nuclei and the nuclei per MGC were counted and the fusion indexes were calculated with formula mentioned below:*

$$FI\% = \frac{\text{Number of nuclei in multinucleated cells}}{\text{Total number of nuclei}} \times 100$$

*Data are means ± standard deviation of the results from five independent experiments (using five buffy coats). *P < 0.05; two-tailed, unpaired Student's t test.*

4.9 Virulence of MAH in *Galleria mellonella* larvae

From our previous experiments, we could already hypothesize that the *lysX* mutation influences the virulence of the MAH pathogen. In order to evaluate the phenotype of *lysX* in vivo, the *G. mellonella* larvae (30 larvae per strain) were infected with wild type, lysX mutant and lysX complemented strains. The survival of the infected larvae was monitored for over 18 days (Fig. 10a). We observed that more death events occurred to the larvae infected with the lysX mutant strain in comparsion to the others. However, the death events started to happen only during later stages of infection (12^{th} day post infection). Upon inspection, we found that the lysX mutant had the highest virulence potency, as the infected larvae exhibited 100% mortality at 18 days after infection. While the wild type strain showed only 40% mortality at the 18^{th} day following infection and the complemented strain was intermediate displaying 65% mortality. The median survival time (time point at 50% survival) was recorded for all the three strains to be undefined in the wild type, 13 days in the lysX mutant-and 15days in the lysX complemented strain (Fig. 10a). The viability of the MAH strains (infection dose -10^6 CFU per larvae) was measured over an infection course of 10 days. Initially, the bacterial numbers decreased (approxiamately 50%) relatively uniformly with all the three strains until 120 hours post infection. Progressively, the bacterial counts in every strain were found to increase between 120 hours and 240 hours after infection. The lysX mutant showed the most strongest and a statistically significant elevation in the growth in vivo out of all the strains. The bacterial loads increased up to 100 fold in the case of infection with lysX mutant whereas the wild-type showed only 10 fold increase (Fig. 10b). Thus the lysX mutant was found to have acquired a higher multiplication capacity within G. melonella than the wild type

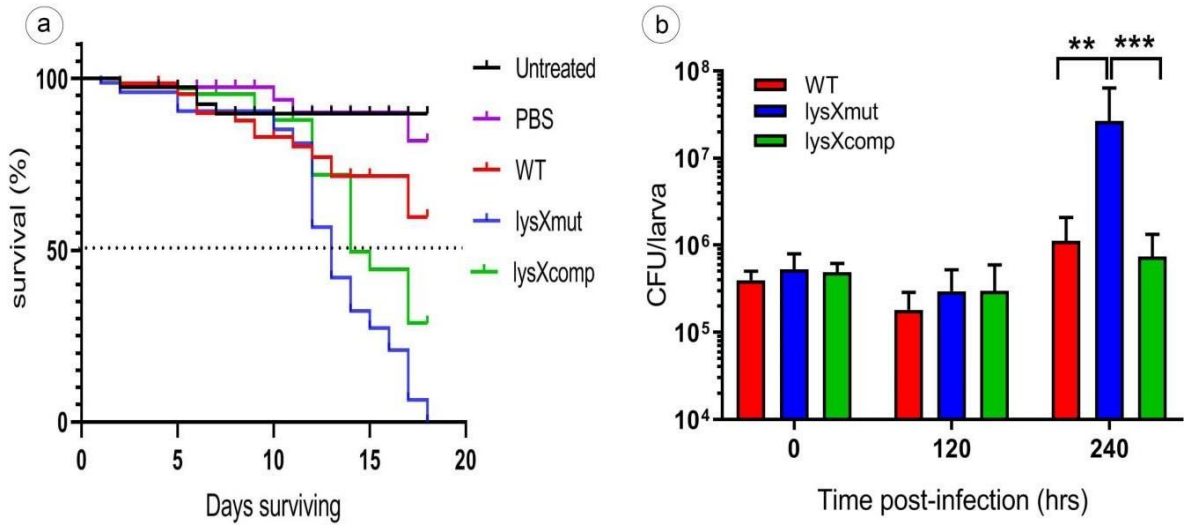

Figure 10: Effect of infection of the MAH strains on the survival of *G. mellonella* and growth of MAH in *G. melonella*. *(a) Survival of G. melonella after infection with 10^6 CFU of the MAH strains (30 per group) wild type (WT), lysX mutant (lysXmut) or lysX complemented strain (lysXcomp) was investigated for 20 days. Untreated larvae and PBS injected were taken as controls. Three independent experiments were conducted. Both the survival and pupation events of the larvae were analyzed. Pupation events are denoted as short dashes. The survival percentages of the three experiments were pooled and displayed in the survival curve. (b) The MAH viability in vivo was measured by sacrificing 3 to 5 larvae per group and plating them on antibiotic treated MB 7H10 plates for CFU quantification on specific time points (days 0, 5 and 10) during the infection study. Data are means ± standard deviation of the results from three independent experiments. * P < 0.05; **P < 0.01; ***P < 0.0001; two-tailed, unpaired Student's t test.*

4.10 MAH GPL expression and its antigenic reactivity

GPLs are highly antigenic membrane lipids of the MAC complex. They are also considered to be potential mediators of virulence due to their immuno-modulatory activity. Therefore, we explored the effect of the *lysX* mutation on GPL expression by extracting the purified GPLs using alkali treatment from the total lipids of the MAH strains. Thin layer chromatography was used to visualize the different patterns of GPL expression of the strains (Fig. 11a). On closer examination, we found that the GPL from the lysX mutant

showed a defective pattern with a lack of a lower band which was present in both the wild type and complemented strains.

Research studies have proven that the anti-GPL antibody levels reveal the disease activity in MAC lung infection[107]. Hence, the reactivity of the GPL extracts of the MAH strains were tested against the sera of cystic fibrosis patients with MAH infections through ELISA assay. The reactivity of the serum of the two tested patients against the GPL was lower in the lysX mutant when compared to the wild type strain (Fig. 11b). Still, the reactivity of the serum from a healthy person was only slightly above the negative control. This reactivity from GPL from the lysX mutant may be to due to the fact of the deficienct GPL pattern observed (Fig. 11a).

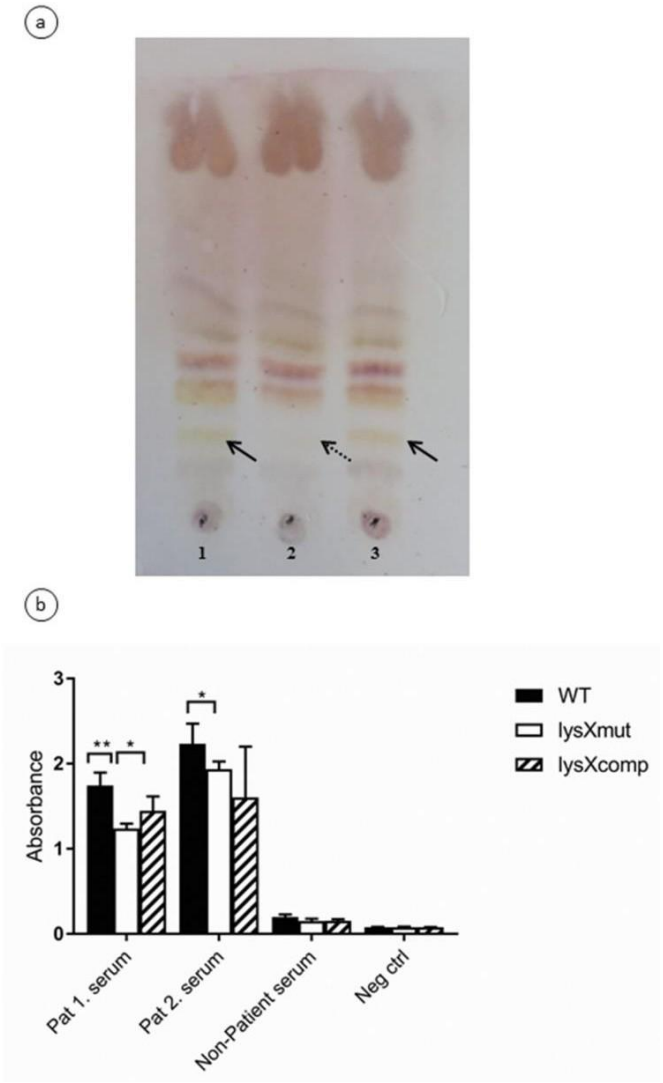

Figure 11: Expression profile of total GPLs from MAH strains and their antigenic reactivity *Thin layer chromatography (TLC) of GPL extracted from MAH strains wild type (Lane 1), lysX mutant (Lane 2) and lysX complemented strain (Lane 3). The GPL expression pattern of the Wild type strain and lysX complemented strain were similar while lysX mutant failed to express a single GPL band at the lowermost-molecular weight position (marked using a dashed arrow).*

*(b) Graph shows the reactivity of sera from two MAH infected patients against MAH GPL extracts from the MAH strains wild type (WT), lysX mutant (lysXmut) and lysX complement (lysXcomp)) using ELISA assay. Healthy individual's sera are included as a control. Data are means ± standard deviation of the results from three independent experiments. *P < 0.05; **P < 0.01; two-tailed, unpaired Student's t test).*

5 Discussion

The NTM group of environmental pathogens are increasingly recognized as a significant cause of morbidity and mortality [108]. Several research studies have also reported a continuous inflation in the worldwide incidence and prevalence of non-tuberculous mycobacteria (NTM) diseases, especially pulmonary *Mycobacterium avium* complex (MAC) diseases [43]. Despite this being a serious global health concern, methods to eradicate the NTM from its infection source and hosts are still under-developed. In general, the NTM are tolerant towards chlorine-based disinfectants [109], and MAC is the most tolerant one [110]. The treatment for MAC infections require prolonged therapy with the use of multiple antibiotics for more than 12 months [12]. Recurrent infections at the end of a completed therapy is also not uncommon due to MAC reinfection (32–48% of cases) [111, 112].Therefore to prevent the occurrence of these infections, strategies need to be developed in order to clear pathogens from infection sources, to vaccinate susceptible people in endemic areas and to treat patients effectively [43]. However, little is known about the role of mycobacterial genes which are involved in the prolonged survival of *M. avium* in the host [113]. Our study was focused on the *lysX* gene, which alters the surface charge of MTB and thereupon decreases the bacteria's vulnerability to the antimicrobial action of the host immune cells [77, 78]. Furthermore, the gene was proven to be an important requisite for MTB adaptation and survival in the host [114]. The experimental work from this thesis unravels the unknown functional aspects of the *lysX* gene in MAH , mainly pertaining to the establishment of infection in the host-organism.

The lysX mutant and the lysX complemented strains from MAH 104 were generated using illegitimate recombination mutagenesis in a previous study conducted in our laboratory [81]. Proteomic analysis of these mycobacterial strains proved that the mutation on the *lysX* gene interferes with the major metabolic pathways, which revealed a novel role of bifunctional protein [82]. Research studies have already illustrated that metabolism underpins the physiology and pathogenesis of mycobacteria [115]. Metabolic flexibility, autonomy and the capacity to resist nutrient stress are the key characteristics of mycobacterial pathogens [116]. In particular, we observed that a majority of the proteins enriched in the lysX mutant strain belonged to the category of fatty acid metabolism. Gene expression studies and metabolomics profiles have also shown that MTB after being phagocytosed by the macrophages, substantially upregulated the genes and their products

involved in fatty acid degradation and metabolism and in cholesterol uptake and consumption [103, 117]. Intracellular MTB remodels its metabolic networks in order to assimilate nutrients from surrounding host tissue and to do so, it switches the carbon metabolism towards β-oxidation pathway and gluconeogenesis via glyoxylate shunt [118, 119]. This metabolic feature enables the bacteria to efficiently utilize the host nutrients (fatty acids as sole carbon source) and contributes towards optimal virulence. Intriguingly, a number of genes in fatty acid β-oxidation (fadA, fadA3, fadA4, fadA5, fadE12, fadE15, echA6, and echA7) and the glyoxylate cycle (icl1, icl2, glcB, sdhA, and sdhB) were upregulated in the MAH lysX mutant [82]. Additionally, a list of virulence-related genes was also differentially upregulated in the mutant. Our results clearly demonstrate a role of LysX in directing the metabolism of MAH to be adapted to different environmental conditions including various stress conditions, along with the in vivo conditions within macrophages.

As the results from the proteome study gave us a hint about the implication of the *lysX* gene with central metabolism, the metabolic phenotypic microarray analysis was performed to identify differential substrate usage. Data analysis showed that the lysX mutant strain lacked the capability to metabolize pyruvic and acetic acid. During infection, the host-derived lipid components are the major carbon source at the infection site. In principle, β-Oxidation of fatty acids turns the fatty acids into potential source of acetate formation, eventually generating acetyl-CoA and to a lesser extent propionyl-CoA [120]. The physiological carbon source cholesterol is usually catabolized into acetyl-CoA, propionyl-CoA, and pyruvate. Further it has been suggested that accumulation of acetate may take place in the course of acetyl-CoA processing by MTB, since acetyl-CoA is a main product of fatty acid degradation pathway [121]. Accordingly, we have also observed an enrichment of the fatty acid degradation pathway in the MAH lysX mutant. Our protein expression analysis also showed that the genes involved in the propionate metabolism and catabolism of cholesterol were strongly upregulated in the lysX mutant and all these might have also led to the accumulation of metabolic substrates such as pyruvate and acetate. To confirm our hypothesis, we quantified the concentration of the pyruvate and as hypothesized, pyruvate was found to be accumulated in the lysXmut strain in comparison to the wild type and lysXcomp complemented strain (Fig. 3). This result also suggests that the lysX mutant strain might have acquired the capability to switch to a metabolism which will be beneficial for the strain to survive in the host under in vivo conditions.

Research studies have reported that excessive metabolic degradation of fatty acids leads to induction of more conversion of fatty acidy into triacylglycerol (TAG). Besides, phosphenol pyruvate and pyruvate have been stated to provide the precursors for de novo TAG synthesis. Also cytoplasmic TAG is one of the major components of intracellular lipid inclusions (ILI) in Mycobacteria [122]. The biosynthetic pathway of TAG diverges from the phospholipid synthesis after the synthesis of phosphatidic acid [76]. During exponential growth, the intracellular TAG may also become accumulated when there is a turnover of phospholipid which thereby enhances the availability of FAS-1 (fatty acid synthesis type-1) products for incorporation [123]. A previous study on an MTB lysX mutant hypothesized that the mutation contributed towards the changes in membrane potential due to the alterations in phospholipid metabolism [78]. In conformance, our MAH strains upon structural investigation using electron microscopy revealed the presence of intracellular lipid-like vacuoles, which was found in abundance in the lysX mutant strains. Studies revealed that this particular phenotype was observed in hypervirulent MTB strains of the W-Beijing Lineage [124]. As the lysX mutant already showed a metabolic alteration which reflected an intracellular metabolic adaptation, these intracellular lipid accumulations would become an added advantage for the bacteria to thrive within the stress-filled environment of the host organism.

Cell wall lipids play a critical role in the development of antibiotic resistance of mycobacterial species [125]. The membrane of mycobacteria comprises of different types of phospholipids: phosphatidylglycerol (PG), phosphatidylethanolamine (PE), phosphatidylinositol (PI), and phosphatidylinositol mannosides (PIMs) [126]. This impenetrable bacterial cell envelope however can be breached by antimicrobial peptides (AMPs). The AMPs are endogenous, cationic peptides which are in general the first line of action by the innate host defense against infection [127]. It has been shown that the enzyme aminoacyl-phosphatidylglcerol synthase catalyzes the amino acylation of the phospholipid PG with alanine or lysine which renders resistance towards these antimicrobial agents, AMPs [128]. This amino acylation of PG results in the reduction of the net negative charge of the bacterial membrane as these aminoacyl-phosphatidylglcerols (eg. lysyl-phosphatidylglycerol (L-PG)) carry an overall positive net charge [129, 130]. Recently, a research study demonstrated that the *lysX* gene from MTB, which encodes a lysyl-tRNA synthetase was responsible for L-PG production, and a MTB lysX deletion mutant was found to be sensitive towards cationic antibiotics and peptides. Also the mutant

exhibited an altered membrane potential when compared to the wild type [77]. In the same way, the MAH lysX mutant from our study also proved to be hypersensitive towards positively charged antibiotics, such as clarithromycin, ethambutol and streptomycin. The complex mycobacterial cell wall contains an outer mycolic acid layer which is linked to the inner peptidoglycan layer via an additional arabinogalactan polymer. The biosynthetic pathways of arabinogalactan and mycolic acids constitute of several efficient drug targets for tuberculosis treatment [131]. The linkage between mycolated arabinogalactan to the peptidoglycan layer involves a key component named as α-L-rhamnopyranosyl residue [132]. Some of the enzymes which participate in the synthesis of rhamnosyl residue (RmlD, RfbD and RfbE) [133, 134] were strongly upregulated in the MAH lysX mutant, which may in part explain the change observed in ethambutol susceptibility. We realized that the complementation did not fully restore the phenotype of the mutant in antibiotic susceptibility testing, however this could be partially explained by the integration locus of the complementing plasmid which differed from the original location of the native gene in the bacterial chromosome [82].

Maloney and colleagues investigated on the phenotypic behavior of a lysX deletion mutant from MTB and displayed the influence of LysX activity on the survival and proliferation of the pathogen upon infection of the host. They hypothesized LysX to be an important necessity factor for acquiring full virulence potential in MTB [77]. The above mentioned results from our study on the MAH lysX mutant was also found to show similar phenotypic traits to those that has been reported in the case of MTB lysX mutant. Both the mutants revealed to be hypersensitive towards cationic antimicrobial agents likewise exhibiting an alteration in the phospholipid metabolism. Also both mutants were hypersensitive towards ROI, RNI and defensing (Ref Mtb). Since the infection studies with the MTB lysX mutant showed growth defects in THP-1 macrophages [135], we examined the intracellular growth proficiency of the MAH lysX mutant in human blood-derived monocytes (from buffy coats). Surprisingly, we discovered that the lysX mutant from MAH exhibited a significant increase in intracellular replication. Earlier studies have shown that the MTB mutants with defective cholesterol utilization displayed reduced survival in macrophages and mice [136, 137]. It was also reported that the MTB possesses the capacity to access and metabolize triacylglycerol from the host lipid storage during infection [138]. Moreover TAG from lipid bodies is considered to be the main energy source under conditions like starvation, oxygen depletion and reactivation in MTB [139].

Our experimental data already confirmed the accumulation of lipid inclusions in the MAH lysX mutant under extracellular conditions and also showed an enrichment of the cholesterol catabolic pathway. These data put together explains the enhanced intracellular survival observed in the lysX mutant of MAH.

One of the factors responsible for this differential behavior between the lysX mutants from MTB and *M. avium* may be explained by the structural differences between the two species. The MAC comprises of unique features such as strain-specific glycopeptidolipids(ssGPL), on its cell wall, which are absent in other mycobacterial species. The genes involved in the GPL synthesis are also implicated in macrophage penetration and some of these these genes were also found to be located in a pathogenicity island of MAH [42, 140]. Also, *M. avium* disposes of the presence of multiple copies of various fatty acid degradation genes (fadD), indicating greater genetic variability to produce variation in cell wall composition which thereby impacts virulence and host specificity [141]. In addition, there exists a variability in the *lysX* gene size between the species - 3531bp (MTB) and 3228bp (MAH) - and the two *lysX* genes exhibit only 81% identity at nucleic acid level [82].

Many investigators assume that these mycobacteria are analogous because they appear to inhabit the same intracellular compartment. From the aforementioned earlier studies, the survival mechanism of one *Mycobacterium* may not necessarily apply to other mycobacteria. *M. avium* and *M. tuberculosis* have been found to differ widely in their interaction with macrophages. Research reports also describe *M. tuberculosis* to be more sensitive than *M. avium* to potential bactericidal molecules, including nitric oxide [142]. Eventually, it points out that *M. avium* adopts distinct strategies to manipulate the host immune response and persist intracellularly. In this context, we focused on studying the interference of the MAH *lysX* gene on the host-pathogen interplay and its contribution to the differential virulence features.

After infecting the host, the mycobacteria encounters a hostile macrophage environment comprising of several stress elements such as the reactive oxygen and nitrogen species (ROS, RNS), acidic pH of phagolysosome compartments and the release of antimicrobial peptides. ROS and RNS promote pathogen killing by damaging its DNA, lipids, and proteins. However, the mycobacteria have devised many stress resistance pathways which enable them to survive and multiply in this hostile environment [143]. In order to go into

detail about the increased intracellular growth of the MAH lysX mutant, we challenged our bacterial strains with host-mediated stresses. On comparing the results, the lysX mutant proved to be more sensitive in the presence of H_2O_2 and DETA-NO than the wild type and complemented strains in the extracellular state. The observed phenotype corresponded with our proteomic data, as the genes which are stated as ROS scavenger genes in MTB were differentially regulated in the MAH lysX mutant. The genes included those encoding catalase (katG) [144], alkylhydroperoxide reductase (ahpC) and thioesterase family protein (MAV_2246) [82]. Habitually, *M. avium* has the potency to tolerate ROS and RNS stress [145].Therefore , this sensitivity effect could be correlated to the impact of the lysX mutation on the defense mechanism of the bacterium. In contrast , the MTB lysX mutant was reported to show no effect on the exposure to H_2O_2 and DETA-NO [146].In the case of MTB infections, the ROS levels induced by the host immune cellsinfluences the survivability of the bacteria inside the host [147, 148], whereas in MAC infections, the resistivity to these host effector molecules does not affect their virulence in the host[149].

Initially, MTB encounters alveolar macrophages and lung epithelial cells during primary infection and studies have shown that these human airway epithelia produce antimicrobial peptides as a part of their antibacterial activity [150]. These peptides are small sized (3-5 kDa) cationic, cytotoxic and oxygen dependent termed as defensins [151]. There exist different classes of defensins , which are variant in their structure and in antimicrobial activity [152]. The cationic defensins cause permeabilization of the cell membrane and leakage of intracellular metabolites through electrostatic binding to the anionic phospholipids in the bacterial membrane [153]. Since, our target *lysX* gene mediates the modification of phosphatidylglycerol with L-lysine, which confers resistance to defensins, we tested the sensitivity of the strains towards Human beta defensin-1. The MAH lysX mutant displayed a substantial decrease in cell viability when compared to the wild type. Also, in the absence of the *lysX* gene, MTB was shown to be susceptible to AMPs in vitro. It was fascinating to observe these differential behavioral aspects of the MAH lysX mutant that even though they exhibited hypersensitivity towards these stresses, they still showed an elevated growth in macrophages. In contrast, the MTB lysX mutant displayed a defective growth in macrophages due to their hypersensitiveness towards host –mediated stresses In general, the MAH causes infection in humans and other mammals by crossing mucosal barriers and they need to resist the action of these antimicrobial peptides (eg. B-defensins, cathelicidin) found in the intestinal and respiratory tract mucosa [50].

Nevertheless, findings also indicate that the components on the surface of the bacteria are also responsible for the susceptibility of the mycobacteria to these antimicrobial peptides. It is also believed that the mycobacteria must possess mechanisms to shift the expression of these membrane molecules depending on their environment [154]. In the same way, our proteomics study also showed a strong upregulation of PhoP in the lysX mutant, which had been described to be a major regulator of bacterial cell wall that provides resistance to antimicrobial peptides as well [155].

Recent study suggests that the β-defensins serves as a link between innate and adaptive immune response as they not only chemoattract macrophages but also play an important role in initiating Th1 inflammatory response [156]. It was also reported that the lysX mutant from MTB induced an elevated secretion of TNF-α and IL-6 cytokines after infecting monocyte-derived macrophages [77]. In our infection studies with PBMC, the MAH lysX mutant also reacted in the same manner, inducing higher levels of cytokine expression (IL-1β, IL- 12, TNFα and IL-10) than the wild type and the complemented strains. The outcome of a mycobacterial infection often depends on the balance between immune activation and inflammation [157]. The expression of TNF-alpha is said to be associated with the multiplication of the virulent MTB strains and it is reported to restrict the intracellular growth of MTB in alveolar macrophages. The intracellular phenotype of the MTB lysX mutant was in conformity with the above stated fact. Nevertheless, in our case the MAH lysX mutant in spite of displaying higher levels of cytokine expression, they still managed to survive and proliferate inside the human monocytes. Although the inflammatory responses are pivotal for contrasting mycobacterial infection [158], still under certain circumstances an extensive immune activation may lead to self-defeating for the host, consequently resulting in the development of the disease and aggravation [157, 159]. Another logic behind this observed phenotype could be the result of differences between the cell wall structure of MTB and MAH. Their distinct cell wall characteristics trigger differential immune response and inflammation, thus manifesting variant pathogenicities [160]. As in *M. avium*, the morphotype and virulence also greatly influence the amount of the cytokine secreted.

Previous studies have proven the capability of MAH cell wall components (e.g., GPL, lipoarabinomannan (LAM) to alter host responses through the disruption of cytokine

networks (especially those associated with Th1-type responses.), which might be either bacteria beneficial or bactericidal based on the structural conformations of these lipids[46, 161]. Proteomic analysis of our strains also revealed a differential regulation of genes in the lysX mutant which were involved in GPL synthesis (MAV_4518, rmt4/mftb, fadE5, sap) and glycerophospholipid metabolism (MAV_1825, fbpB, fbpC) in comparison to that of the wild type.

Normally, the human body reacts to any infectious agents through inflammatory response. However, when this inflammatory state becomes persistent, it may result in irreversible tissue damage [162]. The macrophages on exposure to severe inflammatory stresses fuse with each other forming multinucleated giant cells (MGCs). Beyond this, a chronic inflammation leads to the formation of `Granuloma' which is a focal inflammatory structure consisting of an aggregation of transformed macrophages (MGCs) surrounded by other cell types like leukocytes, lymphocytes and plasma cells [163]. It has been reported that the mycobacterial diseases are granulomatous diseases and the MGCs are a histologic hallmark of granuloma that is suggested to limit tuberculosis infection [60]. Studies have also observed these granulomatous structures in the spleen and liver of *M. avium*-infected mice [164]. However, the function of these inflammatory structures still remains unclear, as it may yield both host-protective and bacteria-beneficial effects; either they can localize the infection preventing it from spreading or they may progress to necrosis of the infected macrophages, *where in the mycobacteria* can significantly alter the immune environment of the granuloma (eg reduction in efficiency to produce bactericidal products such as nitric oxide, increased IL-10 secretion[165]) to facilitate its persistence [166]and thereby enabling the bacteria to disseminate [167, 168]. The MGCs and the mononuclear macrophages are said to have distinct morphological and transcriptional properties. The MGCsare also found to possess the ability to ingest infected apoptotic macrophages and contain high concentrations of nitric oxide [169]. An in vitro infection of macrophages with BCG showed an increased bacterial load in MGCs. Therefore it was suggested that the MGCs have an increased uptake capacity of infected and apoptotic cells but are inefficient in terminating the mycobacteria [170]. In our examination, the infection of IFNγ -activated HBDM with *M. avium* strains resulted in an induction of a higher rate of MGC formation in the lysX mutant than the wild type and complemented strain. As a correlation we found that the gene DprE1, which influences macrophage fusion was strongly overexpressed in the lysX mutant. This gene catalyzes the synthesis of cell-wall arabinans

which activate TLR2 response through lipomannan, thereby triggering the fusion process [171]. DprE1 is also considered as a validated tuberculosis drug target as it also plays a role in the mycobacterial growth and survival [172].

Mycobacterial virulence is referred as the ability of the pathogen to reside within host cells and evade the microbicidal mechanisms of host immune system [173]. Put together, our experimental results already hypothesizes that the mutation of the lysX gene impacts the virulence attributes of MAH. Therefore as a confirmation, we performed in vivo infection experiments employing an invertebrate infection model, *G. mellonella* larvae.

Recently, the *G. mellonella* larvae are increasingly used to study host-pathogen interactions and for the screening of novel drug candidates in a number of microorganisms including Gram-positive, Gram-negative bacteria and fungi [174, 175]. Advantageously, *G. mellonella* shares a high degree of structural and functional similarity to that of the vertebral innate immune system [176, 177]. They also exhibit humoral immune responses by the production of antimicrobial peptides, melanization and through hemolymph clotting. In addition, the cellular immune response of the larval model include phagocytosis, nodulization (multiple hemocytes bind to clusters of bacteria to eliminate them in the hemolymph through activation of prophenoloxidase and melanization [178]), and encapsulation [179]. This model has been reported to be used in several mycobacterial species such as *M. bovis BCG* [180], *M. abscessus*[181],*M. fortuitum* [182], *M. marinum*[182] and *M. aurum*[182]. In our study, we have successfully established *G. melonella* as a suitable in vivo infection model for MAH. We assessed the virulence of the MAH strains by investigating the survival of mycobacteria and the infected host over a period of 10 to 18 days, respectively. From the analysis we found the lysX mutant to be more virulent than the wild type and the complemented strain. The larval group infected with the lysX mutant showed higher number of deaths and resulted in 100% mortality at the end of the experiment though they behaved similar to the wild type at the beginning. On quantification, the lysX mutated strain displayed a remarkable growth (around 100 fold) in vivo particularly between the 5^{th} and the 10^{th} day post infection. The rapid death of the mutant infected larvae could also be correlated with the increased bacterial load observed. Moreover, it was interesting to see that the MAH lysX mutant showed an analogousgrowth pattern in the in vivo galleria model as it was in the *in vitro* model in HBDM, especially during the later stages of infection [82]. This phenotypic behavior of enhanced growth in HMDM and *Galleria* is in agreement with our proteomics data, as we

have seen that *lysX* mutation in MAH instigates a shift in the metabolism which pre-equips the bacteria to survive under intracellular host conditions. We also identified some virulence associated genes (ESX transport systems, EccA3, MAV_4606, MAV_0940; anti-apoptotic pathways, CysK [69], KatG [70], NuoG [71]) differentially regulated in the lysX mutant when compared to the other strains.

In contrast to our results, the lysX mutant from MTB was reported to show growth defects in mice model and was clearly attenuated in guinea pigs [135]. This diversified characteristic feature observed between MAH and MTB may be explained by number of factors. Though the immune responses against MAH and MTB looks similar, they are markedly distinct in the host genetic control of susceptibility and in disease severity [183]. A prominent differentiating factor lies in the cell wall architecture, for eg. *M. avium* does not synthesize phtiocerol dimycocerosate (PDIM) which is reorganized by the macrophage membrane during MTB engulfment, altering the signaling pathways of phagocytic receptors [184]. However, the *M. avium* are equipped with the specialized glycopeptidolipids (GPL) in their cell wall which are absent in MTB and M. leprae. The multifunctional GPLs are involved in biofilm development and in turn important for MAH survival and proliferation in water supply sytems [48, 185]. It is also suggested to play a role in causing infections in immune deficient individuals [186]. Since the GPLs are associated with host-pathogen interactions and the *lysX* gene is also linked with the membrane phospholipid composition, we explored the GPL expression pattern in the MAH strains. On comparison, we found that the lysX mutant had a defective expression pattern. This result was coincidental with our proteomic studies, which showed a differential regulation of the GPL synthesis locus (rmt4, fadE5 & sap) in the lysX mutant strain.

Another study on the MAH GPLs documented about the class of strain specific GPLs(ssGPL), which were competent to interact the macrophage receptors, thus altering the cytokine secretion. It was also illustrated that mutants lacking ssGPL elicited a hypersecretion of pro-inflammatory cytokines such as NF-α, IL-6, IL-12 and RANTES [187]. The increased inflammatory response observed in our lysX mutant may also be explained by the above-stated fact. Research studies state that the GPL core has an immunodominant epitope in MAC strains. It was also demonstrated the whole GPLs as well as components of GPLs possess antigenicity [107]. We analyzed the antigenic reactivity of the GPL extracts from our MAH strains against the sera of MAH infected

patients and the lysX mutant was found yield the least signal of all. This is might be linked to the defective GPL pattern observed.

Latest study on MTB mutants with mutations in the two-component regulatory system genes, mce operon, dosR regulon etc. have shown hypervirulence traits in mouse models [188]. The potential mechanisms of hypervirulence are described as the ability of the pathogen to survive and multiply intracellularly, to interfere with the host immune system (increased expression of inflammatory cytokines and granuloma formation) and higher bacterial burden in vivo [189]. The MAH lysX mutant has also displayed the above mentioned phenotypic traits which are defined to display the phenomenon of hypervirulence [62].

In summary, so far unknown functional aspects of the *lysX* gene from MAH was exposed through this study and the gene was found to play a major role in the modulation of MAH virulence. However to gain a better understanding of *M. avium* pathogenesis, future research needs to concentrate on the mechanisms employed by the mycobacteria to acclimatize themselves to different nutritional situations and to exploit the host's immune response for the enhancement of the anti-inflammatory responses which aid in establishing a persistent infection. . A comparison study between MAH and MTB using *lysX* gene as a tool could be interesting to observe the differences in survival strategies in the mycobacterial species. This would definitely aid in generating potent drug targets which will act specifically on the different mycobacterial species.

6 Summary

Non-tuberculous Mycobacteria (NTM) are an important but often overlooked group of pathogens, especially important in the immunocompromised and patients with pre-existing pulmonary disease. Their condition of environmental bacteria enables them to persist in a wide range of habitats. Although multiple virulence factors of *M. avium* have been proposed, the virulence strategies of *M. avium* are still not fully clear including the mechanisms allowing this environmental bacterium to cause chronic infections in humans.

Lysyl-phosphatidylglycerol, a component of the mycobacterial membrane, contributes to the resistance towards cationic antimicrobial peptides. Its production is catalyzed by LysX, a bifunctional protein with lysyl transferase and lysyl transfer RNA synthetase activity. The main objective of the doctoral project was to characterize the role of the *lysX* gene for growth and host cell interaction of *M. avium* subsp. *hominissuis* (MAH). A considerable impact of the gene *lysX* on the different functional pathways of *M. avium* in particular the central carbon metabolism was demonstrated. Proteomics studies revealed that the lysX mutation led to a metabolic shift which enhanced the suitability of the bacteria to be adaptive towards the living conditions inside host cells. In addition, the mutation also caused an upregulation of lipid synthesis genes which resulted in an intracellular lipid accumulation. The measure of mycobacterial virulence has been stated to depend on the ability of the bacteria to invade, persist and replicate within the hostile macrophage environment. In accordance the lysX mutant already displayed a hypervirulent phenotype, exhibiting an excessive intracellular growth in *in-vitro* (human blood monocytes) and *in-vivo* (*Galleria mellonella*). Additionally, the lysX mutation also resulted in an hyperinflammatory behaviour (increased secretion of cytokines and increased MGC formation), which also indicates a novel functional role of lysX in regards to virulence in *M. avium* species.

Interestingly, the results with respect to the host-pathogen interaction of an MAH with a deficient *lysX* gene obtained in this study contrasted with the results obtained by other authors with a lysX mutant from MTB. This makes it more interesting to further explore on the differential survival strategies of mycobacterial species. The *lysX* gene may also be instrumental in identifying factors involved in molecular pathogenesis of different

mycobacterial diseases, thus benefitting the health systems for developing strategies to combat these hardy pathogens.

7 Zusammenfassung

Nichttuberkulöse Mykobakterien (NTM) sind eine wichtige, aber oft übersehene Gruppe von Krankheitserregern, die besonders wichtig bei immunsupprimierten und Patienten mit bereits bestehenden Lungenerkrankungen sind. Ihre Beschaffenheit als Umweltbakterien ermöglicht es ihnen, in einer Vielzahl von Lebensräumen zu überleben. Obwohl mehrere Virulenzfaktoren von *M. avium* beschrieben wurden, sind die Virulenzstrategien von *M. avium* noch nicht vollständig geklärt, einschließlich der Mechanismen, die es diesem Umweltkeim erlauben, chronische Infektionen beim Menschen zu verursachen.

Lysyl-Phosphatidylglycerol, ein Bestandteil der Mykobakterienmembran, trägt zur Resistenz gegen kationische antimikrobielle Peptide bei. Die Produktion wird durch LysX katalysiert, ein bifunktionelles Protein mit Lysyltransferase- und Lysyltransfer-RNA-Synthetase-Aktivität. Das Hauptziel des Promotionsprojekts war es, die Rolle des *lysX* Gens für das Wachstum und die Wirtszellinteraktion von *M. avium* subsp. *hominissuis* (MAH) zu charakterisieren. Ein erheblicher Einfluss des *lysX* Gens auf verschiedene Stoffwechselwege von *M. avium*, insbesondere auf den zentralen Kohlenstoffstoffwechsel, konnte nachgewiesen werden. Proteomstudien zeigten, dass die lysX-Mutation zu einer metabolischen Verschiebung führte, die die Anpassung der Bakterien an die Lebensbedingungen in den Wirtszellen verbesserte. Darüber hinaus führte die Mutation auch zu einer Hochregulation der Lipidsynthesegene, was zu einer intrazellulären Lipidakkumulation führte. Das Ausmaß der mykobakteriellen Virulenz hängt von der Fähigkeit der Bakterien ab, in die Makrophagen einzudringen, dort zu persistieren und sich zu vermehren. Die lysX-Mutante erwies sich als hypervirulent, da sie sowohl ein übermäßiges intrazelluläres Wachstum *in vitro* (humane Monozyten) als auch ein verstärktes Wachstum *in vivo* (*Galleria mellonella*) aufwies. Darüber hinaus führte die lysX-Mutation auch zu einem hyperinflammatorischen Verhalten (erhöhte Sekretion von Zytokinen und erhöhte MGC-Bildung), was auf eine neuartige funktionelle Rolle von *lysX* bezüglich der Virulenz von *M. avium* hinweist.

Interessanterweise standen die Ergebnisse dieser Studie in Bezug auf die Wirt-Pathogen-Interaktion von MAH mit defektem *lysX* Gen im Gegensatz zu den Ergebnissen anderer Autoren bezüglich einer lysX-Mutante von *M. tuberculosis*. Dies fordert zu weiteren Studien zu den unterschiedlichen Überlebensstrategien verschiedener Mykobakterienarten

heraus. Derartige Untersuchungen können dazu beitragen, Faktoren zu identifizieren, die an der molekularen Pathogenese verschiedener mykobakterieller Erkrankungen beteiligt sind. Dies kann zu neuen Strategien zur Bekämpfung dieser widerstandsfähigen Krankheitserreger beitragen und somit dem Gesundheitswesen zugute kommen.

8 References

1. van Ingen, J., *Mycobacteria*, in *Infectious Diseases*. 2017, Elsevier. p. 1645-1659. e2.
2. Forbes, B.A., et al., *Practice guidelines for clinical microbiology laboratories: mycobacteria*. Clinical microbiology reviews, 2018. **31**(2): p. e00038-17.
3. Organization, W.H., *Global tuberculosis report 2018*. 2018: World Health Organization.
4. Ramazanzadeh, R., et al., *Prevalence and occurrence rate of Mycobacterium tuberculosis Haarlem family multi-drug resistant in the worldwide population: A systematic review and meta-analysis*. Journal of research in medical sciences: the official journal of Isfahan University of Medical Sciences, 2015. **20**(1): p. 78.
5. Magden, E.R., et al., *Chapter 17 - Nonhuman Primates*, in *Laboratory Animal Medicine (Third Edition)*, J.G. Fox, et al., Editors. 2015, Academic Press: Boston. p. 771-930.
6. Reece, S.T. and S.H.E. Kaufmann, *26 - Host Defenses to Intracellular Bacteria*, in *Clinical Immunology (Fifth Edition)*, R.R. Rich, et al., Editors. 2019, Content Repository Only!: London. p. 375-389.e1.
7. Scollard, D.M., et al., *The continuing challenges of leprosy*. Clinical microbiology reviews, 2006. **19**(2): p. 338-381.
8. Sousa, S., et al., *Nontuberculous Mycobacteria Persistence in a Cell Model Mimicking Alveolar Macrophages*. Microorganisms, 2019. **7**(5): p. 113.
9. Tortoli, E., *Clinical manifestations of nontuberculous mycobacteria infections*. Clinical Microbiology and Infection, 2009. **15**(10): p. 906-910.
10. Cassidy, P.M., et al., *Nontuberculous mycobacterial disease prevalence and risk factors: A changing epidemiology*. Clin Infect Dis, 2009. **49**.
11. Gopinath, K. and S. Singh, *Non-Tuberculous mycobacteria in TB-endemic countries: Are we neglecting the danger?* PLoS Neglected Tropical Diseases, 2010. **4**(4).
12. Griffith, D.E., et al., *An official ATS/IDSA statement: Diagnosis, treatment, and prevention of nontuberculous mycobacterial diseases*. American Journal of Respiratory and Critical Care Medicine, 2007. **175**(4): p. 367-416.
13. Tabarsi, P., et al., *Nontuberculous mycobacteria among patients who are suspected for multidrug-resistant tuberculosis - Need for earlier identification of nontuberculosis mycobacteria*. American Journal of the Medical Sciences, 2009. **337**(3): p. 182-184.
14. Prevots, D.R. and T.K. Marras, *Epidemiology of human pulmonary infection with nontuberculous mycobacteria a review*. Clinics in Chest Medicine, 2015. **36**(1): p. 13-34.
15. Thomson, R.M., *Changing epidemiology of pulmonary nontuberculous mycobacteria infections*. Emerging Infectious Diseases, 2010. **16**(10): p. 1576-1583.
16. Adjemian, J., et al., *Spatial clusters of nontuberculous mycobacterial lung disease in the United States*. American Journal of Respiratory and Critical Care Medicine, 2012. **186**(6): p. 553-558.
17. Koh, W.J., et al., *Increasing recovery of nontuberculous mycobacteria from respiratory specimens over a 10-year period in a tertiary referral hospital in South Korea*. Tuberculosis and Respiratory Diseases, 2013. **75**(5): p. 199-204.
18. Namkoong, H., et al., *Epidemiology of pulmonary nontuberculous mycobacterial disease, Japan*. Emerging Infectious Diseases, 2016. **22**(6): p. 1116-1117.
19. Shah, N.M., et al., *Pulmonary Mycobacterium avium-intracellulare is the main driver of the rise in non-tuberculous mycobacteria incidence in England, Wales and Northern Ireland, 2007-2012*. BMC Infectious Diseases, 2016. **16**(1).
20. Wu, M.-L., et al., *NTM drug discovery: status, gaps and the way forward*. Drug Discovery Today, 2018. **23**(8): p. 1502-1519.

21. Talbot, E.A. and B.J. Raffa, *Chapter 92 - Mycobacterium tuberculosis*, in *Molecular Medical Microbiology (Second Edition)*, Y.-W. Tang, et al., Editors. 2015, Academic Press: Boston. p. 1637-1653.
22. Rook, G.A.W., *Mycobacteria, Infection And Immunity*, in *Encyclopedia of Immunology (Second Edition)*, P.J. Delves, Editor. 1998, Elsevier: Oxford. p. 1793-1797.
23. van Ingen, J., *185 - Mycobacteria*, in *Infectious Diseases (Fourth Edition)*, J. Cohen, W.G. Powderly, and S.M. Opal, Editors. 2017, Elsevier. p. 1645-1659.e2.
24. Sarathy, J., V. Dartois, and E. Lee, *The role of transport mechanisms in Mycobacterium tuberculosis drug resistance and tolerance*. Pharmaceuticals, 2012. **5**(11): p. 1210-1235.
25. Boshoff, H.I. and C.E. Barry 3rd, *Tuberculosis—metabolism and respiration in the absence of growth*. Nature Reviews Microbiology, 2005. **3**(1): p. 70.
26. Marrero, J., et al., *Gluconeogenic carbon flow of tricarboxylic acid cycle intermediates is critical for Mycobacterium tuberculosis to establish and maintain infection*. Proc Natl Acad Sci U S A, 2010. **107**.
27. Venugopal, A., et al., *Virulence of Mycobacterium tuberculosis depends on lipoamide dehydrogenase, a member of three multienzyme complexes*. Cell host & microbe, 2011. **9**(1): p. 21-31.
28. Ganapathy, U., et al., *Two enzymes with redundant fructose bisphosphatase activity sustain gluconeogenesis and virulence in Mycobacterium tuberculosis*. Nature communications, 2015. **6**: p. 7912.
29. Basu, P., et al., *The anaplerotic node is essential for the intracellular survival of Mycobacterium tuberculosis*. Journal of Biological Chemistry, 2018. **293**(15): p. 5695-5704.
30. Cosma, C.L., D.R. Sherman, and L. Ramakrishnan, *The secret lives of the pathogenic mycobacteria*. Annual Reviews in Microbiology, 2003. **57**(1): p. 641-676.
31. Pfyffer, G.E., *Mycobacterium: general characteristics, laboratory detection, and staining procedures*, in *Manual of Clinical Microbiology, Eleventh Edition*. 2015, American Society of Microbiology. p. 536-569.
32. Rahman, S.A., et al., *Comparative analyses of nonpathogenic, opportunistic, and totally pathogenic mycobacteria reveal genomic and biochemical variabilities and highlight the survival attributes of Mycobacterium tuberculosis*. MBio, 2014. **5**(6): p. e02020-14.
33. Gagneux, S., *Ecology and evolution of Mycobacterium tuberculosis*. Nature Reviews Microbiology, 2018. **16**(4): p. 202.
34. Mijs, W., et al., *Molecular evidence to support a proposal to reserve the designation Mycobacterium avium subsp. avium for bird-type isolates and 'M. avium subsp. hominissuis' for the human/porcine type of M. avium*. Int J Syst Evol Microbiol, 2002. **52**.
35. Uchiya, K.-i., et al., *Comparative genome analyses of Mycobacterium avium reveal genomic features of its subspecies and strains that cause progression of pulmonary disease*. Scientific reports, 2017. **7**: p. 39750.
36. Orme, I.M. and D.J. Ordway, *Host response to nontuberculous mycobacterial infections of current clinical importance*. Infection and Immunity, 2014. **82**(9): p. 3516-3522.
37. Levy, I., et al., *Multicenter cross-sectional study of nontuberculous mycobacterial infections among cystic fibrosis patients, Israel*. Emerging infectious diseases, 2008. **14**(3): p. 378.
38. Griffith, D.E., et al., *An official ATS/IDSA statement: diagnosis, treatment, and prevention of nontuberculous mycobacterial diseases*. American journal of respiratory and critical care medicine, 2007. **175**(4): p. 367-416.
39. Carter, G., L.S. Young, and L.E. Bermudez, *A subinhibitory concentration of clarithromycin inhibits Mycobacterium avium biofilm formation*. Antimicrobial agents and chemotherapy, 2004. **48**(12): p. 4907-4910.
40. Babrak, L., et al., *The Environment of "Mycobacterium avium subsp. hominissuis" microaggregates induces synthesis of small proteins associated with efficient infection of respiratory epithelial cells*. Infection and Immunity, 2015. **83**(2): p. 625-636.

41. Wu, C.W., et al., *Whole-genome plasticity among Mycobacterium avium subspecies: insights from comparative genomic hybridizations.* J Bacteriol, 2006. **188**.
42. Ignatov, D., et al., *Mycobacterium avium-triggered diseases: pathogenomics.* Cellular microbiology, 2012. **14**(6): p. 808-818.
43. Nishiuchi, Y., T. Iwamoto, and F. Maruyama, *Infection sources of a common non-tuberculous mycobacterial pathogen, Mycobacterium avium complex.* Frontiers in medicine, 2017. **4**: p. 27.
44. Blumenthal, A., et al., *Common and unique gene expression signatures of human macrophages in response to four strains of Mycobacterium avium that differ in their growth and persistence characteristics.* Infection and immunity, 2005. **73**(6): p. 3330-3341.
45. Barrow, W.W., *Processing of mycobacterial lipids and effects on host responsiveness.* Frontiers in bioscience : a journal and virtual library, 1997. **2**: p. d387-400.
46. Schorey, J.S. and L. Sweet, *The mycobacterial glycopeptidolipids: Structure, function, and their role in pathogenesis.* Glycobiology, 2008. **18**.
47. Carter, G., et al., *Characterization of biofilm formation by clinical isolates of Mycobacterium avium.* Journal of medical microbiology, 2003. **52**(9): p. 747-752.
48. Freeman, R., et al., *Roles for Cell Wall Glycopeptidolipid in Surface Adherence and Planktonic Dispersal of Mycobacterium avium.* Applied and Environmental Microbiology, 2006. **72**(12): p. 7554-7558.
49. Li, Y.-j., et al., *Identification of virulence determinants of Mycobacterium avium that impact on the ability to resist host killing mechanisms.* Journal of medical microbiology, 2010. **59**(Pt 1): p. 8.
50. Bevins, C.L. and N.H. Salzman, *Paneth cells, antimicrobial peptides and maintenance of intestinal homeostasis.* Nature Reviews Microbiology, 2011. **9**(5): p. 356.
51. Alonso-Hearn, M., et al., *A Mycobacterium avium subsp. paratuberculosis LuxR regulates cell envelope and virulence.* Innate immunity, 2010. **16**(4): p. 235-247.
52. Cooper, A.M., et al., *Expression of the nitric oxide synthase 2 gene is not essential for early control of Mycobacterium tuberculosis in the murine lung.* Infection and immunity, 2000. **68**(12): p. 6879-6882.
53. Greenwell-Wild, T., et al., *Mycobacterium avium infection and modulation of human macrophage gene expression.* The Journal of Immunology, 2002. **169**(11): p. 6286-6297.
54. Krzywinska, E., J. Krzywinski, and J.S. Schorey, *Phylogeny of Mycobacterium avium strains inferred from glycopeptidolipid biosynthesis pathway genes.* Microbiology, 2004. **150**(6): p. 1699-1706.
55. Krzywinska, E., et al., *Mycobacterium avium 104 deleted of the methyltransferase D gene by allelic replacement lacks serotype-specific glycopeptidolipids and shows attenuated virulence in mice.* Molecular Microbiology, 2005. **56**(5): p. 1262-1273.
56. Bhatnagar, S. and J.S. Schorey, *Elevated mitogen-activated protein kinase signalling and increased macrophage activation in cells infected with a glycopeptidolipid-deficient Mycobacterium avium.* Cellular microbiology, 2006. **8**(1): p. 85-96.
57. Pedrosa, J., et al., *Characterization of the virulence of Mycobacterium avium complex (MAC) isolates in mice.* Clinical & Experimental Immunology, 1994. **98**(2): p. 210-216.
58. Sampaio, E.P., et al., *Mycobacterium abscessus and M. avium trigger Toll-like receptor 2 and distinct cytokine response in human cells.* American journal of respiratory cell and molecular biology, 2008. **39**(4): p. 431-439.
59. Bermudez, L.E., M. Petrofsky, and F. Sangari, *Intracellular phenotype of Mycobacterium avium enters macrophages primarily by a macropinocytosis-like mechanism and survives in a compartment that differs from that with extracellular phenotype.* Cell biology international, 2004. **28**(5): p. 411-419.
60. Shrivastava, P. and T. Bagchi, *IL-10 modulates in vitro multinucleate giant cell formation in human tuberculosis.* PloS one, 2013. **8**(10): p. e77680.

61. Wahl, S.M., et al., *Permissive factors for HIV-1 infection of macrophages.* Journal of leukocyte biology, 2000. **68**(3): p. 303-310.
62. Facchetti, F., et al., *Expression of inducible nitric oxide synthase in human granulomas and histiocytic reactions.* The American journal of pathology, 1999. **154**(1): p. 145-152.
63. Krzywinska, E., et al., *Mycobacterium avium 104 deleted of the methyltransferase D gene by allelic replacement lacks serotype-specific glycopeptidolipids and shows attenuated virulence in mice.* Molecular microbiology, 2005. **56**(5): p. 1262-1273.
64. Li, Y., et al., *A Mycobacterium avium PPE gene is associated with the ability of the bacterium to grow in macrophages and virulence in mice.* Cellular microbiology, 2005. **7**(4): p. 539-548.
65. Danelishvili, L., M.J. Poort, and L.E. Bermudez, *Identification of Mycobacterium avium genes up-regulated in cultured macrophages and in mice.* FEMS microbiology letters, 2004. **239**(1): p. 41-49.
66. Hou, J.Y., J.E. Graham, and J.E. Clark-Curtiss, *Mycobacterium avium genes expressed during growth in human macrophages detected by selective capture of transcribed sequences (SCOTS).* Infection and immunity, 2002. **70**(7): p. 3714-3726.
67. Laurent, J.-P., et al., *Mutational analysis of cell wall biosynthesis in Mycobacterium avium.* Journal of bacteriology, 2003. **185**(16): p. 5003-5006.
68. Marrakchi, H., M.-A. Lanéelle, and M. Daffé, *Mycolic acids: structures, biosynthesis, and beyond.* Chemistry & biology, 2014. **21**(1): p. 67-85.
69. Bannantine, J.P., et al., *Cell wall peptidolipids of Mycobacterium avium: from genetic prediction to exact structure of a nonribosomal peptide.* Molecular microbiology, 2017. **105**(4): p. 525-539.
70. Horgen, L., et al., *Exposure of human peripheral blood mononuclear cells to total lipids and serovar-specific glycopeptidolipids from Mycobacterium avium serovars 4 and 8 results in inhibition of TH1-type responses.* Microbial Pathogenesis, 2000. **29**(1): p. 9-16.
71. Guirado, E., et al., *Characterization of clinical and environmental Mycobacterium avium spp. isolates and their interaction with human macrophages.* PloS one, 2012. **7**(9): p. e45411.
72. Mishra, A.K., et al., *Lipoarabinomannan and related glycoconjugates: structure, biogenesis and role in Mycobacterium tuberculosis physiology and host-pathogen interaction.* FEMS microbiology reviews, 2011. **35**(6): p. 1126-1157.
73. Nizet, V., *Antimicrobial peptide resistance mechanisms of human bacterial pathogens.* Current issues in molecular biology, 2006. **8**(1): p. 11.
74. Camacho, L.R., et al., *Analysis of the Phthiocerol Dimycocerosate Locus of Mycobacterium tuberculosis EVIDENCE THAT THIS LIPID IS INVOLVED IN THE CELL WALL PERMEABILITY BARRIER.* Journal of Biological Chemistry, 2001. **276**(23): p. 19845-19854.
75. Melly, G. and G.E. Purdy, *MmpL Proteins in Physiology and Pathogenesis of M. tuberculosis.* Microorganisms, 2019. **7**(3): p. 70.
76. Crellin, P.K., C.-Y. Luo, and Y.S. Morita, *Metabolism of plasma membrane lipids in mycobacteria and corynebacteria.* Lipid Metabolism, 2013. **6**: p. 119-148.
77. Maloney, E., et al., *The Two-Domain LysX Protein of Mycobacterium tuberculosis Is Required for Production of Lysinylated Phosphatidylglycerol and Resistance to Cationic Antimicrobial Peptides.* PLOS Pathogens, 2009. **5**(7): p. e1000534.
78. Maloney, E., et al., *Alterations in Phospholipid Catabolism in Mycobacterium Tuberculosis LysX Mutant.* Frontiers in Microbiology, 2011. **2**: p. 19.
79. Montoya-Rosales, A., et al., *lysX gene is differentially expressed among Mycobacterium tuberculosis strains with different levels of virulence.* Tuberculosis, 2017. **106**: p. 106-117.
80. Zhao, L.-l., et al., *Mutations in lysX as the new and reliable markers for tuberculosis Beijing and modern Beijing strains.* Tuberculosis, 2016. **97**: p. 33-37.

81. Khattak, F.A., et al., *Illegitimate recombination: An efficient method for random mutagenesis in Mycobacterium avium subsp. hominissuis.* BMC Microbiology, 2012. **12**(1): p. 204.
82. Kirubakar, G., et al., *Proteome analysis of a M. avium mutant exposes a novel role of the bifunctional protein LysX in the regulation of metabolic activity.* Journal of Infectious Diseases, 2018. **218**(2): p. 291-299.
83. Murugaiyan, J., et al., *Label-Free Quantitative Proteomic Analysis of Harmless and Pathogenic Strains of Infectious Microalgae, Prototheca spp.* International journal of molecular sciences, 2016. **18**(1): p. 59.
84. Vizcaíno, J.A., et al., *2016 update of the PRIDE database and its related tools.* Nucleic acids research, 2015. **44**(D1): p. D447-D456.
85. Bochner, B.R., P. Gadzinski, and E. Panomitros, *Phenotype microarrays for high-throughput phenotypic testing and assay of gene function.* Genome research, 2001. **11**(7): p. 1246-1255.
86. Bochner, B.R., *Innovations: New technologies to assess genotype-phenotype relationships.* Nature Reviews Genetics, 2003. **4**(4): p. 309.
87. Bochner, B.R., *Global phenotypic characterization of bacteria.* FEMS microbiology reviews, 2008. **33**(1): p. 191-205.
88. Sanchini, A., et al., *Metabolic phenotype of clinical and environmental Mycobacterium avium subsp. hominissuis isolates.* PeerJ, 2017. **5**: p. e2833.
89. Vaas, L.A., et al., *opm: an R package for analysing OmniLog® phenotype microarray data.* Bioinformatics, 2013. **29**(14): p. 1823-1824.
90. Kanehisa, M., et al., *KEGG as a reference resource for gene and protein annotation.* Nucleic acids research, 2015. **44**(D1): p. D457-D462.
91. Sadykov, M.R., et al., *Inactivation of the Pta-AckA pathway causes cell death in Staphylococcus aureus.* Journal of bacteriology, 2013. **195**(13): p. 3035-3044.
92. Fabrino, D.L., et al., *Porins facilitate nitric oxide-mediated killing of mycobacteria.* Microbes and infection, 2009. **11**(10-11): p. 868-875.
93. Sharbati, J., et al., *Integrated microRNA-mRNA-analysis of human monocyte derived macrophages upon Mycobacterium avium subsp. hominissuis infection.* PLoS One, 2011. **6**.
94. Kunisch, R., E. Kamal, and A. Lewin, *The role of the mycobacterial DNA-binding protein 1 (MDP1) from Mycobacterium bovis BCG in host cell interaction.* BMC Microbiology, 2012. **12**.
95. Kitada, S., et al., *Serodiagnosis of pulmonary disease due to Mycobacterium avium complex with an enzyme immunoassay that uses a mixture of glycopeptidolipid antigens.* Clinical Infectious Diseases, 2002. **35**(11): p. 1328-1335.
96. Mukherjee, R., et al., *Hyperglycosylation of glycopeptidolipid of Mycobacterium smegmatis under nutrient starvation: Structural studies.* Microbiology, 2005. **151**(7): p. 2385-2392.
97. Tatusov, R.L., et al., *The COG database: a tool for genome-scale analysis of protein functions and evolution.* Nucleic acids research, 2000. **28**(1): p. 33-36.
98. Huang, D.W., et al., *The DAVID Gene Functional Classification Tool: a novel biological module-centric algorithm to functionally analyze large gene lists.* Genome biology, 2007. **8**(9): p. R183.
99. Wipperman, M.F., N.S. Sampson, and S.T. Thomas, *Pathogen roid rage: cholesterol utilization by Mycobacterium tuberculosis.* Critical reviews in biochemistry and molecular biology, 2014. **49**(4): p. 269-293.
100. Liu, X., et al., *GlnR-mediated regulation of short-chain fatty acid assimilation in Mycobacterium smegmatis.* Frontiers in microbiology, 2018. **9**: p. 1311.
101. Szklarczyk, D., et al., *The STRING database in 2017: quality-controlled protein-protein association networks, made broadly accessible.* Nucleic acids research, 2016: p. gkw937.

102. Hou, J.Y., J.E. Graham, and J.E. Clark-Curtiss, *Mycobacterium avium genes expressed during growth in human macrophages detected by selective capture of transcribed sequences (SCOTS).* Infect Immun, 2002. **70**.
103. Schnappinger, D., et al., *Transcriptional adaptation of Mycobacterium tuberculosis within macrophages: insights into the phagosomal environment.* Journal of Experimental Medicine, 2003. **198**(5): p. 693-704.
104. Janagama, H.K., et al., *Primary transcriptomes of Mycobacterium avium subsp. paratuberculosis reveal proprietary pathways in tissue and macrophages.* BMC Genomics, 2010. **11**(1): p. 561.
105. Eisenreich, W., et al., *Metabolic host responses to infection by intracellular bacterial pathogens.* Frontiers in Cellular and Infection Microbiology, 2013. **3**: p. 24.
106. Lee, W., et al., *Intracellular Mycobacterium tuberculosis exploits host-derived fatty acids to limit metabolic stress.* Journal of Biological Chemistry, 2013. **288**(10): p. 6788-6800.
107. Kitada, S., et al., *Use of glycopeptidolipid core antigen for serodiagnosis of Mycobacterium avium complex pulmonary disease in immunocompetent patients.* Clinical and Diagnostic Laboratory Immunology, 2005. **12**(1): p. 44-51.
108. Sood, G. and N. Parrish, *Outbreaks of nontuberculous mycobacteria.* Current opinion in infectious diseases, 2017. **30**(4): p. 404-409.
109. Le Dantec, C., et al., *Chlorine disinfection of atypical mycobacteria isolated from a water distribution system.* Appl. Environ. Microbiol., 2002. **68**(3): p. 1025-1032.
110. Taylor, R.H., et al., *Chlorine, chloramine, chlorine dioxide, and ozone susceptibility of Mycobacterium avium.* Appl. Environ. Microbiol., 2000. **66**(4): p. 1702-1705.
111. Wallace Jr, R.J., et al., *Macrolide/azalide therapy for nodular/bronchiectatic Mycobacterium avium complex lung disease.* Chest, 2014. **146**(2): p. 276-282.
112. Lee, B.Y., et al., *Risk factors for recurrence after successful treatment of Mycobacterium avium complex lung disease.* Antimicrobial agents and chemotherapy, 2015. **59**(6): p. 2972-2977.
113. Matern, W.M., J.S. Bader, and P.C. Karakousis, *Genome analysis of Mycobacterium avium subspecies hominissuis strain 109.* Scientific data, 2018. **5**: p. 180277.
114. Rengarajan, J., B.R. Bloom, and E.J. Rubin, *Genome-wide requirements for Mycobacterium tuberculosis adaptation and survival in macrophages.* Proceedings of the National Academy of Sciences, 2005. **102**(23): p. 8327-8332.
115. Rhee, K., *Minding the gaps: metabolomics mends functional genomics.* EMBO reports, 2013. **14**(11): p. 949-950.
116. Warner, D.F., *Mycobacterium tuberculosis metabolism.* Cold Spring Harbor perspectives in medicine, 2015. **5**(4): p. a021121.
117. de Carvalho, L.P.S., et al., *Metabolomics of Mycobacterium tuberculosis reveals compartmentalized co-catabolism of carbon substrates.* Chemistry & biology, 2010. **17**(10): p. 1122-1131.
118. Williams, K.J., et al., *The Mycobacterium tuberculosis β-oxidation genes echA5 and fadB3 are dispensable for growth in vitro and in vivo.* Tuberculosis, 2011. **91**(6): p. 549-555.
119. Lee, J.J., et al., *Glutamate mediated metabolic neutralization mitigates propionate toxicity in intracellular Mycobacterium tuberculosis.* Scientific reports, 2018. **8**(1): p. 8506.
120. Rücker, N., et al., *Acetate dissimilation and assimilation in Mycobacterium tuberculosis depend on carbon availability.* Journal of Bacteriology, 2015. **197**(19): p. 3182-3190.
121. Somashekar, B., et al., *Metabolic profiling of lung granuloma in Mycobacterium tuberculosis infected guinea pigs: ex vivo 1H magic angle spinning NMR studies.* Journal of proteome research, 2011. **10**(9): p. 4186-4195.
122. Maurya, R.K., S. Bharti, and M.Y. Krishnan, *Triacylglycerols: Fuelling the Hibernating Mycobacterium tuberculosis.* Frontiers in Cellular and Infection Microbiology, 2019. **8**(450).

123. Garton, N.J., et al., *Intracellular lipophilic inclusions of mycobacteria in vitro and in sputum.* Microbiology, 2002. **148**(10): p. 2951-2958.
124. Reed, M.B., et al., *The W-Beijing lineage of Mycobacterium tuberculosis overproduces triglycerides and has the DosR dormancy regulon constitutively upregulated.* Journal of bacteriology, 2007. **189**(7): p. 2583-2589.
125. Ghazaei, C., *Mycobacterium tuberculosis and lipids: Insights into molecular mechanisms from persistence to virulence.* Journal of research in medical sciences: the official journal of Isfahan University of Medical Sciences, 2018. **23**.
126. Nieto, L.M., C. Mehaffy, and K.M. Dobos, *The physiology of mycobacterium tuberculosis in the context of drug resistance: a system biology perspective*, in *Mycobacterium-Research and Development*. 2017, IntechOpen.
127. Zasloff, M., *Antimicrobial peptides of multicellular organisms.* nature, 2002. **415**(6870): p. 389.
128. Arendt, W., et al., *Resistance phenotypes mediated by aminoacyl-phosphatidylglycerol synthases.* Journal of bacteriology, 2012. **194**(6): p. 1401-1416.
129. Roy, H. and M. Ibba, *RNA-dependent lipid remodeling by bacterial multiple peptide resistance factors.* Proceedings of the National Academy of Sciences, 2008. **105**(12): p. 4667-4672.
130. Klein, S., et al., *Adaptation of Pseudomonas aeruginosa to various conditions includes tRNA-dependent formation of alanyl-phosphatidylglycerol.* Molecular microbiology, 2009. **71**(3): p. 551-565.
131. Schubert, K., et al., *The Antituberculosis Drug Ethambutol Selectively Blocks Apical Growth in CMN Group Bacteria. mBio 8.* 2017.
132. Ma, Y., F. Pan, and M. McNeil, *Formation of dTDP-rhamnose is essential for growth of mycobacteria.* Journal of bacteriology, 2002. **184**(12): p. 3392-3395.
133. Marolda, C.L. and M.A. Valvano, *Genetic analysis of the dTDP-rhamnose biosynthesis region of the Escherichia coli VW187 (O7: K1) rfb gene cluster: identification of functional homologs of rfbB and rfbA in the rff cluster and correct location of the rffE gene.* Journal of bacteriology, 1995. **177**(19): p. 5539-5546.
134. Ma, Y., et al., *Drug targeting Mycobacterium tuberculosis cell wall synthesis: genetics of dTDP-rhamnose synthetic enzymes and development of a microtiter plate-based screen for inhibitors of conversion of dTDP-glucose to dTDP-rhamnose.* Antimicrobial agents and chemotherapy, 2001. **45**(5): p. 1407-1416.
135. Maloney, E., et al., *The two-domain LysX protein of Mycobacterium tuberculosis is required for production of lysinylated phosphatidylglycerol and resistance to cationic antimicrobial peptides.* PLoS Pathogens, 2009. **5**.
136. Pandey, A.K. and C.M. Sassetti, *Mycobacterial persistence requires the utilization of host cholesterol.* Proceedings of the National Academy of Sciences, 2008. **105**(11): p. 4376-4380.
137. McKinney, J.D., et al., *Persistence of Mycobacterium tuberculosis in macrophages and mice requires the glyoxylate shunt enzyme isocitrate lyase.* Nature, 2000. **406**(6797): p. 735.
138. Daniel, J., et al., *Mycobacterium tuberculosis uses host triacylglycerol to accumulate lipid droplets and acquires a dormancy-like phenotype in lipid-loaded macrophages.* PLoS pathogens, 2011. **7**(6): p. e1002093.
139. Stehr, M., A.A. Elamin, and M. Singh, *Lipid inclusions in mycobacterial infections*, in *Tuberculosis-Current Issues in Diagnosis and Management*. 2013, IntechOpen.
140. Danelishvili, L., et al., *Identification of Mycobacterium avium pathogenicity island important for macrophage and amoeba infection.* Proc Natl Acad Sci U S A, 2007. **104**.
141. Marri, P.R., J.P. Bannantine, and G.B. Golding, *Comparative genomics of metabolic pathways in Mycobacterium species: gene duplication, gene decay and lateral gene transfer.* FEMS Microbiol Rev, 2006. **30**.

142. Gomes, M.S., et al., *Survival of Mycobacterium avium andMycobacterium tuberculosis in Acidified Vacuoles of Murine Macrophages.* Infection and immunity, 1999. **67**(7): p. 3199-3206.
143. Tischler, A.D. and J.D. McKinney, *Contrasting persistence strategies in Salmonella and Mycobacterium.* Current Opinion in Microbiology, 2010. **13**(1): p. 93-99.
144. Voskuil, M.I., et al., *The response of Mycobacterium tuberculosis to reactive oxygen and nitrogen species.* Frontiers in Microbiology, 2011. **2**(MAY).
145. Mehta, P.K., R. Dharra, and M. Kulharia, *Could mycobacterial MelF protein (Rv1936) be used as a potential drug target?* 2018, Future Medicine.
146. Vandal, O.H., et al., *Acid-susceptible mutants of mycobacterium tuberculosis share hypersusceptibility to cell wall and oxidative stress and to the host environment.* Journal of Bacteriology, 2009. **191**(2): p. 625-631.
147. Jamaati, H., et al., *Nitric oxide in the pathogenesis and treatment of tuberculosis.* Frontiers in microbiology, 2017. **8**: p. 2008.
148. Shastri, M.D., et al., *Role of oxidative stress in the pathology and management of human tuberculosis.* Oxidative Medicine and Cellular Longevity, 2018. **2018**.
149. Tomioka, H., et al., *Effector molecules of the host defence mechanism against Mycobacterium avium complex: The evidence showing that reactive oxygen intermediates, reactive nitrogen intermediates, and free fatty acids each alone are not decisive in expression of macrophage antimicrobial activity against the parasites.* Clinical and Experimental Immunology, 1997. **109**(2): p. 248-254.
150. Ganz, T., *Antimicrobial polypeptides in host defense of the respiratory tract.* The Journal of clinical investigation, 2002. **109**(6): p. 693-697.
151. Fu, L., *The potential of human neutrophil peptides in tuberculosis therapy.* The International Journal of Tuberculosis and Lung Disease, 2003. **7**(11): p. 1027-1032.
152. Dong, H., et al., *Defensins: the case for their use against mycobacterial infections.* Journal of immunology research, 2016. **2016**.
153. Lehrer, R.I., A.K. Lichtenstein, and T. Ganz, *Defensins: antimicrobial and cytotoxic peptides of mammalian cells.* Annual review of immunology, 1993. **11**(1): p. 105-128.
154. Motamedi, N., L. Danelishvili, and L.E. Bermudez, *Identification of Mycobacterium avium genes associated with resistance to host antimicrobial peptides.* Journal of Medical Microbiology, 2014. **63**(PART 7): p. 923-930.
155. Ryndak, M., S. Wang, and I. Smith, *PhoP, a key player in Mycobacterium tuberculosis virulence.* Trends in Microbiology, 2008. **16**(11): p. 528-534.
156. Rivas-Santiago, B., et al., *Expression of beta defensin 2 in experimental pulmonary tuberculosis: tentative approach for vaccine development.* Archives of medical research, 2012. **43**(4): p. 324-328.
157. Romagnoli, A., et al., *Clinical isolates of the modern Mycobacterium tuberculosis lineage 4 evade host defense in human macrophages through eluding IL-1β-induced autophagy.* Cell death & disease, 2018. **9**(6): p. 624.
158. Flynn, J., J. Chan, and P. Lin, *Macrophages and control of granulomatous inflammation in tuberculosis.* Mucosal immunology, 2011. **4**(3): p. 271.
159. Petruccioli, E., et al., *Correlates of tuberculosis risk: predictive biomarkers for progression to active tuberculosis.* European Respiratory Journal, 2016. **48**(6): p. 1751-1763.
160. González-Pérez, M., et al., *Virulence and immune response induced by mycobacterium avium complex strains in a model of progressive pulmonary tuberculosis and subcutaneous infection in BALB/c mice.* Infection and Immunity, 2013. **81**(11): p. 4001-4012.
161. Shaler, C.R., et al., *Pulmonary mycobacterial granuloma: increased IL-10 production contributes to establishing a symbiotic host-microbe microenvironment.* The American journal of pathology, 2011. **178**(4): p. 1622-1634.

162. Medzhitov, R., *Origin and physiological roles of inflammation*. Nature, 2008. **454**(7203): p. 428.
163. Kumar, S.N., et al., *Granuloma with langhans giant cells: An overview*. Journal of oral and maxillofacial pathology: JOMFP, 2013. **17**(3): p. 420.
164. Haug, M., et al., *Dynamics of immune effector mechanisms during infection with M ycobacterium avium in C 57 BL / 6 mice*. Immunology, 2013. **140**(2): p. 232-243.
165. Shaler, C.R., et al., *Pulmonary mycobacterial granuloma: Increased IL-10 production contributes to establishing a symbiotic host-microbe microenvironment*. American Journal of Pathology, 2011. **178**(4): p. 1622-1634.
166. Shaler, C.R., et al., *Within the Enemy's Camp: contribution of the granuloma to the dissemination, persistence and transmission of Mycobacterium tuberculosis*. Frontiers in immunology, 2013. **4**: p. 30.
167. McClean, C.M. and D.M. Tobin, *Macrophage form, function, and phenotype in mycobacterial infection: lessons from tuberculosis and other diseases*. Pathogens and disease, 2016. **74**(7).
168. Davis, J.M. and L. Ramakrishnan, *The role of the granuloma in expansion and dissemination of early tuberculous infection*. Cell, 2009. **136**(1): p. 37-49.
169. Gharun, K., et al., *Mycobacteria exploit nitric oxide-induced transformation of macrophages into permissive giant cells*. EMBO Reports, 2017. **18**(12): p. 2144-2159.
170. Gharun, K., et al., *Mycobacteria exploit nitric oxide-induced transformation of macrophages into permissive giant cells*. EMBO reports, 2017. **18**(12): p. 2144-2159.
171. Puissegur, M.-P., et al., *Mycobacterial lipomannan induces granuloma macrophage fusion via a TLR2-dependent, ADAM9-and B1 integrin-mediated pathway*. The Journal of Immunology, 2007. **178**(5): p. 3161-3169.
172. Kolly, G.S., et al., *Assessing the essentiality of the decaprenyl-phospho-d-arabinofuranose pathway in M ycobacterium tuberculosis using conditional mutants*. Molecular microbiology, 2014. **92**(1): p. 194-211.
173. Echeverria-Valencia, G., S. Flores-Villalva, and C.I. Espitia, *Virulence factors and pathogenicity of Mycobacterium*. Mycobacterium-Research and Development. Wellman Ribón, IntechOpen, 2018: p. 231-255.
174. Cook, S.M. and J.D. McArthur, *Developing Galleria mellonella as a model host for human pathogens*. Virulence, 2013. **4**(5): p. 350-353.
175. Tsai, C.J.-Y., J.M.S. Loh, and T. Proft, *Galleria mellonella infection models for the study of bacterial diseases and for antimicrobial drug testing*. Virulence, 2016. **7**(3): p. 214-229.
176. Lionakis, M.S., *Drosophila and Galleria insect model hosts: new tools for the study of fungal virulence, pharmacology and immunology*. Virulence, 2011. **2**(6): p. 521-527.
177. Hoffmann, J.A., *Innate immunity of insects*. Current opinion in immunology, 1995. **7**(1): p. 4-10.
178. Browne, N., M. Heelan, and K. Kavanagh, *An analysis of the structural and functional similarities of insect hemocytes and mammalian phagocytes*. Virulence, 2013. **4**(7): p. 597-603.
179. Kavanagh, K. and E.P. Reeves, *Exploiting the potential of insects for in vivo pathogenicity testing of microbial pathogens*. FEMS microbiology reviews, 2004. **28**(1): p. 101-112.
180. Li, Y., et al., *Galleria mellonella-a novel infection model for the Mycobacterium tuberculosis complex*. Virulence, 2018. **9**(1): p. 1126-1137.
181. Meir, M., T. Grosfeld, and D. Barkan, *Establishment and validation of Galleria mellonella as a novel model organism to study Mycobacterium abscessus infection, pathogenesis, and treatment*. Antimicrobial agents and chemotherapy, 2018. **62**(4): p. e02539-17.
182. Entwistle, F. and P.J. Coote, *Evaluation of greater wax moth larvae, Galleria mellonella, as a novel in vivo model for non-tuberculosis Mycobacteria infections and antibiotic treatments*. Journal of medical microbiology, 2018.

183. Kondratieva, E., et al., *Host genetics in granuloma formation: human-like lung pathology in mice with reciprocal genetic susceptibility to M. tuberculosis and M. avium.* PloS one, 2010. **5**(5): p. e10515.
184. Astarie-Dequeker, C., et al., *Phthiocerol dimycocerosates of M. tuberculosis participate in macrophage invasion by inducing changes in the organization of plasma membrane lipids.* PLoS pathogens, 2009. **5**(2): p. e1000289.
185. Wu, C.-w., et al., *A novel cell wall lipopeptide is important for biofilm formation and pathogenicity of Mycobacterium avium subspecies paratuberculosis.* Microbial pathogenesis, 2009. **46**(4): p. 222-230.
186. Johansen, T.B., et al., *Biofilm formation by Mycobacterium avium isolates originating from humans, swine and birds.* BMC microbiology, 2009. **9**(1): p. 159.
187. Pang, L., et al., *Structure and function of mycobacterium glycopeptidolipids from comparative genomics perspective.* Journal of Cellular Biochemistry, 2013. **114**(8): p. 1705-1713.
188. Shimono, N., et al., *Hypervirulent mutant of Mycobacterium tuberculosis resulting from disruption of the mce1 operon.* Proceedings of the national academy of sciences, 2003. **100**(26): p. 15918-15923.
189. ten Bokum, A.M.C., et al., *The case for hypervirulence through gene deletion in Mycobacterium tuberculosis.* Trends in Microbiology, 2008. **16**(9): p. 436-441.

9 Supplementary Material

9.1 Supplementary Table S1: Complete list of proteins identified in the *M. avium* strains (W: wild-type, M: lysXmut and C: lysXcomp) by Proteome analysis and comparative statistical differential analysis

Key:

- *T-test difference column is log2 fold change,*
- *Minus symobol indicates proteins downregulated in group 1 when compared to that of the group 2*
- *Numbers without symbol are upregulated in group 1 when compared to that of the group 2*
- *Proteins with significant fold changes have a p-value < 0.05*
- *Significant differentially expressed proteins of the lysX mutant compared to the wild type which were used for functional enrichment analysis are indicated in colours (red: upregulation, green: downregulation)*
- *Proteins present in the pathway network (Fig. 2) are highlighted with a star **

Protein names	Gene names (ORF)	Statitical analysis (Student t-test)		
		t-test difference		
		P1M_P1W	P1C_P1M	P1C_P1W
Chromosomal replication initiator protein DnaA	MAH_0001	-0.04	0.35	0.31
DNA polymerase III subunit beta	MAH_0003	-0.05	0.01	-0.05
DNA gyrase subunit B	MAH_0006	0.15	-0.07	0.08
DNA gyrase subunit A	MAH_0007	0.08	-0.02	0.06
Uncharacterized protein	MAH_0008	1.44	-2.76	-1.33
Cell wall synthesis protein CwsA	MAH_0037	0.07	0.39	**0.46**
Peptidyl-prolyl cis-trans isomerase	MAH_0038	**-0.31**	0.04	**-0.27**
Serine/threonine protein kinase	MAH_0043	-0.16	0.25	0.10
Serine/threonine protein kinase	MAH_0044	-0.13	-0.08	-0.21
Ppp protein	MAH_0047	-0.12	0.01	-0.11
Uncharacterized protein	MAH_0049	0.04	-0.14	-0.09
Acetyltransferase	MAH_0061	-0.77	0.23	-0.54
Uncharacterized protein	MAH_0070	-0.62	**-3.72**	**-4.34**
Uncharacterized protein	MAH_0072	-0.11	0.07	-0.05
UPF0301 protein MAH_0074	MAH_0074	0.01	**-0.33**	**-0.32**
Proline-rich 28 kDa antigen	MAH_0076	-1.39	0.55	-0.84
Leucine--tRNA ligase (Leucyl-tRNA synthetase)	MAH_0077	**0.55**	**-0.37**	0.18

Short chain dehydrogenase	MAH_0078	0.18	-0.08	0.10
MarR family transcriptional regulator	MAH_0079	-0.42	0.43	0.01
MmcI protein	MAH_0083	0.16	-0.27	-0.11
Alpha/beta hydrolase	MAH_0084	0.01	-0.21	-0.20
Myo-inositol-1-phosphate synthase	MAH_0089	-0.07	0.07	0.00
PadR family transcriptional regulator	MAH_0090	-0.26	0.41	0.15
30S ribosomal protein S6	MAH_0096	0.08	-0.22	-0.13
Single-stranded DNA-binding protein (SSB)	MAH_0097	0.14	**-0.18**	-0.04
30S ribosomal protein S18	MAH_0098	0.10	0.07	0.17
50S ribosomal protein L9	MAH_0099	-0.04	0.05	0.00
Oxidoreductase, short chain dehydrogenase/reductase	MAH_0109	**0.25**	**-0.36**	-0.12
FAD binding domain-containing protein	MAH_0111	-0.39	0.05	-0.35
Uncharacterized protein	MAH_0137	-0.03	-0.12	-0.15
Uncharacterized protein	MAH_0145	-0.54	0.20	-0.33
Cyclopropane-fatty-acyl-phospholipid synthase	MAH_0146	-0.04	0.08	0.04
Glyoxalase	MAH_0147	**-0.65**	**0.25**	**-0.40**
Uncharacterized protein	MAH_0149	0.23	-0.12	0.11
Oxidoreductase	MAH_0152	0.25	-0.05	0.20
Uncharacterized protein	MAH_0154	**-1.03**	0.73	-0.30
Acyl-CoA dehydrogenase domain-containing protein	MAH_0161	0.21	-0.23	-0.02
Esat-6 like protein esxD	MAH_0169	-0.28	0.53	0.24
Esat-6 like protein esxC	MAH_0170	-0.85	0.37	-0.48
Uncharacterized protein	MAH_0172	-0.02	0.08	0.07
ATPase AAA	MAH_0176	0.03	0.22	0.25
Ferredoxin-dependent glutamate synthase 1	MAH_0181	0.74	-0.41	0.33
Glutamate synthase subunit beta	MAH_0182	0.20	-0.12	0.08
Luciferase-like monooxygenase	MAH_0183	**4.07**	-0.24	**3.83**
Uncharacterized protein	MAH_0193	-0.78	0.14	-0.64
Uncharacterized protein	MAH_0194	-0.19	0.14	-0.05
Superoxide dismutase	MAH_0196	0.35	-0.31	0.04
Prephenate dehydratase (PDT)	MAH_0202	**5.65**	0.36	**6.01**
Phosphoglycerate mutase	MAH_0203	-0.20	0.43	0.23
Uncharacterized protein	MAH_0206	0.00	**5.42**	**5.42**
Serine--tRNA ligase	MAH_0207	0.26	-0.16	0.09
Uncharacterized protein	MAH_0209	-1.12	0.10	-1.02
Uncharacterized protein	MAH_0213	0.20	**-6.64**	**-6.43**
Cof family hydrolase	MAH_0219	0.00	0.00	0.00
UDP-galactopyranose mutase	MAH_0223	0.20	0.27	0.47
Bifunctional udp-galactofuranosyl transferase glft	MAH_0224	-0.30	-0.50	-0.79
Esterase	MAH_0228	0.15	-0.15	0.00
Antigen 85-C protein	MAH_0229	**-0.69**	0.38	-0.31
Fatty-acid-CoA ligase FadD32	MAH_0231	0.04	-0.10	-0.05

Polyketide synthase	MAH_0232	**0.52**	-0.14	0.38
Propionyl-CoA carboxylase beta chain	MAH_0233	0.06	-0.08	-0.02
Short chain dehydrogenase	MAH_0245	**5.22**	-0.24	**4.97**
Nucleoside diphosphate kinase regulator	MAH_0248	-0.21	-0.13	-0.34
O-antigen export system ATP-binding protein RfbB	MAH_0252	**6.13**	-0.07	**6.07**
Uncharacterized protein	MAH_0253	-0.09	-0.25	**-0.34**
Cysteine desulfurase	MAH_0255	-0.31	0.27	-0.04
Quinone oxidoreductase	MAH_0256	0.41	0.13	**0.53**
Uncharacterized protein	MAH_0257	-0.15	-1.07	-1.22
Uncharacterized protein	MAH_0258	**-1.39**	**0.75**	-0.64
Enoyl-CoA hydratase	MAH_0260	-0.14	**0.22**	0.08
Uncharacterized protein	MAH_0261	0.08	-0.15	-0.07
Putative phenylalanine aminotransferase	MAH_0263	-0.38	0.51	0.13
Acyl-CoA dehydrogenase	MAH_0265	0.00	**4.58**	**4.58**
S-adenosyl-L-methionine-dependent methyltransferase	MAH_0266	-0.01	-0.14	-0.15
Lipoprotein LpqH	MAH_0271	**-6.19**	**6.12**	-0.07
Phosphotransferase enzyme family protein	MAH_0277	0.00	**6.64**	**6.64**
Thiopurine S-methyltransferase superfamily protein	MAH_0278	0.00	0.00	0.00
Phosphoglycerate mutase	MAH_0279	-0.06	-0.09	-0.15
Phosphotransferase enzyme family protein	MAH_0280	0.07	-0.27	-0.20
Uncharacterized protein	MAH_0286	-0.11	-0.21	-0.32
Uncharacterized protein	MAH_0288	-0.22	0.03	-0.19
Uncharacterized protein	MAH_0295	-0.67	0.11	-0.56
Uncharacterized protein	MAH_0296	**-0.94**	0.44	-0.51
GntR family transcriptional regulator	MAH_0304	-0.45	0.27	-0.18
Haloalkane dehalogenase	MAH_0322	**5.91**	**-5.91**	0.00
Uncharacterized protein	MAH_0324	**-0.40**	0.21	-0.19
DNA polymerase LigD polymerase subunit	MAH_0327	0.01	-0.21	-0.20
Oxidoreductase	MAH_0332	0.00	**5.56**	**5.56**
Uncharacterized protein	MAH_0342	0.07	-0.12	-0.05
Aspartate transaminase	MAH_0344	0.17	-0.18	-0.01
KanY protein	MAH_0348	0.43	**-0.36**	0.07
N-acetylmuramoyl-L-alanine amidase	MAH_0349	0.34	-0.38	-0.03
Nucleoid-associated protein	MAH_0350	-0.29	0.22	-0.07
Recombination protein RecR	MAH_0351	**-0.40**	0.20	-0.20
CobB/CobQ-like glutamine amidotransferase	MAH_0352	-0.10	**-5.10**	**-5.20**
2-isopropylmalate synthase	MAH_0355	0.41	-0.16	0.26
Aspartokinase	MAH_0356	0.24	0.05	0.29
Aspartate-semialdehyde dehydrogenase (ASA dehydrogenase) (ASADH)	MAH_0357	-0.01	-0.04	-0.04
Thiopurine S-methyltransferase superfamily protein	MAH_0369	-0.13	-0.02	-0.15
PadR family transcriptional regulator	MAH_0372	0.58	-0.26	0.32

ATPase	MAH_0377	0.22	-0.01	0.21
GatB/Yqey domain-containing protein	MAH_0381	**0.49**	-0.20	0.29
Dehydrogenase	MAH_0389	-0.28	-0.17	-0.45
Intracellular protease, PfpI family	MAH_0390	-0.56	0.04	**-0.52**
Sigma activity regulator	MAH_0397	-0.05	-0.03	-0.08
Anti-sigma factor antagonist	MAH_0398	**-0.35**	0.07	-0.28
Uncharacterized protein	MAH_0405	0.08	-0.01	0.07
Secreted protein	MAH_0407	0.08	0.46	0.54
Membrane carboxypeptidase (Penicillin-binding protein)	MAH_0408	-0.10	-0.14	-0.24
Anion-transporting ATPase	MAH_0410	0.37	-0.30	0.07
Anion-transporting ATPase	MAH_0411	0.20	0.01	0.22
Uncharacterized protein	MAH_0412	-0.40	0.24	-0.17
Translation initiation inhibitor	MAH_0413	-0.27	0.17	-0.10
Metallo-beta-lactamase	MAH_0414	0.08	-0.29	-0.22
Crp/Fnr family transcriptional regulator protein	MAH_0415	0.33	0.13	**0.46**
Uncharacterized protein	MAH_0422	-1.55	0.18	-1.37
Acetyl-coenzyme A synthetase (AcCoA synthetase)	MAH_0424	0.19	-0.21	-0.03
Uncharacterized protein	MAH_0430	**0.40**	**-0.60**	-0.19
HAD-superfamily protein subfamily protein IB hydrolase	MAH_0431	0.00	0.00	0.00
Uncharacterized protein	MAH_0439	-0.07	0.13	0.06
Cold shock protein A	MAH_0441	**-0.70**	0.05	**-0.65**
DNA topoisomerase 1 (DNA topoisomerase I)	MAH_0443	**-0.31**	**0.38**	0.08
RmlB2 protein	MAH_0447	**5.49**	-0.29	**5.20**
Inorganic pyrophosphatase	MAH_0452	-0.39	0.35	-0.05
Hypoxanthine-guanine phosphoribosyltransferase	MAH_0456	0.20	-0.08	0.12
Zinc-binding dehydrogenase	MAH_0461	0.04	-0.31	-0.28
Monooxygenase	MAH_0462	0.11	0.00	0.11
Alpha/beta hydrolase	MAH_0463	0.07	-0.19	-0.12
Dioxygenase	MAH_0464	-0.66	0.55	-0.11
GTP cyclohydrolase 1	MAH_0466	0.08	-0.15	-0.07
2-amino-4-hydroxy-6-hydroxymethyldihydropteridine pyrophosphokinase	MAH_0469	0.00	0.00	0.00
Uncharacterized protein	MAH_0472	-0.13	0.08	-0.05
Chalcone/stilbene synthase	MAH_0473	-0.22	1.43	1.21
Aspartate 1-decarboxylase	MAH_0475	-0.42	-0.11	-0.53
Type III pantothenate kinase	MAH_0476	-0.71	0.47	-0.25
Lysine--tRNA ligase	MAH_0477	0.12	0.06	0.19
LSR2 protein	MAH_0478	-0.40	0.36	-0.04
ATP-dependent chaperone ClpB	MAH_0479	0.43	-0.16	0.27
Antibiotic biosynthesis monooxygenase domain-containing protein	MAH_0486	**-0.54**	0.35	-0.19
Carbonic anhydrase (Carbonate dehydratase)	MAH_0489	**-0.69**	0.12	**-0.57**

Uncharacterized protein	MAH_0490	-1.04	**0.88**	-0.16
DNA integrity scanning protein DisA (Cyclic di-AMP synthase)	MAH_0491	0.07	-0.06	0.01
Uncharacterized protein	MAH_0493	0.07	-0.11	-0.04
Transcriptional regulator	MAH_0494	**-0.52**	**0.30**	-0.22
2-C-methyl-D-erythritol 4-phosphate cytidylyltransferase	MAH_0495	0.12	-0.25	-0.13
2-C-methyl-D-erythritol 2,4-cyclodiphosphate synthase (MECDP-synthase)	MAH_0496	**5.44**	-0.70	**4.74**
Cysteine--tRNA ligase	MAH_0497	0.50	0.28	0.79
Uncharacterized protein	MAH_0500	-0.15	1.20	1.05
TetR family transcriptional regulator	MAH_0511	0.24	-0.06	0.18
Oxidoreductase	MAH_0512	-1.43	**0.58**	-0.85
Pigment production hydroxylase	MAH_0515	**-0.47**	0.01	-0.46
2-hydroxy-6-oxo-6-phenylhexa-2,4-dienoate hydrolase	MAH_0516	-0.62	0.16	-0.45
FadE31 protein	MAH_0523	-0.13	0.16	0.03
Short chain dehydrogenase	MAH_0526	-0.10	-0.01	-0.11
Acetyl-CoA acetyltransferase	MAH_0528	-0.06	0.18	0.12
Coenzyme A transferase	MAH_0533	-1.67	0.95	-0.72
Short-chain dehydrogenase/reductase SDR	MAH_0536	-0.09	0.06	-0.02
Acetyl-CoA acetyltransferase	MAH_0539	-0.15	0.18	0.03
Cytochrome P450	MAH_0540	-0.22	-0.08	-0.30
Acyl-CoA dehydrogenase	MAH_0541	0.12	-0.12	0.00
FadE29 protein	MAH_0542	**-0.58**	**0.44**	-0.15
Uncharacterized protein	MAH_0543	**-0.59**	0.11	-0.47
MaoC-like dehydratase	MAH_0544	-0.47	0.20	-0.27
Lipid-transfer protein	MAH_0545	-0.08	-0.05	-0.13
UfaA2 protein	MAH_0547	-0.07	0.09	0.02
3-ketosteroid 1-dehydrogenase	MAH_0548	-0.27	0.41	0.13
2-hydroxypenta-2,4-dienoate hydratase	MAH_0549	0.52	-1.09	-0.57
Acetaldehyde dehydrogenase	MAH_0550	-0.22	0.20	-0.03
4-hydroxy-2-oxovalerate aldolase (HOA)	MAH_0551	-0.42	**0.56**	0.14
Uncharacterized protein	MAH_0553	0.07	0.11	0.18
Short chain dehydrogenase	MAH_0554	-0.28	-0.75	-1.03
Uncharacterized protein	MAH_0555	-0.47	-0.32	-0.78
Rieske (2Fe-2S) domain-containing protein	MAH_0557	0.18	0.02	0.20
Acetyl-CoA acetyltransferase	MAH_0560	0.02	-0.12	-0.10
Lipid-transfer protein	MAH_0561	-0.05	0.23	**0.19**
Uncharacterized protein	MAH_0562	0.17	-0.06	0.11
FMN-dependent monooxygenase	MAH_0563	-0.10	**-0.40**	-0.49
Uncharacterized protein	MAH_0564	-0.58	0.09	-0.49
Cytochrome P450	MAH_0565	0.00	0.00	0.00
Enoyl-CoA hydratase	MAH_0567	-0.09	0.09	-0.01
Acyl-CoA synthetase	MAH_0568	-0.22	0.14	-0.08

Acyl-CoA dehydrogenase fadE27	MAH_0575	-0.01	-0.14	-0.14
FadE26_1 protein	MAH_0576	0.40	-0.21	0.19
3-ketoacyl-ACP reductase	MAH_0578	0.34	-0.18	0.15
UDP-forming alpha,alpha-trehalose-phosphate synthase	MAH_0591	-0.24	0.15	-0.09
Uncharacterized protein	MAH_0592	**-0.83**	0.21	**-0.61**
Enoyl-CoA hydratase/carnithine racemase	MAH_0595	-0.15	0.14	-0.01
Short chain dehydrogenase	MAH_0596	-0.21	0.29	0.09
Uncharacterized protein	MAH_0600	-0.52	0.10	-0.41
Lipoprotein LpqH	MAH_0604	-1.46	-0.06	-1.52
Uncharacterized protein	MAH_0609	0.08	-0.13	-0.05
DNA-binding response regulator PhoP	MAH_0610	**5.36**	0.06	**5.42**
HIT domain-containing protein	MAH_0612	**0.44**	**-0.72**	-0.28
Steroid delta-isomerase	MAH_0613	-0.23	-0.02	-0.25
Alcohol dehydrogenase B	MAH_0614	0.02	-0.03	-0.01
Oxidoreductase	MAH_0623	-0.94	1.13	0.18
Phosphoribosylamine--glycine ligase	MAH_0625	-0.01	0.13	**0.12**
Adenylosuccinate lyase (ASL)	MAH_0630	-0.59	0.16	-0.43
Phosphoribosylaminoimidazole-succinocarboxamide synthase	MAH_0633	0.09	-0.23	-0.14
PtrBa protein	MAH_0634	**-0.54**	0.16	-0.38
Fumarate reductase/succinate dehydrogenase flavoprotein domain-containing protein	MAH_0640	**4.33**	0.26	**4.58**
Zn-dependent hydrolase	MAH_0641	**0.30**	**-0.46**	-0.16
Phosphoribosylformylglycinamidine synthase subunit PurS	MAH_0643	-0.29	0.09	-0.20
Phosphoribosylformylglycinamidine synthase subunit PurQ	MAH_0644	**0.24**	**-0.15**	0.09
Cupin domain-containing protein	MAH_0647	**-0.53**	0.13	**-0.40**
29 kDa antigen Cfp29	MAH_0648	-0.05	-0.12	-0.17
Dyp-type peroxidase	MAH_0650	-0.06	0.28	0.22
Probable M18 family aminopeptidase 2	MAH_0651	-0.74	0.03	-0.71
Phosphoribosylformylglycinamidine synthase subunit PurL	MAH_0654	0.21	-0.18	0.04
Phosphoribosylformylglycinamidine cyclo-ligase	MAH_0658	-0.58	0.12	-0.46
Uncharacterized protein	MAH_0659	-0.44	0.38	-0.06
Glycine cleavage T-protein	MAH_0660	0.44	**-0.37**	0.07
UPF0678 fatty acid-binding protein-like protein	MAH_0662	-0.11	-0.04	-0.15
SseC protein	MAH_0663	-0.57	0.13	-0.43
Sulfurtransferase	MAH_0664	0.07	-0.22	-0.15
Transcriptional regulator	MAH_0668	0.07	-0.10	-0.03
Phosphate-specific transport system accessory protein PhoU	MAH_0674	0.19	0.11	0.30
Acyl-[acyl-carrier protein] desaturase DesA1	MAH_0677	0.11	-0.15	-0.04
Cold-shock DNA-binding protein family	MAH_0691	**-1.38**	**1.14**	-0.24
Enoyl-CoA hydratase/isomerase	MAH_0706	-0.08	0.35	0.27
Acetyl-CoA acetyltransferase	MAH_0709	**7.18**	0.14	**7.31**

NarL_1 protein	MAH_0712	0.37	-0.64	-0.27
Amidohydrolase	MAH_0731	-0.63	**0.50**	-0.13
Short chain dehydrogenase	MAH_0736	0.08	-0.11	-0.04
Carveol dehydrogenase	MAH_0737	-0.28	0.39	0.11
Transcriptional regulator	MAH_0738	-0.13	0.50	0.37
Uncharacterized protein	MAH_0743	-0.89	-0.85	-1.74
Amidohydrolase 2	MAH_0748	0.95	-0.65	0.30
Acetyl-CoA acetyltransferase	MAH_0750	-0.87	-0.13	-1.01
Uncharacterized protein	MAH_0755	**5.35**	**-5.35**	0.00
Cytochrome P450	MAH_0788	**5.24**	-0.29	**4.95**
Dehydrogenase	MAH_0790	-0.17	-0.09	-0.26
Aldehyde dehydrogenase	MAH_0791	**-0.25**	0.03	-0.22
L-carnitine dehydratase/bile acid-inducible protein F	MAH_0792	-0.07	-0.12	-0.19
Amidohydrolase 2	MAH_0817	-0.09	0.19	0.09
Pdc protein	MAH_0823	0.00	**-0.45**	-0.45
Cyclase/dehydrase	MAH_0824	-0.89	-0.52	-1.41
Cyclase/dehydrase	MAH_0826	-0.55	0.10	-0.44
Acetyl-CoA acetyltransferase (*fadA*)*	MAH_0829	**0.41**	-0.15	0.26
Acyl-CoA dehydrogenase (*fadB*)*	MAH_0830	**0.46**	-0.13	0.32
Methyltransferase type 12	MAH_0831	0.87	-0.40	0.47
Methyltransferase type 12	MAH_0832	**4.83**	0.64	**5.47**
F420-dependent oxidoreductase	MAH_0833	0.04	0.04	0.07
Luciferase family protein	MAH_0836	-0.01	0.01	0.00
Antibiotic biosynthesis monooxygenase domain-containing protein	MAH_0837	0.23	-0.31	-0.09
DNA or RNA helicase of superfamily protein II	MAH_0840	0.00	0.00	0.00
Uncharacterized protein	MAH_0842	0.86	-0.47	0.40
Cyclic pyranopterin monophosphate synthase accessory protein	MAH_0843	-0.23	**-0.63**	-0.86
Molybdenum cofactor synthesis domain-containing protein	MAH_0844	-0.29	**0.35**	0.06
CspB protein	MAH_0850	-0.14	0.09	-0.05
Glutathione S-transferase	MAH_0852	**0.75**	**-0.22**	**0.53**
Cyclase/dehydrase	MAH_0858	0.17	0.53	0.70
MarR family transcriptional regulator	MAH_0860	0.16	0.16	0.31
Phosphoserine aminotransferase	MAH_0864	0.18	-0.12	0.06
NADPH:adrenodoxin oxidoreductase fprB	MAH_0866	**6.27**	**-6.27**	0.00
Glyoxalase	MAH_0867	-0.12	0.00	-0.12
Citrate synthase 2	MAH_0868	0.29	-0.19	0.09
Citrate synthase(*gltA1/prpC*)*	MAH_0870	**0.38**	-0.24	0.13
Uncharacterized protein	MAH_0872	0.16	-0.18	-0.02
Two component transcriptional regulator	MAH_0874	-0.04	-0.12	-0.16
Enoyl-CoA hydratase (*echA6*)*	MAH_0880	**0.56**	-0.23	**0.34**
Metallo-beta-lactamase	MAH_0881	0.11	**-0.57**	-0.46

Uncharacterized protein	MAH_0884	-0.50	0.12	**-0.37**
Uncharacterized protein	MAH_0885	0.31	-0.47	-0.16
Uncharacterized protein	MAH_0888	-0.31	0.08	-0.23
Oxidoreductase	MAH_0893	-0.02	0.01	-0.02
Short chain dehydrogenase	MAH_0897	-0.11	0.30	0.19
Phosphate-binding protein PstS	MAH_0898	**0.69**	**-0.55**	0.14
Non-homologous end joining protein Ku	MAH_0901	-0.32	0.10	-0.23
Bifunctional 2-hydroxyhepta-2,4-diene-1,7-dioate isomerase	MAH_0908	**0.56**	**-0.60**	-0.04
S-adenosyl-L-methionine-dependent methyltransferase	MAH_0909	-0.15	-0.18	-0.33
EchA12_1 protein	MAH_0910	0.22	-0.39	-0.18
Oxidoreductase	MAH_0911	0.08	-0.05	0.04
Stas domain-containing protein	MAH_0912	-1.18	**0.63**	-0.55
P-aminobenzoate N-oxygenase AurF	MAH_0914	**3.80**	-0.57	**3.23**
Glucose-6-phosphate isomerase (GPI) (*pgi*)*	MAH_0918	**0.41**	-0.18	0.23
Chorismate mutase	MAH_0919	0.02	-0.02	0.00
Succinyl-CoA ligase [ADP-forming] subunit beta	MAH_0923	0.06	-0.05	0.02
Succinyl-CoA ligase [ADP-forming] subunit alpha	MAH_0924	-0.25	0.15	-0.11
Luciferase family protein	MAH_0926	**0.24**	-0.08	0.16
Phosphoribosylglycinamide formyltransferase	MAH_0929	-0.05	0.12	0.07
Bifunctional purine biosynthesis protein PurH	MAH_0930	-0.16	0.29	0.13
Uncharacterized protein	MAH_0931	-0.42	0.36	-0.07
Mg-chelatase subunit ChlI	MAH_0932	**0.23**	**-0.21**	0.02
Morphine 6-dehydrogenase	MAH_0934	0.27	-0.16	0.11
Enoyl-CoA hydratase (*echA7*)*	MAH_0936	**0.37**	**-0.44**	-0.07
Acyl-CoA dehydrogenase domain-containing protein (*fadE12*)*	MAH_0937	**0.30**	-0.06	0.24
Carbamoyl-phosphate synthase L subunit (*accA2*)*	MAH_0938	**0.61**	-0.37	0.24
Acetyl-CoA carboxylase carboxyltransferase	MAH_0939	**0.47**	**-0.51**	-0.04
Acyl-CoA dehydrogenase domain-containing protein	MAH_0940	0.31	0.05	0.36
Uncharacterized protein	MAH_0941	-0.39	-0.02	-0.41
Two component response transcriptional regulator MprA	MAH_0943	-0.01	**-0.63**	**-0.64**
Protease	MAH_0945	**0.25**	**-0.27**	-0.02
MoaB2 protein	MAH_0946	0.06	-0.20	-0.13
Large-conductance mechanosensitive channel	MAH_0947	**-1.51**	**1.26**	-0.25
Regulatory protein, FmdB family protein	MAH_0949	0.29	-0.37	-0.09
UTP-glucose-1-phosphate uridylyltransferase	MAH_0951	-0.05	-0.05	-0.09
Molybdopterin biosynthesis protein moeA	MAH_0952	-0.01	0.15	0.14
ISAfe7, transposase OrfA	MAH_0956	**-0.48**	1.34	0.86
Uncharacterized protein	MAH_0963	-0.38	0.19	-0.19
Phosphoheptose isomerase	MAH_0975	**-5.71**	**4.45**	-1.26
Arginine deiminase (ADI)	MAH_0981	-0.01	0.11	0.10

Methyltransferase FkbM	MAH_0990	0.07	-0.50	-0.43
Chain length determinant protein	MAH_0992	-1.18	0.22	-0.96
Uncharacterized protein	MAH_1010	0.00	**5.80**	**5.80**
Methionine--tRNA ligase	MAH_1013	0.38	-0.30	0.08
Long-chain-fatty-acid--CoA ligase	MAH_1018	-0.16	0.02	-0.13
50S ribosomal protein L25 (General stress protein CTC)	MAH_1020	0.23	-0.38	-0.15
Retinol dehydrogenase	MAH_1021	0.20	-0.01	0.19
Arsenate reductase	MAH_1023	0.09	-0.04	0.06
Ribose-phosphate pyrophosphokinase (RPPK)	MAH_1024	0.05	-0.09	-0.04
Bifunctional protein GlmU	MAH_1025	0.21	-0.09	0.12
TetR-family transcriptional regulator	MAH_1026	-0.21	-0.53	-0.75
Nucleoside triphosphate pyrophosphohydrolase	MAH_1029	0.53	-1.45	-0.92
Enolase	MAH_1031	-0.14	0.03	-0.11
Winged helix family two component transcriptional regulator	MAH_1036	-2.31	0.92	-1.39
EsaT-6 like protein EsxN	MAH_1044	-0.50	0.22	-0.28
ESAT-6-like protein	MAH_1045	-0.32	0.30	-0.02
Long-chain-fatty-acid-CoA ligase	MAH_1054	-0.01	0.62	0.61
Enoyl-CoA hydratase	MAH_1063	0.10	0.02	0.12
3-hydroxyisobutyryl-CoA hydrolase	MAH_1064	-0.15	0.03	-0.12
Acetyl-CoA acetyltransferase (*fadA3*)*	MAH_1066	**0.21**	**-0.16**	0.05
CysM2 protein	MAH_1069	-0.12	-0.08	-0.20
Cystathionine gamma-synthase	MAH_1071	-0.33	-0.22	-0.55
Transcription elongation factor GreA (Transcript cleavage factor GreA)	MAH_1072	0.16	-0.13	0.03
Mycothiol S-conjugate amidase	MAH_1074	-0.01	-0.23	-0.23
Steroid delta-isomerase	MAH_1077	**-0.35**	0.16	-0.19
Serine hydroxymethyltransferase (SHMT) (Serine methylase)	MAH_1083	**0.43**	**-0.30**	0.13
DesA2 protein	MAH_1084	0.11	-0.19	-0.08
Fumarate hydratase class II (Fumarase C)	MAH_1089	0.19	-0.16	0.04
Fructose-1,6-bisphosphatase	MAH_1090	0.07	-0.07	0.00
Dienelactone hydrolase	MAH_1092	0.19	-0.09	0.11
Cholesterol dehydrogenase	MAH_1094	**5.06**	-0.22	**4.84**
Exodeoxyribonuclease 7 small subunit	MAH_1095	-0.17	0.08	-0.09
Uncharacterized protein	MAH_1097	0.14	-0.17	-0.02
4-hydroxy-3-methylbut-2-enyl diphosphate reductase	MAH_1098	0.20	0.48	0.68
Ribosome-binding ATPase YchF	MAH_1100	0.07	-0.06	0.00
Uncharacterized protein	MAH_1103	**-0.67**	0.52	-0.15
Glyoxalase	MAH_1106	0.31	-0.36	-0.05
Antibiotic biosynthesis monooxygenase	MAH_1110	0.00	0.17	0.17
Glucose-6-phosphate 1-dehydrogenase (G6PD)	MAH_1113	-0.01	-0.29	-0.29
6-phosphogluconate dehydrogenase	MAH_1114	0.10	-0.09	0.00
BpoB protein	MAH_1115	**-0.70**	0.14	-0.56

Oxidoreductase, short chain dehydrogenase/reductase	MAH_1125	0.04	0.23	0.27
Aldehyde dehydrogenase	MAH_1136	**-0.82**	**0.99**	0.17
Acetyl-CoA acetyltransferase	MAH_1137	**-0.21**	**0.14**	-0.08
Carnitinyl-CoA dehydratase	MAH_1138	-0.54	0.39	-0.14
Enoyl-CoA hydratase	MAH_1144	-0.19	0.04	-0.14
Alpha-methylacyl-CoA racemase	MAH_1145	-0.35	0.11	-0.24
Uncharacterized protein	MAH_1146	-0.12	**0.33**	0.21
GntR family transcriptional regulator	MAH_1151	0.07	-0.08	-0.01
Pyridoxamine 5'-phosphate oxidase	MAH_1153	0.16	**-0.39**	-0.23
Uncharacterized protein	MAH_1154	-0.53	0.51	-0.02
HhH-GPD family protein	MAH_1155	-0.28	-0.39	-0.68
Putative pterin-4-alpha-carbinolamine dehydratase (PHS)	MAH_1161	-0.11	-0.14	-0.25
Uncharacterized protein	MAH_1162	-0.10	-0.11	-0.21
GTP-binding protein TypA/BipA	MAH_1168	0.19	-0.27	-0.08
TetR family transcriptional regulator	MAH_1170	**5.38**	**-5.38**	0.00
Ferredoxin	MAH_1176	-0.21	-0.23	-0.44
N-succinyldiaminopimelate aminotransferase	MAH_1177	0.02	0.01	0.03
PPE family protein	MAH_1183	-0.42	0.84	0.41
Adenylyl-sulfate kinase	MAH_1184	-0.42	-0.19	**-0.61**
Sulfate adenylyltransferase	MAH_1185	0.11	0.18	0.29
Uncharacterized protein	MAH_1186	-0.21	0.15	-0.06
Hydrolase, alpha/beta hydrolase family protein	MAH_1201	**0.65**	**-0.55**	0.09
2,3,4,5-tetrahydropyridine-2,6-dicarboxylate N-succinyltransferase	MAH_1204	0.15	-0.10	0.05
Long-chain-acyl-CoA synthetase	MAH_1212	-0.15	0.38	0.23
Glucose-1-phosphate adenylyltransferase	MAH_1218	0.46	**-0.44**	0.02
ABC transporter-like protein	MAH_1222	**5.15**	**-5.15**	0.00
O-methyltransferase, family protein 3	MAH_1224	-0.02	-0.19	-0.21
Trypsin	MAH_1227	-0.10	0.20	0.10
Iron-sulfur cluster carrier protein	MAH_1229	0.31	-0.21	0.10
Mg/Co/Ni transporter MgtE	MAH_1232	0.00	**6.15**	**6.15**
SugC protein	MAH_1238	-0.32	0.15	-0.17
Malate dehydrogenase (*mdh*)*	MAH_1241	**0.15**	-0.07	0.08
Short chain alcohol dehydrogenase	MAH_1245	0.56	-0.30	0.27
Alpha-ketoglutarate decarboxylase	MAH_1246	0.33	-0.15	0.18
ATP-dependent RNA helicase DeaD	MAH_1263	0.04	-0.01	0.03
Oxidoreductase, FAD-binding	MAH_1267	-0.14	0.04	-0.09
Monooxygenase	MAH_1271	-0.22	0.27	0.06
HIT family protein	MAH_1274	**5.44**	**-5.44**	0.00
Amidase (*amiB2*)*	MAH_1275	**5.40**	-1.21	***4.19***
Uncharacterized protein	MAH_1278	0.66	-0.14	0.52
Carbonic anhydrase	MAH_1296	-0.18	**0.36**	0.19
Uncharacterized protein	MAH_1297	0.11	-0.13	-0.02

StaS protein	MAH_1300	0.19	-0.02	0.17
Glyoxalase/bleomycin resistance protein/dioxygenase	MAH_1301	-0.28	0.03	-0.25
Glyoxalase/bleomycin resistance protein/dioxygenase	MAH_1302	-0.20	-0.05	-0.26
Steroid delta-isomerase	MAH_1306	-0.70	0.29	-0.41
Uncharacterized protein	MAH_1310	**-4.41**	0.00	**-4.41**
Arginine--tRNA ligase	MAH_1314	**5.43**	0.03	**5.46**
Diaminopimelate decarboxylase (DAP decarboxylase) (DAPDC)	MAH_1315	0.15	**-0.41**	-0.26
Homoserine dehydrogenase	MAH_1316	0.21	-0.03	0.19
Threonine synthase	MAH_1317	0.04	-0.12	-0.08
Transcription termination factor Rho	MAH_1319	-0.12	0.07	-0.05
50S ribosomal protein L31	MAH_1320	0.15	0.04	0.19
Peptide chain release factor 1 (RF-1)	MAH_1321	-0.17	0.20	0.04
Translation factor (SUA5)	MAH_1323	0.12	-0.13	0.00
ATP synthase subunit b (ATP synthase F(0) sector subunit b)	MAH_1328	-0.23	0.55	0.32
F0F1 ATP synthase subunit delta	MAH_1329	-0.15	0.46	0.31
ATP synthase subunit alpha	MAH_1330	**0.20**	**-0.19**	0.01
ATP synthase gamma chain (ATP synthase F1 sector gamma subunit)	MAH_1331	0.01	0.08	0.09
ATP synthase subunit beta	MAH_1332	0.07	**-0.20**	-0.13
ATP synthase epsilon chain (ATP synthase F1 sector epsilon subunit)	MAH_1333	-0.06	-0.02	-0.08
ATP:cob(I)alamin adenosyltransferase	MAH_1335	0.08	-0.29	-0.22
UDP-N-acetylglucosamine 1-carboxyvinyltransferase	MAH_1336	0.75	-0.22	0.53
Methylated-DNA--protein-cysteine methyltransferase	MAH_1338	-0.95	**-4.41**	**-5.36**
Methylmalonyl-CoA epimerase	MAH_1346	-0.03	0.07	0.04
Acetyl-CoA acetyltransferase (*fadA4*)*	MAH_1347	**0.33**	**-0.21**	0.12
Thioredoxin	MAH_1348	-0.14	-0.15	-0.29
1,4-alpha-glucan branching enzyme GlgB	MAH_1349	-0.09	-0.15	-0.24
Alpha-1,4 glucan phosphorylase	MAH_1351	**0.45**	**-0.38**	0.07
Nicotinate phosphoribosyltransferase	MAH_1353	-0.52	-0.68	-1.20
ATP-dependent Clp protease adapter protein ClpS	MAH_1354	-0.75	-0.11	-0.86
Transcriptional regulator	MAH_1355	**0.34**	-0.30	0.05
Metal-dependent hydrolase of the beta-lactamase III	MAH_1359	-0.41	0.35	-0.07
Ribonuclease PH (RNase PH)	MAH_1360	-0.14	-0.01	-0.16
Uncharacterized protein	MAH_1368	**-1.88**	1.08	-0.80
Acyl-CoA dehydrogenase	MAH_1374	-0.14	**-0.62**	-0.76
3-ketoacyl-ACP reductase	MAH_1375	**0.47**	-0.29	0.18
Acyl-CoA dehydrogenase	MAH_1378	0.12	1.07	1.18
TetR family transcriptional regulator	MAH_1393	0.11	-0.25	-0.14
Uncharacterized protein	MAH_1396	**4.73**	**-4.73**	0.00

AccD4_2 protein (MAV_1608)*	MAH_1415	**5.11**	0.08	**5.19**
Alpha/beta hydrolase	MAH_1423	**-0.50**	0.23	-0.27
Anti-anti-sigma factor	MAH_1426	**-0.57**	0.28	-0.29
Amidohydrolase	MAH_1431	-0.45	0.49	0.04
Uncharacterized protein	MAH_1446	**-0.72**	0.40	-0.32
Fatty acid synthase fas	MAH_1454	0.82	-0.14	0.68
Holo-[acyl-carrier-protein] synthase (Holo-ACP synthase)	MAH_1455	0.19	0.26	0.45
Uncharacterized protein	MAH_1456	0.14	**-5.89**	**-5.75**
Alkyl hydroperoxide reductase/ Thiol specific antioxidant/ Mal allergen	MAH_1457	0.18	**-0.22**	-0.05
Oligoribonuclease	MAH_1467	0.23	-0.16	0.07
ATP-binding protein	MAH_1468	0.08	-0.56	-0.49
Short chain dehydrogenase	MAH_1469	**0.45**	-0.36	0.09
AccD1 protein	MAH_1473	0.39	-0.44	-0.05
Acetyl-/propionyl-coenzyme A carboxylase subunit alpha	MAH_1474	0.24	-0.19	0.05
FadE19 protein	MAH_1475	0.08	-0.14	-0.06
Acyl dehydratase	MAH_1476	0.23	-0.29	-0.06
CitE protein	MAH_1477	-0.01	-0.02	-0.02
Enoyl-CoA hydratase	MAH_1481	-0.03	0.00	-0.04
Uncharacterized protein	MAH_1484	0.78	0.27	1.05
Acyltransferase	MAH_1487	0.00	0.00	0.00
ABC transporter ATP-binding protein	MAH_1491	0.28	-0.11	0.17
Uncharacterized protein	MAH_1494	-0.04	**-5.46**	**-5.50**
Alpha-amylase	MAH_1496	0.29	0.00	0.29
Uncharacterized protein	MAH_1500	-0.14	0.08	-0.05
Aminopeptidase N	MAH_1501	0.44	-0.20	0.25
DsbA oxidoreductase	MAH_1502	0.10	-0.09	0.01
Ribose-5-phosphate isomerase B	MAH_1503	0.05	0.00	0.04
Trigger factor (TF)	MAH_1506	-0.18	-0.10	**-0.28**
ATP-dependent Clp protease proteolytic subunit	MAH_1507	**0.42**	-0.24	0.18
ATP-dependent Clp protease proteolytic subunit	MAH_1508	0.03	-0.07	-0.04
ATP-dependent Clp protease ATP-binding subunit ClpX	MAH_1510	0.12	-0.12	0.00
2-oxoglutarate--ferredoxin oxidoreductase alpha subunit	MAH_1511	-0.03	0.02	-0.01
2-oxoglutarate ferredoxin oxidoreductase subunit beta	MAH_1512	0.16	-0.10	0.07
Probable molybdenum cofactor guanylyltransferase	MAH_1513	**0.19**	**-0.24**	-0.05
Valine--tRNA ligase	MAH_1517	0.78	-0.38	0.40
FolC protein	MAH_1518	-0.30	0.18	-0.12
Nucleoside diphosphate kinase (NDK) (NDP kinase)	MAH_1520	**0.30**	-0.24	0.06
Rne protein	MAH_1521	-0.06	-0.08	-0.14
50S ribosomal protein L21	MAH_1522	-0.09	0.25	0.16

50S ribosomal protein L27	MAH_1523	-0.38	0.22	-0.16
GTPase Obg	MAH_1524	0.04	-0.03	0.01
Glutamate 5-kinase	MAH_1525	0.00	0.00	0.00
NAD synthetase	MAH_1530	-0.65	-0.22	-0.86
Gamma-glutamyl phosphate reductase (GPR)	MAH_1540	-0.17	0.09	-0.08
Ribosomal silencing factor RsfS	MAH_1544	-0.02	-0.46	-0.48
Phosphoglycerate mutase	MAH_1545	0.00	0.01	0.01
Dihydrodipicolinate reductase N-terminus domain-containing protein	MAH_1550	-0.24	0.15	-0.09
Pyridoxamine 5'-phosphate oxidase	MAH_1558	-0.65	0.39	-0.26
Pimeloyl-CoA dehydrogenase	MAH_1559	-0.10	0.01	-0.09
Acyl-CoA dehydrogenase	MAH_1560	-0.20	0.13	-0.08
30S ribosomal protein S20	MAH_1564	**-0.80**	**0.88**	0.08
CBS domain-containing protein	MAH_1570	-0.59	0.41	-0.18
Glycoside hydrolase 15-like protein	MAH_1574	-0.13	-0.18	-0.31
Sulfate/thiosulfate import ATP-binding protein CysA	MAH_1579	0.00	**4.77**	**4.77**
Acyl-[acyl-carrier protein] desaturase DesA1	MAH_1585	0.25	-0.06	0.19
Low molecular weight antigen MTB12	MAH_1635	**-0.67**	0.13	-0.54
Low molecular weight antigen MTB12	MAH_1636	**-0.63**	0.37	-0.26
Uncharacterized protein	MAH_1639	5.18	0.50	**5.69**
Chaperone protein DnaJ	MAH_1642	**0.35**	-0.21	0.15
Uncharacterized protein	MAH_1653	0.49	-0.89	-0.39
ArsR family transcriptional regulator	MAH_1655	**5.45**	-0.66	**4.80**
Glycine--tRNA ligase	MAH_1656	**0.52**	**-0.31**	0.22
Cysteine synthase	MAH_1670	**-0.24**	-0.03	**-0.28**
Major membrane protein 1	MAH_1673	0.24	**-0.35**	-0.10
Cysteine desulfurase	MAH_1674	0.12	-0.16	-0.04
Sulfotransferase	MAH_1677	**-4.40**	0.00	**-4.40**
Acyl-CoA oxidase	MAH_1693	0.41	-0.16	0.25
Modulator of DNA gyrase	MAH_1705	-0.25	-0.14	-0.39
CalR5 protein	MAH_1706	0.29	-0.26	0.03
Uncharacterized protein	MAH_1707	-0.59	1.38	0.79
Methyltransferase, UbiE/COQ5 family protein	MAH_1725	-0.20	0.20	0.00
Uncharacterized protein	MAH_1730	**-0.21**	0.17	-0.04
Chaperone protein HtpG (Heat shock protein HtpG) (High temperature protein G)	MAH_1731	-0.07	-0.09	-0.16
Luciferase family protein	MAH_1733	-0.27	-0.01	-0.29
MgtE intracellular domain protein	MAH_1735	-0.19	0.05	-0.14
Acetyl-CoA C-acyltransferase (*fadA5*)*	MAH_1740	**5.62**	-0.09	**5.53**
CysQ_2 protein	MAH_1742	-0.24	0.00	-0.25
Haloalkane dehalogenase	MAH_1743	-0.55	**0.72**	0.16
Sulfurtransferase	MAH_1753	0.06	0.10	0.16
Acyl-CoA synthase*	MAH_1787	**5.03**	**-5.03**	0.00
NAD dependent epimerase/dehydratase	MAH_1789	0.11	-0.01	0.10

Cupin domain-containing protein	MAH_1813	-0.08	-0.03	-0.12
Aldo/keto reductase	MAH_1816	**0.42**	**-0.30**	0.11
Threonine--tRNA ligase	MAH_1820	0.03	-0.06	-0.03
Diadenosine tetraphosphate	MAH_1821	0.05	-0.27	-0.23
Pyridoxal 5'-phosphate synthase subunit PdxS (PLP synthase subunit PdxS)	MAH_1826	0.21	-0.20	0.01
TesB2 protein	MAH_1827	0.34	0.11	**0.45**
Pyridoxal 5'-phosphate synthase subunit PdxT	MAH_1828	**5.00**	**-5.00**	0.00
Probable transcriptional regulatory protein MAH_1829	MAH_1829	0.03	-0.13	-0.11
Holliday junction ATP-dependent DNA helicase RuvA	MAH_1836	-0.33	0.23	-0.11
4-aminobutyrate aminotransferase	MAH_1840	0.45	-0.09	0.37
Peptidyl-prolyl cis-trans isomerase (PPIase)	MAH_1848	0.38	**-5.68**	**-5.30**
Histidine--tRNA ligase	MAH_1850	0.09	0.26	0.35
Dihydrodipicolinate synthetase	MAH_1859	0.18	-0.15	0.03
Metallopeptidase, zinc binding	MAH_1860	**-1.26**	0.85	-0.40
Aspartyl-tRNA synthetase	MAH_1863	0.12	0.11	0.23
Uncharacterized protein	MAH_1864	**5.94**	**-5.94**	0.00
Deazaflavin-dependent nitroreductase family protein	MAH_1868	0.03	-0.20	-0.17
Uncharacterized protein	MAH_1870	-0.61	0.63	0.02
Uncharacterized protein	MAH_1876	-0.48	-0.03	-0.51
Uncharacterized protein	MAH_1877	-0.82	0.38	-0.44
Secondary thiamine-phosphate synthase enzyme	MAH_1878	-0.19	-0.19	-0.39
Alanine--tRNA ligase	MAH_1879	0.18	-0.12	0.06
Chorismate synthase (CS)	MAH_1893	**0.48**	**-0.25**	0.23
3-dehydroquinate synthase	MAH_1895	0.50	-0.31	0.19
3-dehydroquinate dehydratase (3-dehydroquinase)	MAH_1896	**4.50**	0.11	**4.61**
PepQ protein	MAH_1898	-0.02	-0.11	-0.12
Elongation factor P	MAH_1899	-0.07	-0.03	-0.09
N utilization substance protein B homolog (Protein NusB)	MAH_1900	0.00	0.00	0.00
Bifunctional protein PyrR	MAH_1916	0.05	-0.25	-0.20
Aspartate carbamoyltransferase	MAH_1917	0.53	-0.35	0.18
Dihydroorotase (DHOase)	MAH_1918	0.33	-0.09	0.24
Carbamoyl-phosphate synthase small chain	MAH_1920	**0.29**	**-0.45**	-0.16
Carbamoyl-phosphate synthase large chain	MAH_1921	0.23	0.05	0.28
TobE protein	MAH_1923	-0.28	0.00	-0.27
Integration host factor	MAH_1924	0.04	-0.01	0.03
Guanylate kinase	MAH_1925	-0.77	-0.38	-1.15
DNA-directed RNA polymerase subunit omega (RNAP omega subunit)	MAH_1926	-0.34	0.05	-0.29
S-adenosylmethionine synthase (AdoMet synthase)	MAH_1928	0.09	0.00	0.08
Alpha/beta hydrolase	MAH_1930	-0.12	0.15	0.03

Ribulose-phosphate 3-epimerase (*rpe*)*	MAH_1937	**5.31**	0.12	**5.43**
Riboflavin biosynthesis protein RibD	MAH_1938	0.14	**-6.07**	**-5.93**
LprG protein	MAH_1940	0.22	-0.28	-0.06
Riboflavin synthase subunit alpha	MAH_1941	0.41	**-5.65**	**-5.24**
Riboflavin biosynthesis protein RibBA	MAH_1942	-0.26	0.21	-0.05
6,7-dimethyl-8-ribityllumazine synthase (DMRL synthase) (LS) (Lumazine synthase)	MAH_1943	0.07	-0.26	-0.18
Putative sporulation transcription regulator WhiA	MAH_1951	0.00	0.16	0.16
Phospholipid/glycerol acyltransferase	MAH_1961	-0.08	-0.14	**-0.23**
Glyceraldehyde-3-phosphate dehydrogenase (*gap*)*	MAH_1965	**0.19**	**-0.10**	0.09
Phosphoglycerate kinase	MAH_1966	0.04	-0.10	-0.06
Triosephosphate isomerase (TIM) (TPI)	MAH_1967	0.19	-0.06	0.13
General stress protein 69	MAH_1972	**0.72**	**-0.62**	0.10
Uncharacterized protein	MAH_1974	0.11	0.13	0.24
6-phosphogluconolactonase	MAH_1975	0.09	-0.19	-0.10
OpcA protein	MAH_1976	0.11	0.00	0.10
Glucose-6-phosphate 1-dehydrogenase (G6PD) (*zwf*)*	MAH_1977	**5.47**	**-5.47**	0.00
Transaldolase	MAH_1978	0.04	0.00	0.04
Transketolase	MAH_1979	0.13	-0.01	0.12
NADPH--quinone reductase	MAH_1981	0.14	-0.17	-0.03
ABC transporter ATP-binding subunit	MAH_1985	-0.18	-0.19	-0.37
FeS assembly protein SufB	MAH_1988	0.24	**-0.38**	-0.14
FeS assembly protein SufD	MAH_1989	0.00	-0.16	-0.16
ABC transporter ATP-binding subunit	MAH_1990	0.10	-0.05	0.05
27 kDa lipoprotein antigen	MAH_1996	-0.36	-0.92	-1.27
Acyl-CoA dehydrogenase (*fadE15*)*	MAH_1998	**0.38**	**-0.25**	0.13
Thioredoxin	MAH_1999	-0.13	**-0.68**	**-0.81**
Enoyl-CoA hydratase	MAH_2000	-1.30	-0.26	-1.56
Aconitate hydratase	MAH_2004	0.04	0.01	0.06
Uncharacterized protein	MAH_2005	-0.39	0.20	-0.19
MoxR protein	MAH_2008	**0.78**	**-0.51**	0.27
Uncharacterized protein	MAH_2009	0.72	-2.73	-2.02
FabG1 protein	MAH_2012	-0.06	0.02	-0.04
Enoyl-[acyl-carrier-protein] reductase [NADH]	MAH_2013	0.14	-0.02	0.12
Secreted protein	MAH_2017	-0.28	0.30	0.03
Methylmalonyl-CoA mutase, small subunit	MAH_2026	-0.12	-0.01	-0.13
Methylmalonyl-CoA mutase	MAH_2027	-0.14	0.32	0.18
Arginine/ornithine transport system ATPase	MAH_2028	-0.51	0.25	-0.26
NAD dependent epimerase/dehydratase	MAH_2033	-0.02	0.11	0.08
MtfB protein	MAH_2035	**0.70**	-0.43	0.27
Methyltransferase MtfC	MAH_2038	-0.25	0.25	0.00
Glycosyltransferase 28	MAH_2040	0.47	0.44	0.91
Daunorubicin resistance ATP-binding protein	MAH_2056	-0.10	0.03	-0.07

Uncharacterized protein	MAH_2058	0.42	0.71	1.13
Uncharacterized protein	MAH_2060	-0.44	-0.11	-0.54
2-nitropropane dioxygenase, NPD	MAH_2065	0.29	-0.30	-0.02
Oxidoreductase, short chain dehydrogenase/reductase	MAH_2075	**0.32**	0.01	0.32
Ketoacyl reductase	MAH_2076	**0.32**	-0.09	**0.23**
Fatty-acid-CoA ligase fadD11_1	MAH_2081	**-5.22**	**4.25**	-0.98
Uncharacterized protein	MAH_2084	0.12	-0.33	-0.20
L-threonine dehydratase	MAH_2085	0.05	-0.31	-0.26
NlpC/P60 family protein	MAH_2093	0.37	0.09	0.46
Quinolinate synthase A	MAH_2108	-0.96	0.34	-0.62
Uncharacterized protein	MAH_2111	1.33	-0.38	0.95
Histidinol dehydrogenase (HDH)	MAH_2112	-0.12	-0.02	-0.14
Histidinol-phosphate aminotransferase	MAH_2113	0.00	-0.13	-0.14
Imidazoleglycerol-phosphate dehydratase (IGPD)	MAH_2114	-0.08	0.01	-0.07
Imidazole glycerol phosphate synthase subunit HisH	MAH_2115	0.51	0.14	0.64
Phosphoribosyl isomerase A	MAH_2116	-0.26	0.10	-0.16
ImpA protein	MAH_2117	-0.37	0.68	0.31
Imidazole glycerol phosphate synthase subunit HisF	MAH_2118	-0.26	0.14	-0.12
Phosphoribosyl-AMP cyclohydrolase (PRA-CH)	MAH_2119	-0.01	-0.45	-0.46
BcpB protein	MAH_2121	0.25	-0.63	-0.39
Anthranilate synthase component I	MAH_2122	**-0.44**	0.26	-0.18
Indole-3-glycerol phosphate synthase	MAH_2124	-0.22	0.20	-0.02
Tryptophan synthase beta chain	MAH_2125	-0.30	0.04	-0.26
Tryptophan synthase alpha chain	MAH_2126	0.01	-0.05	-0.04
Pyruvate kinase (*pykA*)*	MAH_2129	**0.42**	**-0.31**	0.12
TesB1 protein	MAH_2130	-0.16	-0.50	-0.66
Response regulator	MAH_2139	0.15	-0.08	0.08
Lipid-transfer protein	MAH_2140	-0.75	0.20	-0.55
Nucleic acid-binding protein	MAH_2141	**-0.51**	0.23	-0.28
DNA polymerase I	MAH_2142	**0.44**	**-0.35**	0.09
30S ribosomal protein S1	MAH_2145	-0.07	-0.10	-0.17
Dephospho-CoA kinase/protein folding accessory domain-containing protein	MAH_2146	0.02	0.00	0.02
UvrABC system protein B (Protein UvrB) (Excinuclease ABC subunit B)	MAH_2156	0.01	-0.12	-0.10
Universal stress protein UspA-like protein	MAH_2160	-0.22	0.04	-0.18
Hydrolase	MAH_2161	0.07	-0.13	-0.05
Uncharacterized protein	MAH_2163	0.00	0.00	0.00
Translation initiation factor IF-3	MAH_2175	-0.21	0.26	0.04
50S ribosomal protein L35	MAH_2176	-0.64	**0.76**	0.12
50S ribosomal protein L20	MAH_2177	-0.42	0.27	-0.15
Phenylalanine--tRNA ligase alpha subunit	MAH_2182	0.02	-0.16	-0.15
N-acetyl-gamma-glutamyl-phosphate reductase	MAH_2184	-0.41	0.41	0.00

(AGPR)				
Arginine biosynthesis bifunctional protein ArgJ	MAH_2185	-0.12	-0.06	-0.18
Acetylornithine aminotransferase (ACOAT)	MAH_2187	-0.27	0.22	-0.04
Ornithine carbamoyltransferase (OTCase)	MAH_2188	**-0.35**	0.16	-0.19
Arginine repressor	MAH_2189	**-0.57**	0.24	-0.33
Argininosuccinate synthase	MAH_2190	-0.08	0.04	-0.04
Argininosuccinate lyase (ASAL)	MAH_2191	-0.40	0.10	-0.30
Acyl-CoA synthetase	MAH_2207	-0.19	-0.43	-0.62
TPR repeat-containing protein	MAH_2216	-1.15	-0.93	-2.08
NAD kinase	MAH_2220	0.05	-0.08	-0.02
Uncharacterized protein	MAH_2223	-0.12	0.08	-0.04
CTP synthase	MAH_2224	0.00	0.11	0.11
Catechol-O-methyltransferase	MAH_2227	-0.06	-0.12	-0.18
SpoOJ regulator protein	MAH_2228	-0.10	-0.07	-0.17
Segregation and condensation protein B	MAH_2230	-0.29	-0.02	-0.31
Cytidylate kinase (CK)	MAH_2232	**-0.43**	0.22	-0.21
GTPase Der (GTP-binding protein EngA)	MAH_2233	**4.29**	-0.42	**3.87**
AsnB_1 protein	MAH_2239	0.42	0.21	0.64
GNAT family acetyltransferase	MAH_2240	**0.36**	-0.11	0.25
Fumarate reductase/succinate dehydrogenase	MAH_2269	**5.21**	**-5.21**	0.00
2,3-dihydroxybiphenyl 1,2-dioxygenase	MAH_2270	**-0.48**	0.19	-0.30
Hydroxylase	MAH_2271	**-0.42**	**0.27**	-0.15
Alpha/beta hydrolase	MAH_2276	0.56	-0.42	0.15
CsbD-like protein	MAH_2279	-0.59	0.18	-0.41
Oxidoreductase	MAH_2303	0.01	0.06	0.07
Arylsulfatase	MAH_2304	-0.10	-0.10	-0.20
Uncharacterized protein	MAH_2324	-0.25	0.04	-0.20
Uncharacterized protein	MAH_2354	0.27	0.05	0.32
Ftsk/SpoIIIE family protein	MAH_2355	0.78	-0.55	0.23
Uncharacterized protein	MAH_2370	-0.22	0.06	-0.16
Subtilase	MAH_2372	-0.15	0.35	0.20
ATPase AAA	MAH_2374	-0.47	**-4.50**	**-4.97**
PPE family protein	MAH_2379	0.30	-0.42	-0.12
PPE family protein	MAH_2380	**0.88**	**-0.66**	0.22
Uncharacterized protein	MAH_2381	0.18	0.08	0.26
PPE family protein	MAH_2385	**-5.31**	0.00	**-5.31**
Succinate dehydrogenase/fumarate reductase flavoprotein subunit	MAH_2393	-0.49	0.29	-0.20
Uncharacterized protein	MAH_2395	0.31	-0.23	0.08
Protein translocase subunit SecA	MAH_2396	0.20	-0.10	0.09
Glycine cleavage system H protein	MAH_2401	**-0.58**	0.41	-0.17
Forkhead-associated protein	MAH_2402	-0.15	-0.08	-0.24
MerR family transcriptional regulator	MAH_2403	-0.04	-0.34	-0.39
Uncharacterized protein	MAH_2404	-0.69	0.16	**-0.53**

MerR family transcriptional regulator	MAH_2405	0.00	-0.13	-0.13
Glycine dehydrogenase (decarboxylating)	MAH_2406	0.22	-0.72	-0.51
Uncharacterized protein	MAH_2409	-0.16	0.39	0.22
Malate synthase G (*glcB*) *	MAH_2410	**0.36**	-0.13	0.23
Inosine 5-monophosphate dehydrogenase	MAH_2417	-0.24	**-0.29**	-0.52
6-phosphogluconate dehydrogenase, decarboxylating	MAH_2418	0.24	0.00	0.24
Uncharacterized protein	MAH_2421	0.14	-0.01	0.13
Oxidoreductase	MAH_2424	**0.33**	**-0.33**	-0.01
Short chain dehydrogenase	MAH_2425	**0.32**	**-0.35**	-0.04
Alanine and proline rich secreted protein apa	MAH_2430	-0.08	-0.08	-0.16
Probable phosphoketolase	MAH_2434	**0.89**	-0.33	**0.55**
Anthranilate dioxygenase reductase	MAH_2440	-0.10	0.12	0.03
Uncharacterized protein	MAH_2444	-0.30	**0.36**	0.06
Alkyl hydroperoxide reductase AhpD	MAH_2449	0.42	**-0.42**	-0.01
Alkyl hydroperoxide reductase	MAH_2450	**1.07**	**-0.91**	0.16
Uncharacterized protein	MAH_2452	-0.19	-0.03	-0.23
Enoyl-CoA hydratase/isomerase	MAH_2454	0.12	-0.13	-0.01
Ferroxidase	MAH_2456	0.12	**-0.86**	-0.74
Carboxymuconolactone decarboxylase	MAH_2458	**-0.33**	**0.66**	0.34
Glutamine synthetase catalytic domain	MAH_2460	**-5.02**	0.00	**-5.02**
Short chain dehydrogenase	MAH_2466	-0.17	0.30	0.12
Cyclase/dehydrase	MAH_2467	-0.07	0.29	0.22
Antigen 85-B	MAH_2470	**-0.52**	0.32	-0.19
AdhA_2 protein	MAH_2473	0.11	-0.22	-0.12
Uncharacterized protein	MAH_2477	-0.37	0.05	-0.32
Oxidoreductase, 2-nitropropane dioxygenase	MAH_2478	-0.02	0.11	0.08
S-adenosyl-L-methionine-dependent methyltransferase	MAH_2482	0.00	-0.03	-0.03
Uncharacterized protein	MAH_2484	**3.94**	1.24	**5.18**
Activator of Hsp90 ATPase 1 family protein	MAH_2498	0.10	**-5.36**	**-5.26**
Isocitrate lyase (*icl2*)*	MAH_2501	**0.37**	-0.27	0.09
Limonene 1,2-monooxygenase	MAH_2503	0.02	0.15	0.18
Uncharacterized protein	MAH_2504	-0.03	0.04	0.02
Uncharacterized protein	MAH_2508	**-6.02**	**5.16**	-0.87
Probable thiol peroxidase	MAH_2511	-0.12	-0.02	-0.15
Acyl-CoA dehydrogenase domain-containing protein	MAH_2514	**-0.84**	**0.61**	-0.23
NAD dependent epimerase/dehydratase	MAH_2515	-0.04	0.11	0.07
Glycosyl hydrolases family protein 16	MAH_2520	0.05	0.66	0.71
Secreted protein	MAH_2523	**-0.50**	0.22	-0.28
Catalase-peroxidase (CP)	MAH_2528	**-0.61**	0.34	-0.27
Ferric uptake regulator family protein	MAH_2529	-0.23	0.30	0.07
FAD dependent oxidoreductase	MAH_2532	0.00	0.00	0.00
Uncharacterized protein	MAH_2533	-0.43	-0.03	-0.46

PPE family protein	MAH_2535	-0.54	0.04	-0.50
Uncharacterized protein	MAH_2538	**-0.78**	0.32	-0.46
Cutinase	MAH_2540	-1.02	-0.12	**-1.14**
Uncharacterized protein	MAH_2546	-0.31	-0.13	-0.44
Glucose-6-phosphate 1-dehydrogenase (G6PD)	MAH_2548	0.16	-0.13	0.04
S-adenosyl-L-methionine-dependent methyltransferase	MAH_2549	0.06	-0.22	-0.16
Citrate lyase beta chain	MAH_2550	-0.44	0.10	-0.34
Hydrolase, peptidase M42 family protein	MAH_2551	0.34	0.04	0.39
Peptidyl-prolyl cis-trans isomerase	MAH_2555	-0.29	0.57	0.28
TetR family transcriptional regulator	MAH_2576	-0.26	0.13	-0.13
Amidohydrolase	MAH_2620	-0.41	0.03	-0.38
FabG3_1 protein	MAH_2627	-0.47	0.08	-0.39
Universal stress protein family protein	MAH_2629	**-0.54**	**0.70**	0.16
Universal stress protein family protein	MAH_2630	0.24	0.11	0.36
Uncharacterized protein	MAH_2631	-0.23	0.25	0.02
Uncharacterized protein	MAH_2633	-0.14	0.13	-0.01
Uncharacterized protein	MAH_2634	-0.24	0.35	0.11
Acyl-CoA thioesterase	MAH_2637	-0.82	0.70	-0.12
Aldo/keto reductase	MAH_2640	0.08	-0.12	-0.04
Uncharacterized protein	MAH_2663	-0.50	0.33	-0.17
RNA polymerase-binding protein RbpA	MAH_2686	-0.20	-0.01	-0.21
Polyprenol-monophosphomannose synthase ppm1	MAH_2687	-0.20	-0.02	-0.22
Dienelactone hydrolase	MAH_2691	**0.31**	-0.20	0.11
Pyridoxamine 5'-phosphate oxidase	MAH_2692	-0.30	0.13	-0.17
Nitrilase/cyanide hydratase and apolipoprotein N-acyltransferase	MAH_2707	0.14	**-0.45**	-0.31
Proline dipeptidase	MAH_2710	**4.77**	-0.52	**4.25**
Uncharacterized protein	MAH_2712	0.00	-0.05	-0.05
DNA-binding protein	MAH_2716	-0.35	-0.30	-0.65
Proteasome accessory factor B	MAH_2717	0.32	**-0.47**	-0.15
Pup--protein ligase	MAH_2718	-0.22	0.23	0.00
Proteasome subunit alpha	MAH_2719	0.02	-0.19	-0.17
Proteasome subunit beta	MAH_2720	**0.30**	**-0.34**	-0.04
Prokaryotic ubiquitin-like protein Pup	MAH_2721	-0.35	0.04	-0.32
Uncharacterized protein	MAH_2722	0.11	0.01	0.12
Uncharacterized protein	MAH_2723	**-0.83**	0.55	-0.28
AAA ATPase forming ring-shaped complexes (Proteasome-associated ATPase)*	MAH_2724	**0.40**	**-0.24**	0.16
Mercuric reductase	MAH_2730	-0.15	0.59	0.43
ATP phosphoribosyltransferase (ATP-PRT) (ATP-PRTase)	MAH_2732	-0.14	-0.05	-0.19
Phosphoribosyl-ATP pyrophosphatase (PRA-PH)	MAH_2733	**-0.45**	0.06	-0.39
B12-dependent methionine synthase	MAH_2745	**3.78**	0.13	**3.91**
L-cysteine:1D-myo-inositol 2-amino-2-deoxy-	MAH_2760	-0.10	0.24	0.14

alpha-D-glucopyranoside ligase				
Inositol monophosphatase	MAH_2761	**4.66**	0.35	**5.01**
Uncharacterized protein	MAH_2763	0.33	-0.05	0.27
Uncharacterized protein	MAH_2764	0.30	-1.23	-0.93
Uncharacterized protein	MAH_2765	-0.17	-0.24	-0.40
Uncharacterized protein	MAH_2770	-0.29	-0.08	**-0.36**
Uncharacterized protein	MAH_2771	0.21	-0.15	0.07
Wag31 protein	MAH_2779	-0.21	0.01	**-0.20**
Cell division protein SepF	MAH_2781	0.53	-0.84	-0.31
Uncharacterized protein	MAH_2782	-0.01	-0.13	-0.14
Cell division protein FtsZ	MAH_2784	0.19	-0.38	-0.19
UDP-N-acetylmuramate--L-alanine ligase	MAH_2786	**0.54**	**-0.45**	0.09
UDP-N-acetylmuramoyl-tripeptide--D-alanyl-D-alanine ligase	MAH_2791	-0.01	-0.02	-0.03
UDP-N-acetylmuramyl-tripeptide synthetase	MAH_2792	-0.08	-0.02	-0.10
Transcriptional regulator MraZ	MAH_2796	**0.73**	**-0.69**	0.04
Uncharacterized protein	MAH_2800	0.41	**-0.41**	-0.01
Regulatory protein	MAH_2803	**-0.34**	0.08	-0.26
3-deoxy-D-arabinoheptulosonate-7-phosphate synthase	MAH_2806	0.32	-0.01	0.31
1-acylglycerol-3-phosphate O-acyltransferase(*AGPAT*)*	MAH_2810	**5.26**	-0.96	**4.30**
Cyclase/dehydrase	MAH_2813	0.30	-0.18	0.12
Acyl-CoA dehydrogenase	MAH_2816	0.02	0.13	0.15
NLP/P60 family protein	MAH_2819	0.56	-0.21	0.35
QcrC protein	MAH_2825	**-0.40**	0.17	-0.23
QcrA protein	MAH_2826	-0.32	**0.82**	0.49
QcrB protein	MAH_2827	0.00	**5.52**	**5.52**
Membrane protein MmpS3	MAH_2830	**5.14**	**-5.14**	0.00
CtaC protein	MAH_2832	-0.88	**0.77**	-0.11
Adenosine kinase	MAH_2834	0.29	-0.11	0.18
HesB/YadR/YfhF family protein	MAH_2836	**0.42**	**-0.67**	**-0.25**
Branched-chain-amino-acid aminotransferase	MAH_2842	-0.06	0.00	-0.06
Aminomethyltransferase	MAH_2843	**0.50**	**-0.58**	-0.08
Probable cytosol aminopeptidase (Leucine aminopeptidase) (Leucyl aminopeptidase)	MAH_2844	**0.30**	-0.18	0.12
Dihydrolipoamide acetyltransferase	MAH_2848	0.03	-0.10	-0.07
Integral membrane protein	MAH_2852	**5.79**	**-5.79**	0.00
Glutamine synthetase	MAH_2854	0.04	-0.05	-0.01
Thioesterase	MAH_2856	**-5.71**	**5.15**	-0.57
GlnA2 protein	MAH_2858	0.16	0.02	0.19
Alpha/beta hydrolase	MAH_2859	0.11	-0.23	-0.12
3-methyl-2-oxobutanoate hydroxymethyltransferase	MAH_2862	0.42	-0.15	0.28
Uncharacterized protein	MAH_2864	0.00	0.00	0.00
Adenylate cyclase	MAH_2866	-0.41	0.26	-0.15

Bifunctional RNase H/acid phosphatase	MAH_2871	0.18	-0.43	-0.25
Uncharacterized protein	MAH_2872	-0.15	0.09	-0.06
GTP cyclohydrolase 1 type 2 homolog	MAH_2873	-0.26	0.04	-0.21
Alkyl hydroperoxide reductase/ Thiol specific antioxidant/ Mal allergen	MAH_2882	-0.16	0.04	-0.13
Uncharacterized protein	MAH_2883	-0.11	-0.01	-0.13
Pyruvate dehydrogenase E1 component	MAH_2885	0.19	-0.14	0.05
ACP S-malonyltransferase	MAH_2887	-0.27	-0.04	-0.31
Acyl carrier protein (ACP)	MAH_2888	**-0.54**	0.20	-0.33
3-oxoacyl-(Acyl carrier protein) synthase II	MAH_2889	**-0.33**	0.17	-0.17
3-oxoacyl-(Acyl carrier protein) synthase II	MAH_2890	0.11	-0.12	-0.01
Propionyl-CoA carboxylase	MAH_2891	-0.16	0.07	-0.09
Transcriptional regulator	MAH_2899	**5.54**	**-5.54**	0.00
AdhE2 protein	MAH_2900	0.31	-0.01	0.30
Metallo-beta-lactamase	MAH_2901	-0.28	0.36	0.08
Dihydrodipicolinate reductase N-terminus domain-containing protein	MAH_2905	0.12	0.54	0.67
Acyl carrier protein	MAH_2911	**-1.20**	**0.78**	-0.41
Serine esterase cutinase	MAH_2912	0.37	-0.49	-0.12
Uncharacterized protein	MAH_2941	-0.29	-0.07	-0.36
Amidohydrolase	MAH_2950	-0.24	0.27	0.02
Uncharacterized protein	MAH_2959	**4.41**	**-4.41**	0.00
Methionine-R-sulfoxide reductase	MAH_2972	-0.06	0.00	-0.06
Thiopurine S-methyltransferase superfamily protein	MAH_2974	0.11	-0.17	-0.06
Chlorite dismutase	MAH_2975	0.28	0.03	0.30
Enoyl-CoA hydratase	MAH_2978	-0.56	-0.17	-0.73
Uncharacterized protein	MAH_2979	0.42	**-0.82**	-0.40
Ribonuclease D	MAH_2980	**4.55**	**-4.55**	0.00
CBS domain-containing protein	MAH_2982	0.01	0.75	0.76
TrkA protein	MAH_2986	0.02	0.10	0.12
TrkB protein	MAH_2987	-0.03	0.07	0.04
OB-fold nucleic acid binding domain-containing protein	MAH_2989	-0.12	-0.31	**-0.43**
Uncharacterized protein	MAH_2991	-0.13	-0.08	-0.21
Deoxyuridine 5'-triphosphate nucleotidohydrolase	MAH_2992	0.38	-0.21	0.17
Uncharacterized protein	MAH_2994	-0.44	0.03	-0.40
PpgK protein	MAH_2997	-0.09	-0.21	-0.30
RNA polymerase sigma factor SigA	MAH_2998	**0.39**	-0.31	0.08
Uncharacterized protein	MAH_3004	-0.54	0.21	-0.33
Iron-dependent repressor IdeR	MAH_3007	0.05	-0.09	-0.04
Conserved alanine and leucine rich protein	MAH_3012	-0.48	0.24	-0.24
Thymidylate synthase	MAH_3014	-0.01	-0.22	-0.24
UPF0678 fatty acid-binding protein-like protein	MAH_3015	-0.86	-0.24	**-1.11**
Transcriptional repressor NrdR	MAH_3016	-0.05	-0.08	-0.13

LexA repressor	MAH_3018	-0.20	-0.08	-0.28
Uncharacterized protein	MAH_3019	-0.47	**0.50**	0.02
Long-chain specific acyl-CoA dehydrogenase	MAH_3020	0.15	-0.12	0.03
GTPase HflX (GTP-binding protein HflX)	MAH_3021	-0.44	0.41	-0.03
Conserved alanine and arginine rich protein	MAH_3027	-0.58	0.42	-0.16
Protein RecA (Recombinase A)	MAH_3031	0.12	-0.10	0.02
Uncharacterized protein	MAH_3036	0.00	0.00	0.00
35kd antigen	MAH_3039	0.04	-0.15	-0.11
Antibiotic biosynthesis monooxygenase domain-containing protein	MAH_3045	-0.24	0.33	0.09
3-ketoacyl-(Acyl-carrier-protein) reductase	MAH_3046	-0.12	0.04	-0.07
Hydrolase of the metallo-beta-lactamase	MAH_3048	-0.58	0.48	-0.11
4-hydroxy-tetrahydrodipicolinate synthase (HTPA synthase)	MAH_3049	-0.22	0.25	0.03
Thymidylate synthase ThyX (TS) (TSase)	MAH_3050	-0.90	1.24	0.34
Uncharacterized protein	MAH_3052	-0.31	0.10	-0.21
Uncharacterized protein	MAH_3053	**-0.37**	0.01	**-0.36**
Uncharacterized protein	MAH_3062	0.14	-0.24	-0.10
Dihydrofolate reductase	MAH_3063	-0.20	-0.54	-0.74
Alanine rich hydrolase	MAH_3065	-0.04	0.65	0.61
3-ketoacyl-(Acyl-carrier-protein) reductase	MAH_3067	**0.45**	-0.06	**0.38**
Multimeric flavodoxin WrbA	MAH_3072	0.00	0.00	0.00
4-hydroxy-tetrahydrodipicolinate reductase (HTPA reductase)	MAH_3074	0.12	-0.16	-0.04
Uncharacterized protein	MAH_3083	**-0.62**	**0.57**	-0.06
Dioxygenase	MAH_3085	-0.79	0.98	0.19
Polyribonucleotide nucleotidyltransferase	MAH_3087	0.21	-0.16	0.05
30S ribosomal protein S15	MAH_3088	-0.29	0.46	0.16
Riboflavin biosynthesis protein	MAH_3089	**5.08**	-0.53	**4.55**
Iron repressor protein	MAH_3090	-0.37	0.18	-0.19
Lipid-transfer protein	MAH_3092	-0.22	0.17	-0.06
Enoyl-CoA hydratase	MAH_3100	0.27	**-0.32**	-0.05
DHH family protein	MAH_3102	-0.35	0.54	0.19
Ribosome-binding factor A	MAH_3103	0.01	-0.13	-0.11
Translation initiation factor IF-2	MAH_3104	0.09	-0.05	0.03
Transcription termination/antitermination protein NusA	MAH_3106	0.10	-0.06	0.03
Ribosome maturation factor RimP	MAH_3107	-0.29	-0.08	-0.37
Proline--tRNA ligase (Prolyl-tRNA synthetase)	MAH_3110	-0.05	-0.03	-0.08
Uncharacterized protein	MAH_3111	0.00	**5.44**	**5.44**
Chelatase	MAH_3116	-0.21	-0.03	-0.24
Acetyltransferase, gnat family protein	MAH_3117	-0.37	-0.15	-0.51
Methionine aminopeptidase (MAP) (MetAP)	MAH_3131	0.15	0.15	0.29
4-hydroxy-3-methylbut-2-en-1-yl diphosphate synthase (flavodoxin)	MAH_3135	0.00	0.11	0.11
Ribosome-recycling factor (RRF) (Ribosome-	MAH_3142	-0.08	0.00	-0.07

releasing factor)				
Uridylate kinase	MAH_3143	0.34	-0.43	-0.09
CsbD-like protein	MAH_3144	**-1.49**	**0.84**	-0.65
ChaB family protein	MAH_3150	-0.54	-0.09	-0.63
Elongation factor Ts (EF-Ts)	MAH_3153	0.02	-0.10	-0.07
30S ribosomal protein S2	MAH_3154	-0.38	**0.57**	0.19
Lactate 2-monooxygenase	MAH_3157	**0.42**	**-0.37**	0.05
Siderophore utilization protein	MAH_3158	**0.52**	**-0.34**	0.18
NAD dependent epimerase/dehydratase	MAH_3164	**5.68**	**-5.68**	0.00
ANTAR domain-containing protein	MAH_3165	-0.33	0.44	0.11
Uncharacterized protein	MAH_3166	0.09	-0.26	-0.17
50S ribosomal protein L19	MAH_3169	-0.03	-0.05	-0.08
tRNA (guanine-N(1)-)-methyltransferase	MAH_3171	-0.40	0.44	0.05
UPF0109 protein	MAH_3173	-0.07	-0.02	-0.09
30S ribosomal protein S16	MAH_3174	-0.27	0.20	-0.07
Amidohydrolase	MAH_3179	0.00	**4.15**	**4.15**
Signal recognition particle protein (Fifty-four homolog)	MAH_3180	-0.16	0.10	-0.06
Nitrogen regulatory protein PII	MAH_3184	-0.11	0.17	0.05
Signal recognition particle receptor FtsY (SRP receptor)	MAH_3186	-0.77	**-4.58**	**-5.35**
Chromosome partition protein Smc	MAH_3187	**6.08**	-0.34	**5.74**
Uncharacterized protein	MAH_3189	**0.44**	**-0.47**	-0.02
Ribonuclease 3	MAH_3192	-0.20	0.18	-0.02
Uncharacterized protein	MAH_3193	-0.68	-0.18	-0.86
Uncharacterized protein	MAH_3194	0.27	**-0.40**	-0.13
Phosphopantetheine adenylyltransferase	MAH_3234	0.11	0.00	0.11
Uncharacterized protein	MAH_3237	-0.73	**1.16**	0.43
Alpha/beta hydrolase	MAH_3238	0.38	-0.41	-0.02
2,5-diketo-D-gluconic acid reductase A	MAH_3239	**-0.16**	0.05	-0.11
50S ribosomal protein L28	MAH_3245	-0.03	-0.46	-0.49
D-alanine--D-alanine ligase	MAH_3254	-0.08	0.35	0.27
Glycerol-3-phosphate dehydrogenase [NAD(P)+]	MAH_3255	0.18	**-0.72**	-0.54
Polyphosphate kinase	MAH_3257	-0.04	0.02	-0.02
DNA-binding protein HU	MAH_3259	-0.42	**0.67**	0.24
3-isopropylmalate dehydratase small subunit	MAH_3260	**-0.45**	**0.53**	0.07
3-isopropylmalate dehydratase large subunit	MAH_3261	**-0.44**	**0.43**	-0.01
Pyridoxamine 5'-phosphate oxidase	MAH_3263	0.23	-0.31	-0.08
Glutamate--tRNA ligase (Glutamyl-tRNA synthetase)	MAH_3264	0.43	-0.28	0.16
5-carboxymethyl-2-hydroxymuconate delta-isomerase	MAH_3265	0.23	-0.20	0.03
3-isopropylmalate dehydrogenase	MAH_3267	-0.01	-0.06	-0.07
D-3-phosphoglycerate dehydrogenase	MAH_3268	**0.19**	**-0.17**	0.01
NAD(P)H:quinone oxidoreductase, type IV	MAH_3270	-0.78	**-4.33**	**-5.11**

Ketol-acid reductoisomerase	MAH_3271	**-0.19**	0.16	-0.03
Acetolactate synthase 3 regulatory subunit	MAH_3272	0.28	-0.20	0.07
Acetolactate synthase	MAH_3273	-0.03	0.39	0.36
Aspartyl/glutamyl-tRNA(Asn/Gln) amidotransferase subunit B	MAH_3278	0.25	-0.10	0.15
6-phosphofructokinase	MAH_3280	0.45	**-0.46**	-0.01
Glutamyl-tRNA(Gln) amidotransferase subunit A (Glu-ADT subunit A)	MAH_3281	0.25	-0.09	0.16
Aspartyl/glutamyl-tRNA(Asn/Gln) amidotransferase subunit C (Asp/Glu-ADT subunit C)	MAH_3282	-0.20	0.09	-0.11
ACT domain-containing protein	MAH_3283	0.46	-0.19	0.27
DNA ligase (Polydeoxyribonucleotide synthase [NAD(+)])	MAH_3290	0.00	**5.41**	**5.41**
Electron transfer flavoprotein, alpha subunit	MAH_3297	0.04	-0.01	0.03
Electron transfer protein, beta subunit	MAH_3298	-0.21	0.10	-0.11
Immunogenic protein MPB64/MPT64	MAH_3324	0.00	0.00	0.00
Enoyl-CoA hydratase	MAH_3327	-0.04	0.12	0.08
Nudix hydrolase	MAH_3328	0.05	-0.17	-0.12
Molybdenum ABC transporter ATPase	MAH_3329	-0.22	-0.25	-0.46
Phosphoserine phosphatase	MAH_3330	0.19	0.04	0.23
Cytochrome c oxidase subunit 1	MAH_3331	-1.16	0.99	-0.17
NADP-dependent alcohol dehydrogenase c	MAH_3334	**0.68**	-0.15	0.54
Ribonucleoside-diphosphate reductase subunit beta	MAH_3336	-0.15	0.09	-0.07
TetR family transcriptional regulator	MAH_3340	-0.09	0.04	-0.05
Ribonucleoside-diphosphate reductase	MAH_3341	-0.11	0.14	0.03
Secreted protein	MAH_3344	0.07	-0.31	-0.24
Acyl-CoA dehydrogenase	MAH_3357	0.23	0.14	**0.38**
3-hydroxyacyl-CoA dehydrogenase type-2	MAH_3358	-0.05	0.18	0.13
Phosphoglucomutase	MAH_3394	**0.65**	**-0.48**	0.18
Uncharacterized protein	MAH_3398	**5.16**	-0.34	**4.82**
Citrate lyase beta subunit, CitE_2	MAH_3400	0.10	-0.22	-0.12
Hemerythrin HHE cation binding domain-containing protein	MAH_3401	-0.84	-0.08	-0.92
SsrA-binding protein (Small protein B)	MAH_3419	**4.76**	0.24	**5.00**
Cell division ATP-binding protein FtsE	MAH_3421	0.26	-0.18	0.08
Peptide chain release factor 2 (RF-2)	MAH_3424	0.09	-0.07	0.02
NADPH:adrenodoxin oxidoreductase FprA	MAH_3425	-0.09	0.03	-0.06
Flavin-nucleotide-binding protein	MAH_3426	0.21	-0.16	0.05
Universal stress protein	MAH_3428	-0.32	0.48	0.16
Nitric-oxide reductase subunit B	MAH_3429	-0.92	1.50	0.58
SPFH domain-containing protein/band 7 family protein	MAH_3431	-1.03	0.42	-0.61
FadE24 protein	MAH_3436	0.19	0.16	0.35
Acyl-CoA dehydrogenase	MAH_3437	0.17	0.12	0.29
Zinc-binding dehydrogenase	MAH_3438	0.11	-0.30	-0.19

Acyl-CoA dehydrogenase*	MAH_3443	**-5.32**	**6.09**	0.77
YceI like family protein	MAH_3447	**0.53**	**-0.44**	0.09
Two-component system response regulator	MAH_3448	0.06	-0.02	0.04
NADH-quinone oxidoreductase subunit B	MAH_3450	0.29	-0.17	0.12
NADH-quinone oxidoreductase subunit C	MAH_3451	-0.11	-0.08	-0.19
NADH-quinone oxidoreductase subunit D	MAH_3452	0.15	0.15	0.30
NADH dehydrogenase subunit E	MAH_3453	**-0.36**	0.23	-0.13
NADH-quinone oxidoreductase subunit F	MAH_3454	-0.15	0.16	0.02
NADH-quinone oxidoreductase	MAH_3455	0.02	-0.03	0.00
NADH-quinone oxidoreductase subunit I	MAH_3457	-0.22	0.06	-0.16
NADH dehydrogenase subunit J	MAH_3458	-0.63	**0.64**	0.01
TetR family transcriptional regulator	MAH_3473	-1.45	0.62	-0.83
Phosphotransferase enzyme family protein	MAH_3474	-0.43	0.36	-0.07
Uncharacterized protein	MAH_3475	-0.16	0.09	-0.08
Chemotaxis response regulator	MAH_3485	0.45	-1.27	-0.82
Catalase	MAH_3487	**-0.60**	0.26	-0.34
Rho termination factor	MAH_3488	**-1.51**	**0.97**	-0.54
CsbD-like protein	MAH_3494	**-1.19**	**0.62**	-0.58
Thiamine pyrophosphate protein	MAH_3510	**-0.65**	0.51	-0.15
Aldo/keto reductase	MAH_3515	**0.51**	-0.14	**0.37**
Glycogen operon protein GlgX homolog	MAH_3517	-0.45	0.16	-0.29
S-(Hydroxymethyl)glutathione dehydrogenase	MAH_3518	-0.44	1.13	0.70
Dehydrogenase	MAH_3520	**5.01**	0.93	**5.94**
MerR family transcriptional regulator	MAH_3522	-0.24	-0.12	-0.36
Pyridoxamine 5'-phosphate oxidase	MAH_3527	0.03	0.11	0.14
Uncharacterized protein	MAH_3528	-0.63	**0.62**	-0.01
Response regulator receiver domain-containing protein	MAH_3530	**-0.49**	0.06	**-0.43**
Uncharacterized protein	MAH_3540	0.00	0.00	0.00
Uncharacterized protein	MAH_3546	0.09	-0.27	-0.18
Glutathione peroxidase	MAH_3547	**-0.31**	0.12	-0.19
Immunogenic protein MPT64	MAH_3548	-0.13	0.17	0.05
UPF0182 protein MAH_3549	MAH_3549	**5.84**	0.29	**6.13**
Uncharacterized protein	MAH_3551	0.44	-0.36	0.09
ABC transporter ATP-binding protein	MAH_3553	0.03	-0.17	-0.14
NADH pyrophosphatase	MAH_3558	0.01	-0.09	-0.08
Ion channel membrane protein	MAH_3559	0.06	**-0.72**	-0.65
Uncharacterized protein	MAH_3565	0.41	-0.22	0.19
Uncharacterized protein	MAH_3569	0.13	-0.13	0.00
RhlE protein	MAH_3572	**-0.47**	**0.39**	-0.08
Soj/parA-related protein	MAH_3574	-0.04	0.13	0.08
Sensor histidine kinase	MAH_3581	-2.02	0.36	-1.66
Anti-sigma factor	MAH_3583	-0.52	0.14	-0.38
RNA polymerase sigma factor	MAH_3584	0.20	-0.21	-0.01

Short chain dehydrogenase	MAH_3585	0.20	-0.14	0.06
Oxidoreductase, short chain dehydrogenase/reductase	MAH_3588	**-5.42**	0.00	**-5.42**
Uncharacterized protein	MAH_3594	-0.10	0.77	0.67
3-phosphoshikimate 1-carboxyvinyltransferase	MAH_3595	0.53	**-6.04**	**-5.51**
Uncharacterized protein	MAH_3607	**-0.92**	0.41	-0.52
PvdS protein	MAH_3608	0.45	-0.83	-0.38
Protein translocase subunit SecA	MAH_3616	0.05	0.08	0.13
S30AE family protein	MAH_3617	**-0.54**	0.44	-0.10
Lipoprotein LpqB	MAH_3619	0.27	0.23	0.50
DNA-binding response regulator	MAH_3621	0.04	-0.32	-0.28
dTMP kinase	MAH_3622	-0.62	0.24	-0.38
Adenosylhomocysteinase	MAH_3623	0.12	-0.02	0.10
Mannose-6-phosphate isomerase, class I	MAH_3630	0.38	-0.26	0.12
Uncharacterized protein	MAH_3631	0.15	-0.06	0.09
Phosphomannomutase/phosphoglucomutase	MAH_3632	-0.05	0.15	0.10
2-phospho-L-lactate transferase	MAH_3636	0.00	0.00	0.00
Mannose-1-phosphate guanylyltransferase	MAH_3640	-0.55	0.65	0.10
RmlD protein	MAH_3642	**5.16**	0.05	**5.21**
Uncharacterized protein	MAH_3645	-0.29	0.37	0.08
S-adenosyl-L-methionine-dependent methyltransferase	MAH_3647	-0.03	-0.12	-0.16
YfdE protein	MAH_3648	0.16	0.05	0.20
Serine/threonine protein kinase	MAH_3649	**-0.76**	**0.69**	-0.08
Two-component system response regulator	MAH_3651	-0.29	0.01	-0.28
Response regulator receiver modulated serine phosphatase	MAH_3653	-0.39	0.05	-0.34
Acyl-CoA dehydrogenase	MAH_3654	0.15	-0.28	-0.13
N5-carboxyaminoimidazole ribonucleotide mutase (N5-CAIR mutase)	MAH_3655	0.12	**-0.28**	-0.16
N5-carboxyaminoimidazole ribonucleotide synthase (N5-CAIR synthase)	MAH_3656	-0.05	0.04	-0.01
Biotin-[acetyl-CoA-carboxylase] ligase	MAH_3659	**0.56**	-0.35	0.21
AccD5 protein	MAH_3661	0.02	-0.09	-0.06
Uncharacterized protein	MAH_3662	-0.14	-0.14	-0.28
Sulfurtransferase	MAH_3664	0.16	-0.21	-0.06
Fe-S metabolism associated domain-containing protein	MAH_3665	-0.01	**-0.41**	**-0.42**
AccA3 protein	MAH_3666	0.23	-0.21	0.02
RsbW protein	MAH_3669	-0.16	0.18	0.02
AsnC family transcriptional regulator	MAH_3674	-0.58	0.52	-0.06
TetR family transcriptional regulator	MAH_3677	-0.39	0.40	0.01
PPE family protein	MAH_3684	-0.37	0.30	-0.07
L308_f3_97	MAH_3690	-0.30	0.02	-0.28
Amidase	MAH_3692	**0.34**	-0.11	0.23
Cutinase Cut3	MAH_3693	-0.35	**0.45**	0.10

Purine nucleoside phosphorylase	MAH_3694	0.68	-0.45	0.23
Uncharacterized protein	MAH_3698	-0.16	0.04	-0.12
Adenosine deaminase	MAH_3703	0.44	-0.32	0.11
Cytidine deaminase	MAH_3705	0.50	-0.92	-0.42
Succinate dehydrogenase flavoprotein subunit (*sdhA*)*	MAH_3708	**0.70**	-0.27	0.43
Succinate dehydrogenase iron-sulfur subunit (*sdhB*)*	MAH_3709	**0.32**	**-0.40**	-0.09
Tryptophan--tRNA ligase (Tryptophanyl-tRNA synthetase)	MAH_3720	-0.02	-0.10	-0.13
Isocitrate dehydrogenase [NADP]	MAH_3722	0.28	-0.17	0.11
Isocitrate dehydrogenase, NADP-dependent	MAH_3723	0.14	0.05	0.19
O-acetylhomoserine aminocarboxypropyltransferase	MAH_3724	0.17	-0.24	-0.07
Methyltransferase	MAH_3726	-0.17	0.26	0.09
Bifunctional protein FolD	MAH_3730	-0.01	-0.10	-0.11
NADH:flavin oxidoreductase	MAH_3731	-0.07	0.14	0.07
ATP/GTP-binding protein	MAH_3735	0.21	-0.75	-0.54
Roadblock/LC7 family protein	MAH_3737	-0.66	0.07	-0.59
SAM-dependent methyltransferase	MAH_3739	0.00	0.18	0.18
Nitroreductase	MAH_3741	0.39	-0.29	0.10
Trehalose 6-phosphate phosphatase	MAH_3744	2.39	-0.84	1.54
MaoC family protein	MAH_3745	0.00	0.18	0.18
Uncharacterized protein	MAH_3746	**-1.22**	**0.90**	-0.32
Inosine-uridine preferring nucleoside hydrolase	MAH_3749	0.29	0.99	1.28
3-oxoacyl-(Acyl carrier protein) synthase II	MAH_3750	**0.34**	-0.04	0.31
GMP synthase [glutamine-hydrolyzing]	MAH_3755	0.28	-0.31	-0.03
Beta-phosphoglucomutase hydrolase	MAH_3757	-0.05	0.12	0.07
Glycoside hydrolase 65, central catalytic	MAH_3758	-0.73	1.44	0.71
Inosine 5-monophosphate dehydrogenase	MAH_3762	-0.01	0.04	0.03
Inosine-5'-monophosphate dehydrogenase	MAH_3763	0.07	-0.14	-0.07
Uncharacterized protein	MAH_3771	0.00	**4.45**	**4.45**
60 kDa chaperonin (GroEL protein) (Protein Cpn60)	MAH_3772	0.15	**-0.18**	-0.03
10 kDa chaperonin (GroES protein) (Protein Cpn10)	MAH_3773	-0.15	-0.13	-0.28
Uncharacterized protein	MAH_3778	0.10	-0.59	-0.49
Alanine racemase (*alr*)*	MAH_3780	**4.86**	0.11	**4.97**
Glutamate decarboxylase	MAH_3781	0.13	-0.08	0.05
Bifunctional NAD(P)H-hydrate repair enzyme (Nicotinamide nucleotide repair protein)	MAH_3782	0.17	-0.24	-0.07
Glutamine--fructose-6-phosphate aminotransferase [isomerizing]	MAH_3785	0.58	-0.58	0.00
Oxidoreductase	MAH_3789	-0.31	-0.09	-0.40
Phosphoglucosamine mutase	MAH_3792	**5.09**	**-5.09**	0.00
30S ribosomal protein S9	MAH_3793	-0.16	0.28	0.12
50S ribosomal protein L13	MAH_3794	-0.12	**0.26**	0.14

Cutinase	MAH_3802	0.00	0.00	0.00
50S ribosomal protein L17	MAH_3805	-0.09	0.23	0.13
DNA-directed RNA polymerase subunit alpha (RNAP subunit alpha)	MAH_3806	0.01	-0.07	-0.06
30S ribosomal protein S4	MAH_3807	-0.07	0.01	-0.06
30S ribosomal protein S11	MAH_3808	-0.56	**0.50**	-0.06
30S ribosomal protein S13	MAH_3809	-0.07	**0.38**	0.32
Translation initiation factor IF-1	MAH_3810	0.04	0.18	0.22
Uncharacterized protein	MAH_3811	**0.51**	-0.36	0.15
F420-dependent methylene-tetrahydromethanopterin reductase	MAH_3812	**0.80**	**-0.53**	0.27
dTDP-glucose 4,6-dehydratase	MAH_3813	0.09	-0.09	0.00
dTDP-4-dehydrorhamnose 3,5-epimerase	MAH_3814	0.00	0.09	0.08
Methylmalonate-semialdehyde dehydrogenase	MAH_3824	0.16	-0.07	0.09
Acyl-CoA dehydrogenase	MAH_3825	**6.60**	-0.02	**6.57**
3-hydroxyisobutyrate dehydrogenase (HIBADH)	MAH_3826	-0.16	0.19	0.03
MarR family transcriptional regulator	MAH_3827	**4.55**	1.41	**5.96**
Methionine aminopeptidase (MAP) (MetAP)	MAH_3840	0.00	-0.44	-0.44
Adenylate kinase	MAH_3841	-0.14	-0.02	**-0.16**
S-adenosyl-L-methionine-dependent methyltransferase	MAH_3843	-0.64	0.23	-0.42
Uncharacterized protein	MAH_3844	0.06	-0.10	-0.04
2-hydroxyacid dehydrogenase	MAH_3846	0.04	-0.13	-0.09
L-fuculose-phosphate aldolase	MAH_3847	-0.26	0.05	-0.21
S-adenosyl-L-methionine-dependent methyltransferase	MAH_3852	0.33	-0.29	0.04
Signal peptide peptidase SppA, 67K type	MAH_3854	**0.75**	**-0.55**	0.20
50S ribosomal protein L15	MAH_3856	-0.64	**0.71**	0.07
50S ribosomal protein L30	MAH_3857	-0.26	**0.43**	0.16
30S ribosomal protein S5	MAH_3858	0.20	0.00	0.20
50S ribosomal protein L18	MAH_3859	-0.21	0.25	0.04
50S ribosomal protein L6	MAH_3860	-0.25	**0.36**	0.11
30S ribosomal protein S8	MAH_3861	-0.14	0.31	0.17
50S ribosomal protein L5	MAH_3863	0.06	0.01	0.07
50S ribosomal protein L24	MAH_3864	-0.44	0.42	-0.02
50S ribosomal protein L14	MAH_3865	-0.08	0.35	0.27
Arylsulfatase	MAH_3871	**4.63**	-0.03	**4.61**
30S ribosomal protein S17	MAH_3872	-0.34	0.26	-0.07
50S ribosomal protein L29	MAH_3873	0.04	**-0.37**	**-0.33**
50S ribosomal protein L16	MAH_3874	-0.21	**0.50**	0.29
30S ribosomal protein S3	MAH_3875	-0.14	0.10	-0.04
50S ribosomal protein L22	MAH_3876	-0.10	**0.23**	0.13
30S ribosomal protein S19	MAH_3877	-0.40	**0.46**	0.06
50S ribosomal protein L2	MAH_3878	-0.16	**0.23**	0.07
50S ribosomal protein L23	MAH_3879	0.09	-0.12	-0.04

50S ribosomal protein L4	MAH_3880	-0.07	0.05	-0.03
50S ribosomal protein L3	MAH_3881	-0.10	**0.34**	0.24
30S ribosomal protein S10	MAH_3882	0.01	-0.03	-0.01
TetR family transcriptional regulator	MAH_3883	-0.91	1.24	0.32
Heme/flavin dehydrogenase, mycofactocin system	MAH_3887	**5.58**	-0.59	**4.99**
Ferredoxin reductase	MAH_3894	-0.14	-0.06	-0.20
Membrane protein	MAH_3896	**-4.72**	**3.41**	-1.31
Elongation factor Tu (EF-Tu)	MAH_3898	0.03	**-0.16**	-0.13
Elongation factor G (EF-G)	MAH_3899	0.07	-0.10	-0.03
30S ribosomal protein S7	MAH_3900	-0.17	0.56	0.39
30S ribosomal protein S12	MAH_3901	-0.24	0.39	0.15
TetR family transcriptional regulator	MAH_3902	-0.10	-0.26	-0.37
Enoyl-CoA hydratase	MAH_3905	0.60	-0.03	0.57
Enoyl-CoA hydratase	MAH_3907	0.63	-0.03	0.60
Acyl-CoA dehydrogenase	MAH_3908	**3.81**	0.12	**3.93**
DNA-directed RNA polymerase subunit beta' (RNAP subunit beta')	MAH_3910	-0.04	0.19	0.15
DNA-directed RNA polymerase subunit beta (RNAP subunit beta)	MAH_3911	0.09	-0.05	0.04
ABC transporter ATP-binding protein	MAH_3912	-0.24	0.18	-0.07
50S ribosomal protein L7/L12	MAH_3915	0.06	-0.13	-0.07
50S ribosomal protein L10	MAH_3916	0.16	**-0.23**	-0.07
Alpha-mannosidase	MAH_3920	0.25	**-5.63**	**-5.37**
Uncharacterized protein	MAH_3921	0.15	-0.16	-0.02
ABC transporter	MAH_3922	0.04	-0.57	-0.53
Methoxy mycolic acid synthase 1	MAH_3924	-0.02	0.18	0.16
Methoxy mycolic acid synthase	MAH_3925	-0.12	0.06	-0.06
DGPF domain-containing protein	MAH_3926	**-0.87**	0.48	-0.40
50S ribosomal protein L1	MAH_3928	-0.14	0.19	0.05
50S ribosomal protein L11	MAH_3929	-0.04	0.00	-0.04
Transcription termination/antitermination protein NusG	MAH_3930	-0.14	-0.02	-0.17
Preprotein translocase subunit SecE	MAH_3931	-0.50	**2.83**	2.33
UPF0336 protein MAH_3932	MAH_3932	0.25	-0.13	0.12
(3R)-hydroxyacyl-ACP dehydratase subunit HadB	MAH_3933	0.06	-0.21	-0.15
UPF0336 protein MAH_3934	MAH_3934	-0.09	0.01	-0.08
50S ribosomal protein L33	MAH_3935	-0.21	**0.51**	0.30
Uncharacterized protein	MAH_3936	-0.11	-0.16	-0.27
Metallo-beta-lactamase	MAH_3937	**-0.48**	**0.32**	-0.16
Uncharacterized protein	MAH_3938	**-0.91**	**0.98**	0.06
Enoyl-CoA hydratase	MAH_3939	0.52	**-1.35**	-0.83
Cyanate hydratase (Cyanase)	MAH_3943	**0.40**	**-0.59**	-0.19
S-adenosyl-L-methionine-dependent methyltransferase	MAH_3962	0.38	-0.10	0.28

S-adenosyl-L-methionine-dependent methyltransferase	MAH_3963	-0.09	-0.17	-0.27
Uncharacterized protein	MAH_3966	**-0.97**	**0.93**	-0.05
ANTAR domain-containing protein	MAH_3967	-0.43	-0.14	-0.57
Uncharacterized protein	MAH_3973	-0.11	0.11	0.00
UPF0234 protein	MAH_3987	-0.01	-0.10	-0.11
Glycerol-3-phosphate dehydrogenase [NAD(P)+]	MAH_3989	-0.41	0.18	-0.22
GrcC1 protein	MAH_3993	0.47	-0.05	0.42
Alpha/beta hydrolase	MAH_4001	0.26	**-0.43**	-0.16
Acyl-CoA synthetase	MAH_4004	0.04	0.25	**0.29**
Deazaflavin-dependent nitroreductase family protein	MAH_4007	-0.21	0.28	0.07
1,4-dihydroxy-2-naphthoyl-CoA synthase (DHNA-CoA synthase)	MAH_4008	0.30	-0.18	0.12
Short chain dehydrogenase	MAH_4009	0.27	-0.84	-0.57
Glyoxalase	MAH_4010	0.65	-0.49	0.16
Uncharacterized protein	MAH_4013	-0.37	-0.29	-0.66
Uncharacterized protein	MAH_4018	-1.20	0.84	-0.36
3-oxoacyl-[acyl-carrier-protein] synthase 3	MAH_4024	0.00	0.00	0.00
Uncharacterized protein	MAH_4027	0.04	0.17	0.21
Phosphoglycerate mutase	MAH_4032	-0.20	0.00	-0.20
Glutamate-1-semialdehyde 2,1-aminomutase (GSA)	MAH_4033	0.15	**-0.29**	-0.14
Uncharacterized protein	MAH_4035	-0.33	0.36	0.03
2-dehydropantoate 2-reductase(Ketopantoate reductase)	MAH_4037	-1.12	-0.20	-1.32
Uncharacterized protein	MAH_4043	0.29	-0.23	0.06
Uroporphyrinogen-III synthase	MAH_4050	-0.83	0.03	-0.79
Porphobilinogen deaminase (PBG)	MAH_4051	0.04	0.09	0.13
Uncharacterized protein	MAH_4056	-0.52	0.08	-0.44
Uncharacterized protein	MAH_4057	**-1.00**	0.47	-0.52
HAD-superfamily protein subfamily protein IB hydrolase	MAH_4059	-0.02	-0.08	-0.10
UPF0336 protein MAH_4060	MAH_4060	0.14	-0.12	0.02
Cyclopropane-fatty-acyl-phospholipid synthase 2	MAH_4061	0.00	-0.15	-0.15
Uncharacterized protein	MAH_4064	**-0.60**	**0.69**	0.08
Pyrroline-5-carboxylate reductase (P5C reductase) (P5CR)	MAH_4065	**0.56**	-0.31	0.25
Ppx/GppA phosphatase	MAH_4069	**0.44**	-0.34	0.10
Uncharacterized protein	MAH_4070	**-5.22**	**4.53**	-0.69
RegX3 protein	MAH_4073	-0.27	0.24	-0.04
2,3-bisphosphoglycerate-dependent phosphoglycerate mutase	MAH_4075	-0.18	-0.12	-0.30
Uncharacterized protein	MAH_4076	-0.58	0.22	-0.35
Oxidoreductase	MAH_4079	0.00	-0.09	-0.09
Uncharacterized protein	MAH_4082	0.29	**-0.45**	-0.15
Carbon-nitrogen hydrolase	MAH_4083	0.06	0.19	0.25

Conserved membrane protein	MAH_4084	-0.41	-0.21	-0.62
Heparin binding hemagglutinin hbha	MAH_4088	0.06	0.34	**0.40**
XRE family transcriptional regulator	MAH_4089	-0.55	0.09	-0.46
UmaA2 protein	MAH_4092	0.02	-0.01	0.01
3-hydroxybutyryl-CoA dehydrogenase	MAH_4094	0.19	0.00	0.20
Isocitrate lyase (*icl1*)*	MAH_4095	**0.56**	-0.24	0.32
Acyl-ACP thioesterase	MAH_4096	0.11	-0.14	-0.03
Dihydrolipoyl dehydrogenase (IpdA)*	MAH_4100	**0.30**	-0.10	0.20
Eptc-inducible aldehyde dehydrogenase	MAH_4104	-0.01	-0.09	-0.10
Enoyl-CoA hydratase	MAH_4107	-0.01	-0.11	-0.12
Uncharacterized protein	MAH_4108	**-0.71**	0.38	-0.33
Uncharacterized protein	MAH_4114	0.26	-0.33	-0.06
Glyoxalase	MAH_4115	**5.81**	-0.01	**5.79**
Amidohydrolase	MAH_4116	0.16	0.08	0.24
Uncharacterized protein	MAH_4118	-0.14	0.10	-0.04
60 kDa chaperonin (GroEL protein) (Protein Cpn60)	MAH_4120	0.06	-0.11	-0.05
Cupin domain-containing protein	MAH_4122	-0.12	0.36	0.24
Short chain dehydrogenase	MAH_4123	**0.75**	**-0.66**	0.09
Molybdopterin biosynthesis protein MoeA	MAH_4124	0.06	-0.11	-0.05
Phosphatidylserine decarboxylase proenzyme	MAH_4126	-0.02	0.02	0.00
Uncharacterized protein	MAH_4137	**4.98**	**-4.98**	0.00
Peptide deformylase (PDF)	MAH_4138	-0.16	-0.47	-0.62
Transmembrane protein	MAH_4141	-0.01	0.04	0.03
Uncharacterized protein	MAH_4143	-0.22	**-0.64**	-0.86
Phosphomethylpyrimidine synthase	MAH_4144	0.05	0.10	0.15
Uncharacterized protein	MAH_4146	0.00	0.00	0.00
Peptidase, M28 family protein	MAH_4151	-0.37	0.90	0.53
Uncharacterized protein	MAH_4155	-0.67	0.46	-0.21
Thiamine-phosphate synthase (TP synthase) (TPS)	MAH_4160	-0.56	0.84	0.28
Serine/threonine protein kinase	MAH_4164	0.10	-0.09	0.00
TetR family transcriptional regulator	MAH_4166	**3.98**	0.10	**4.07**
F420-dependent glucose-6-phosphate dehydrogenase (FGD) (G6PD)	MAH_4174	**0.23**	**-0.24**	-0.01
Glutaryl-CoA dehydrogenase	MAH_4180	0.48	-0.42	0.06
Long-chain specific acyl-CoA dehydrogenase	MAH_4181	0.49	-0.71	-0.22
O-succinylhomoserine sulfhydrylase	MAH_4186	0.18	-0.13	0.05
Uncharacterized protein	MAH_4187	-0.12	-0.09	-0.21
Phosphoribosylglycinamide formyltransferase 2	MAH_4188	**0.59**	**-0.58**	0.02
Thioesterase	MAH_4189	-0.05	-0.06	-0.11
Adenylosuccinate synthetase (AMPSase) (AdSS)	MAH_4190	-0.19	0.09	-0.10
Uncharacterized protein	MAH_4195	-0.89	0.52	-0.36
Succinyl-CoA:3-ketoacid-coenzyme A transferase 1	MAH_4198	-0.08	0.13	0.04

Orotate phosphoribosyltransferase (OPRT) (OPRTase)	MAH_4202	0.27	-0.15	0.12
Chaperone protein ClpB	MAH_4205	0.27	**-0.35**	-0.08
FAD dependent oxidoreductase domain-containing protein	MAH_4209	-0.43	0.82	0.38
Uncharacterized protein	MAH_4215	**-0.45**	**0.47**	0.01
Chaperone protein DnaJ	MAH_4218	**-0.55**	0.25	**-0.30**
Protein GrpE (HSP-70 cofactor)*	MAH_4219	**-0.22**	-0.02	-0.24
Chaperone protein DnaK (HSP70) (Heat shock 70 kDa protein)	MAH_4220	-0.18	-0.06	**-0.24**
Uncharacterized protein	MAH_4221	-0.05	0.27	0.22
Uncharacterized protein	MAH_4228	0.14	0.18	0.32
Ferredoxin, 4Fe-4S	MAH_4229	-0.55	0.73	0.18
Aminotransferase AlaT	MAH_4231	**-0.35**	0.25	-0.10
Glucose-1-phosphate thymidylyltransferase	MAH_4233	0.00	-0.12	-0.12
Uncharacterized protein	MAH_4234	-0.66	**0.48**	-0.18
Uncharacterized protein	MAH_4235	0.00	0.00	0.00
Deoxycytidine triphosphate deaminase (dCTP deaminase)	MAH_4241	0.00	-0.15	-0.15
ErfK/YbiS/YcfS/YnhG family protein	MAH_4247	-0.62	0.77	0.15
Glycosyl hydrolases family protein 16	MAH_4257	-0.42	**0.39**	-0.04
Oxidoreductase, zinc-binding	MAH_4258	-0.01	-0.27	-0.27
Uncharacterized protein	MAH_4260	-0.10	**-4.96**	**-5.06**
Uncharacterized protein	MAH_4265	0.02	-0.08	-0.06
AtsG protein	MAH_4272	-1.21	**-4.65**	**-5.86**
Trans-aconitate 2-methyltransferase	MAH_4273	-0.01	0.00	-0.01
Subtilase	MAH_4276	-0.19	0.43	0.24
ATPase AAA	MAH_4285	**5.61**	-0.20	5.41
S-adenosyl-L-methionine-dependent methyltransferase	MAH_4287	0.25	**-0.42**	-0.16
Glyoxalase/bleomycin resistance protein/dioxygenase	MAH_4299	-0.01	0.09	0.08
FadE6 protein	MAH_4302	0.10	0.02	0.12
Uncharacterized protein	MAH_4303	**-0.38**	**0.33**	-0.05
Acyl-CoA synthetase	MAH_4304	**-1.34**	**1.34**	0.00
TetR family transcriptional regulator	MAH_4307	-0.23	0.19	-0.04
Allophanate hydrolase subunit 1	MAH_4309	0.29	-0.39	-0.10
Uncharacterized protein	MAH_4310	0.14	-0.21	-0.07
Uncharacterized protein	MAH_4319	-0.29	0.33	0.04
Succinate dehydrogenase flavoprotein subunit	MAH_4321	-0.02	0.17	0.15
Fumarate reductase iron-sulfur subunit	MAH_4322	**-0.31**	0.21	-0.09
NADH-FMN oxidoreductase	MAH_4324	0.04	-0.18	-0.14
Acyl-CoA dehydrogenase	MAH_4326	0.32	0.13	0.44
Acetyl-CoA acetyltransferase	MAH_4327	**0.34**	-0.18	0.16
3-ketoacyl-(Acyl-carrier-protein) reductase	MAH_4328	**0.53**	**-0.27**	**0.26**
MaoC like domain-containing protein	MAH_4329	**0.86**	-0.05	0.81

Acetolactate synthase *(ilvB)**	MAH_4346	**0.57**	-0.24	0.33
Succinic semialdehyde dehydrogenase (*gabD1)**	MAH_4347	**0.37**	**-0.36**	0.01
Ribonucleotide-diphosphate reductase subunit beta	MAH_4348	-0.57	0.38	-0.19
Phosphotriesterase-like protein	MAH_4352	-0.04	0.13	0.10
Uncharacterized protein	MAH_4354	-0.46	**0.45**	-0.01
Aldehyde dehydrogenase	MAH_4358	-0.19	0.10	-0.09
Uncharacterized protein	MAH_4361	**-0.60**	0.23	-0.37
AMP-dependent synthetase and ligase	MAH_4362	-0.34	**-5.50**	**-5.84**
Enoyl-CoA hydratase	MAH_4363	-0.05	-0.10	-0.15
p40 protein	MAH_4369	0.48	-0.88	-0.41
Phosphoenolpyruvate carboxykinase [GTP] (PEP carboxykinase)	MAH_4375	0.09	0.03	0.13
Uncharacterized protein	MAH_4380	0.23	**-5.62**	**-5.40**
Peptidase M13	MAH_4388	0.04	0.30	0.34
ErfK/YbiS/YcfS/YnhG family protein	MAH_4397	**-0.47**	0.01	**-0.46**
Uncharacterized protein	MAH_4399	**0.82**	**-1.02**	-0.20
Dihydroxy-acid dehydratase (DAD)	MAH_4400	**0.33**	-0.09	**0.24**
O-methyltransferase	MAH_4403	**0.50**	**-0.44**	0.06
Lysophospholipase	MAH_4408	0.06	-0.03	0.03
Uncharacterized protein	MAH_4410	-0.14	-0.41	-0.55
YhhW protein	MAH_4413	0.00	0.00	0.00
Uncharacterized protein	MAH_4420	-0.50	**-3.45**	**-3.95**
Mce-family protein mce1c	MAH_4424	-0.38	-0.66	-1.04
Long-chain-fatty-acid-CoA ligase	MAH_4429	0.09	0.11	0.19
Cyclase/dehydrase	MAH_4431	0.18	-0.19	-0.01
AdhE protein	MAH_4433	**5.56**	0.71	**6.28**
Uncharacterized protein	MAH_4446	-0.38	0.34	-0.04
Uncharacterized protein	MAH_4449	0.22	-0.23	-0.01
FabG3_2 protein	MAH_4452	0.07	0.06	0.13
Homoserine dehydrogenase	MAH_4453	0.37	-1.65	-1.28
TetR family transcriptional regulator	MAH_4454	-0.16	0.13	-0.03
Uncharacterized protein	MAH_4455	-1.40	1.07	-0.33
NAD(P) transhydrogenase subunit beta	MAH_4456	0.13	-0.67	-0.55
PntAA protein	MAH_4458	0.38	**-0.51**	-0.14
Uncharacterized protein	MAH_4459	0.55	0.93	1.48
Acyl-CoA dehydrogenase fadE2	MAH_4460	0.26	-0.11	0.15
Peroxisomal multifunctional enzyme type 2	MAH_4462	0.22	-0.12	0.10
Aldehyde dehydrogenase	MAH_4463	-0.10	0.24	0.14
Peptide methionine sulfoxide reductase MsrA	MAH_4476	-0.09	0.05	-0.05
Uncharacterized protein	MAH_4487	**4.76**	**-4.76**	0.00
FadE1_3 protein	MAH_4497	-0.17	**0.33**	0.16
ZbpA protein	MAH_4498	0.25	-0.09	0.16
Antigen 85-C (*fbpC*)*	MAH_4508	**0.56**	**-0.54**	0.02

Uncharacterized protein	MAH_4510	0.13	**-0.52**	**-0.40**
Elongation factor G	MAH_4514	**4.04**	1.74	**5.78**
Acyl-CoA synthetase*	MAH_4515	**-5.25**	**5.34**	0.09
Zinc-binding dehydrogenase	MAH_4521	**0.77**	**-0.70**	0.08
O-methyltransferase, family protein 3	MAH_4524	**0.65**	-0.29	0.36
Aldehyde dehydrogenase	MAH_4526	0.00	0.00	0.00
Uncharacterized protein	MAH_4540	**-0.70**	**0.47**	-0.23
DltE protein	MAH_4547	0.31	-0.10	0.21
Methyltransferase type 11	MAH_4551	**0.66**	**-0.49**	0.17
Uncharacterized protein	MAH_4552	-0.20	-0.08	-0.28
Short chain dehydrogenase	MAH_4561	-0.75	0.00	-0.75
Uncharacterized protein	MAH_4564	0.01	0.10	0.11
TetR family transcriptional regulator	MAH_4574	-0.21	0.22	0.01
NAD dependent epimerase/dehydratase	MAH_4576	-0.02	0.06	0.04
Acyl dehydratase	MAH_4585	-0.23	0.01	-0.22
Uncharacterized protein	MAH_4589	0.27	-0.22	0.05
Fructose-1,6-bisphosphate aldolase	MAH_4592	-0.03	0.02	-0.01
Anti-anti-sigma factor	MAH_4593	-0.44	0.28	-0.17
Amidohydrolase	MAH_4598	**-0.54**	**0.48**	-0.06
Uncharacterized protein	MAH_4606	**5.71**	-1.04	**4.67**
Uncharacterized protein	MAH_4609	0.67	-1.49	-0.82
Uncharacterized protein	MAH_4612	-0.94	0.57	-0.37
PcnA protein	MAH_4615	-0.38	-0.12	-0.51
Virulence factor mvin family protein	MAH_4621	-0.09	-0.46	-0.56
Thioredoxin reductase	MAH_4624	0.17	0.00	0.17
Thioredoxin	MAH_4625	-0.14	-0.09	-0.23
ParB-like partition proteins	MAH_4628	0.06	-0.13	-0.07
Chromosome partitioning protein parA	MAH_4629	-0.04	0.19	0.15
R3H domain-containing protein	MAH_4632	**-0.40**	0.04	-0.36
50S ribosomal protein L34	MAH_4636	-0.17	**-4.65**	**-4.82**

9.2 Supplementary Table S2a: Pathway analysis via DAVID of differentially regulated genes of *M. avium hominissuis* lysX mutant in comparison to wild type

Pathways	Percentage of differentially regulated genes	*p* - value
Upregulated genes		
Biosynthesis of secondary metabolites	26.5	1.75×10^{-11}
Citrate cycle (TCA cycle)	3.8	5.95×10^{-11}
Glyoxylate and dicarboxylate metabolism	8.3	2.99×10^{-11}
Butanoate metabolism	68.2	3.8×10^{-3}
Fatty acid metabolism	68.2	0.01
Propanoate metabolism	60.6	0.03
Pyruvate metabolism	5.30	0.05
Downregulated genes		
Amino-acid biosynthesis	8.60	8.3×10^{-3}
Valine, leucine and isoleucine biosynthesis	4.90	7.5×10^{-3}
2-Oxocarboxylic acid metabolism	4.90	0.03

Percentage: involved genes/total of up- or down-regulated genes.

p-value: modified Fisher exact *p*-value.

9.2.1 Supplementary Table S2b: Functional enrichment analysis of differentially regulated genes of *M. avium hominissuis* lysX mutant in comparison to wild type strain 104 using STRING

	number of differentially regulated genes	FDR
Upregulated genes		
Biosynthesis of secondary metabolites*	45	1.9×10^{-11}
Glyoxylate and dicarboxylate metabolism*	12	9.53×10^{-7}
Butanoate metabolism*	12	1.05×10^{-5}
Pyruvate metabolism*	9	1.27×10^{-3}
Fatty acid metabolism*	10	1.73×10^{-3}
Citrate cycle (TCA cycle)*	7	1.86×10^{-3}
Oxidative phosphorylation	8	2.22×10^{-3}
Lysine degradation	8	2.22×10^{-3}
Valine, leucine and isoleucine degradation	10	2.32×10^{-3}
Fatty acid degradation	9	4.87×10^{-3}
Tryptophan metabolism	8	4.87×10^{-3}
Propanoate metabolism*	9	5.03×10^{-3}
Glycine, serine and threonine metabolism	6	5.83×10^{-3}
Glutathione metabolism	4	5.83×10^{-3}
Glycolysis / Gluconeogenesis	7	6.5×10^{-3}
Synthesis and degradation of ketone bodies	4	7.07×10^{-3}
Terpenoid backbone biosynthesis	5	0.01
Benzoate degradation	6	0.04
Downregulated genes		
Amino-acid biosynthesis*	10	0.02
Valine, leucine and isoleucine biosynthesis*	4	0.02
Oxidative phosphorylation	9	1.29×10^{-4}

*the pathways found by both DAVID and STRING analysis

FDR – false discovery rate

9.3 Supplementary Table S3: Genes differentially regulated in the *M.avium* lysX mutant compared to the wild type, which were reported to be associated with infection of macrophages (12-16) classified into COG (cluster of orthologous groups) groups

UPREGULATED GENES

COG Category		Gene Name	Product Description	Possible functions
Cellular Processes and Signalling				
Cell wall/membrane/envelope biogenesis (M)				
	MAV_2337	*murC*	UDP-N-acetylmuramate--L-alanine ^ ligase	Cell cycle, cell division, cell wall organization, peptidoglycan biosynthetic process
	MAV_5183	*fbpC*	Antigen 85-C (diacylglycerol O-acyltransferase / trehalose O-mycolyltransferase)	Glycerolipid metabolism
	MAV_2269		Integral membrane protein	Integral component of membrane
Post-translational modification, protein turnover, and chaperones (O)				
	MAV_2400	*mpa*	Proteasome-associated ATPase	proteasomal protein catabolic process
	MAV_0013		Peptidyl-prolyl cis-trans isomerase	protein folding,Cationic antimicrobial peptide (CAMP) resistance
	MAV_1713	*clpP1*	ATP-dependent Clp protease proteolytic subunit	serine-type endopeptidase activity
	MAV_2023	*dnaJ*	Chaperone protein DnaJ	DNA replication, protein folding, response to heat
Defense mechanisms (V)				
	MAV_0940		Cytochrome P450 superfamily protein	heme binding, iron ion binding, monooxygenase activity, oxidoreductase activity
	MAV_2839		Alkylhydroperoxide reductase	cell redox homeostasis, oxidoreductase activity,
	MAV_2909		PPE family protein	Mycobacteria virulence

Information Storage and processing				
Translation, ribosomal structure and biogenesis (J)				
	MAH_1314	*argS*	Arginine--tRNA ligase	arginyl-tRNA aminoacylation
Transcription (K)				
	MAV_3595	*sigA*	RNA polymerase sigma factor SigA	transcription initiation from bacterial-type RNA polymerase promoter
	MAV_1309		Transcriptional regulator, TetR family protein	regulation of transcription, DNA-templated
	MAV_0701	*phoP*	DNA-binding response regulator PhoP	phosphorelay signal transduction system, two-component system, OmpR family, response regulator
	MAV_4420		Transcriptional regulator, MarR family protein	transcription, DNA-templated
Replication, recombination and repair (L)				
	MAV_3155		DNA polymerase I	Purine and pyrimidine metabolism, DNAreplication,base repair, nucleotide excision repair, homologous recombination
Metabolism				
Energy production and conversion (C)				
	MAV_0344		Citrate synthase 2	Tricarboxylic acid cycle, glyoxylate cycle
	MAV_4687	*lpdA*	Dihydrolipoyl dehydrogenase	Cell redox homeostasis , tricarboxylic acid cycle, glyoxylate cycle, pyruvate metabolism, proponoate metabolism
	MAV_1525	*atpA*	ATP synthase F1, alpha subunit	Oxidative phosphorylation
	MAV_2298		Cytochrome c family protein	Electron carrier activity, Heme binding, iron ion binding, oxidative phosphorylation
	MAV_2781	*aceA*	Isocitrate lyase	Carboxylic acid metabolic process, glyoxylate cycle
	MAV_4682	*aceA*	Isocitrate lyase	Carboxylic acid metabolic process, glyoxylate cycle
	MAV_2880	*glcB*	Malate synthase G	Tricarboxylic acid cycle, glyoxylate cycle, pyruvate metabolism
	MAV_1380	*mdh*	Malate dehydrogenase	Carbohydrate metabolic process, tricarboxylic acid cycle,glyoxylate clycle, pyruvate metabolism

	MAV_4299	*sdhA*	Succinate dehydrogenase flavoprotein subunit	electron transport chain, tricarboxylic acid cycle, oxidative phosphorylation, butanoate metabolism
	MAV_4300	*sdhB*	succinate dehydrogenase iron-sulfur subunit	tricarboxylic acid cycle, oxidative phosphorylation, butanoate metabolism
Amino acid transport and metabolism (E)				
	MAV_4935	*ilvB*	Thiamine pyrophosphate enzyme	Valine, leucine, and isoleucine biosynthesis, butanoate metabolism
	MAV_3413	*aroQ*	3-dehydroquinate dehydratase	Aromatic amino acid family biosynthetic process, chorismate biosynthetic process
	MAV_2379	*metH*	Methionine synthase	Cysteine and methionine metabolism, Selenocompound metabolism, metabolism of cofactors and vitamins
Carbohydrate transport and metabolism (G)				
	MAV_3329	*zwf*	Glucose-6-phosphate 1-dehydrogenase	Pentose phosphate pathway, glutathione metabolism
Coenzyme transport and metabolism (H)				
	MAV_3678	*ribF*	Riboflavin biosynthesis protein	FAD and FMN biosynthetic process, riboflavin metabolism
	MAV_4871		ATPase, AAA family protein	ATP binding
	MAV_1719	*mobA*	molybdenum cofactor guanylyltransferase	Folate biosynthesis, GTP binding
	MAV_3482	*pdxT*	Pyridoxal 5'-phosphate synthase subunit PdxT	glutamine metabolic process, pyridoxal phosphate biosynthetic process, vitamin B6 metabolism
Lipid transport and metabolism (I)				
	MAV_4915		Acetyl-CoA acetyltransferase	Fatty acid degradation, ketone body biosynthesis, lysine degradation, pyruvate metabolism, proponoate metabolism, two-component system
	MAV_1544		Acetyl-CoA acetyltransferase	Fatty acid degradation, ketone body biosynthesis, lysine degradation, pyruvate metabolism, proponoate metabolism, two-component system

MAV_2127		Acetyl-CoA acetyltransferase	Fatty acid degradation, ketone body biosynthesis, lysine degradation, pyruvate metabolism, proponoate metabolism, two-component system
MAV_0980		Acetyl-CoA acetyltransferase	Fatty acid degradation, ketone body biosynthesis, lysine degradation, pyruvate metabolism, proponoate metabolism, two-component system
MAV_1090		Acetyl-CoA carboxylase carboxyltransferase	Ligase activity, transferase activity
MAV_4418	*fadE8*	Acyl-CoA dehydrogenase family protein member 8	Acyl-CoA dehydrogenase activity, flavin adenine dinucleotide binding
MAV_4500		Putative acyl-CoA dehydrogenase	Acyl-CoA dehydrogenase activity, flavin adenine dinucleotide binding
MAV_1088	*fadE12*	Acyl-CoA dehydrogenase	Acyl-CoA dehydrogenase activity, flavin adenine dinucleotide binding
MAV_1087		Enoyl-CoA hydratase	Fatty acid degradation, Geraniol degradation, lysine degradation, benzoate degradation, proponoate metabolism,butanoate metabolism
MAV_0981		Putative acyl-CoA dehydrogenase	fatty acid beta-oxidation, Geraniol degradation, lysine degradation, benzoate degradation, proponoate metabolism, butanoate metabolism
MAV_1225		3-beta hydroxysteroid dehydrogenase/ isomerase family protein	Steroid degradation
MAV_1089		Carbamoyl-phosphate synthase L chain, ATP binding domain	Valine, leucine and isoleucine degradation, glyoxylate and dicarboxylate metabolism, proponoate metabolism
MAV_2313		1-acylglycerol-3-phosphate O-acyltransferase	Glycerolipid metabolism, Glycerophospholipid metabolism
MAV_4343		3-oxoacyl-[acyl-carrier-protein] synthase 2	Fatty acid synthesis
MAV_1572		3-oxoacyl-[acyl-carrier-protein] r eductase	Fatty acid biosynthesis, biotin metaboilsm, biosynthesis of unsaturated fatty acids

	MAV_4916		Oxidoreductase, short chain dehydrogenase/ reductase family protein	Fatty acid biosynthesis, biotin metaboilsm, biosynthesis of unsaturated fatty acids
	MAV_0218	*pks13*	Polyketide synthase 13	Lipid biosynthesis proteins
	MAV_4917		MaoC like domain protein	fatty acid biosynthetic process, oxidation-reduction process
	MAV_0572	*ispF*	2-C-methyl-D-erythritol 2,4-cyclodiphosphate synthase	Isopentenyl diphosphate biosynthetic process, methylerythritol 4-phosphate pathway, terpenoid backbone biosynthesis

DOWNREGULATED GENES

Cellular Processes and Signalling

Cell wall/membrane/envelope biogenesis (M)				
	MAV_1098	*mscL*	Large conductance mechanosensitive channel protein	Ion channel activity
	MAV_0306		Lipoprotein LpqH	Pathogenesis, host cell surface receptor binding,
Post-translational modification, protein turnover, and chaperones (O)				
	MAV_4807	*grpE*	molecular chaperone GrpE	Protein folding, stress response
	MAV_4806	*dnaJ*	Chaperone protein DnaJ	DNAreplication, protein folding, response to heat
Defense mechanisms (V)				
	MAV_2905		Ppe family protein	Mycobacteria virulence

Metabolism

Amino acid transport and metabolism (C)				
	MAV_3837	*leuD*	3-isopropylmalate dehydratase small subunit	leucine biosynthetic process
	MAV_3838	*leuC*	3-isopropylmalate dehydratase large subunit	leucine biosynthetic process
Lipid transport and metabolism (I)				
	MAV_5190		Acyl-CoA synthase	metabolic process
	MAV_2192		3-oxoacyl-[acyl-carrier-protein] synthase 1	Fatty acid biosynthesis
	MAV_2193	*acpP*	Acyl carrier protein	Fatty acid biosynthesis
Inorganic ion transport and metabolism (P)				
	MAV_3021		Biphenyl-2,3-diol 1,2-dioxygenase 1	xenobiotic catabolic process, iron ion binding
	MAV_2753	*katG*	Catalase-peroxidase	Phenylalanine and tryptophan metabolism,response to oxidative stress

9.4 Supplementary Table S4a: List of the substrates equally used by both the strains- wild type (MAH 104) and mutant lysXmut in the metabolic microarray analysis

The number and letter of each substrate indicate the exact position in the PM plate.

PMI

Carbon substrates

1,"C05 -Tween 20"

2,"D05 - Tween 40"

3,"E05 - Tween 80"

4,"C09 - D-Glucose"

5,"F07 - Propionic Acid"

PM3

Nitrogen substrates

6,"G10 - D,L-a-Amino-Caprylic Acid"

9.4.1 Supplementary Table S4b: List of the substrates differentially used by the strains- wild type (MAH 104) and mutant lysXmut in the metabolic microarray analysis

The number and letter of each substrate indicate the exact position in the PM plate.

PM1

Carbon substrates

1,“H07 – Glucuronamide“

2,“H05 - D-Psicose”

3,”C08 - Acetic acid” *

4,”G09 - Mono-methyl succinate”

5,”G10 – Methyl pyruvate”

6,”H08 - Pyruvic acid” *

PM2

Carbon substrates

7,”F08 - Sebacic acid”

8,”B03 - b-D-Allose”

9,”D12 - Butyric acid”

10,”E02 - Caproic acid”

PM3

Nitrogen substrates

11,”E09 - D-Galactosamine”

12,”A09 - L-Asparagine”

13,”A11 - L-Cysteine”

.

PM3

Phosphorous substrates

14,”B05 - Carbamyl phosphate”

15,”A03 - Sodium pyrophosphate”

* The differentially used substrates with statistical significance are underlined. Significant differences between isolates were calculated by comparison of mean point estimates and their 95% confidence intervals for the parameter A using the functions ´extract´ and ´ci-plot´ within the R-opm package (42).

9.5 Supplementary Table S5: The pathway analysis of substrates differentially used in the metabolic microarray analysis by the lysX mutant strain when compared to the wild type (MAH 104)

The pathways were obtained by using the "KEGG pathway database".

Substrate	Pathways associated
Acetic acid	Glycolysis / Gluconeogenesis *
	Taurine and hypotaurine metabolism
	Pyruvate metabolism**
	Propanoate metabolism**
	C5-Branched dibasic acid metabolism
	Methane metabolism
	Sulphur metabolism
	Biosynthesis of secondary metabolites**
	Microbial metabolism in diverse environments
	Biosynthesis of antibiotics
	Carbon metabolism
	Degradation of aromatic compounds
Pyruvic acid	Glycolysis / Gluconeogenesis *
	Taurine and hypotaurine metabolism
	Pyruvate metabolism**
	Microbial metabolism in diverse environments
	Degradation of aromatic compounds
	Citrate cycle (TCA)**
	Pentose phosphate pathway
	Cysteine and methionine metabolism
	Benzoate degradation*
	Pentose and glucuronate interconversions
	Ascorbate and aldarate metabolism
	Alanine, aspartate and glutamate metabolism
	Glycine, serine and threonine metabolism*
	Monobactam biosynthesis
	Valine, leucine and isoleucine biosynthesis**
	Arginine and proline metabolism
	Tyrosine metabolism
	Phenylalanine metabolism
	D-Alanine metabolism

*- Pathways enriched according to DAVID or STRING analysis**- Pathways enriched according to both DAVID and STRING analysis

10 List of Publications

1. **Greana Kirubakar**, Jayaseelan Murugaiyan, Christoph Schaudinn, Flavia Dematheis, Gudrun Holland, Murat Eravci, Christoph Weise, Uwe Roesler, Astrid Lewin, Proteome Analysis of a *M. avium* Mutant Exposes a Novel Role of the Bifunctional Protein LysX in the Regulation of Metabolic Activity, *The Journal of Infectious Diseases*, Volume 218, Issue 2, 15 July 2018, Pages 291–299, https://doi.org/10.1093/infdis/jiy100

(Original paper - Published)

2. **Greana Kirubakar**, Hubert Schaefer, Volker Rickerts, Carsten Schwarz, Astrid Lewin, LysX interferes with the pathogenic behavior of Mycobacterium avium hominissuis.

Submitted to *Virulence* (Original paper – under revision)

11 Self-Declaration

This thesis is a presentation of my original research work. Wherever contributions of others are involved, every effort was made to indicate this clearly, with due reference to the literature and acknowledgement of collaborative research and discussions. The thesis contains no material which has been accepted for the award of any other degree or diploma in any University.

Greana Kirubakar
27.08.2019